

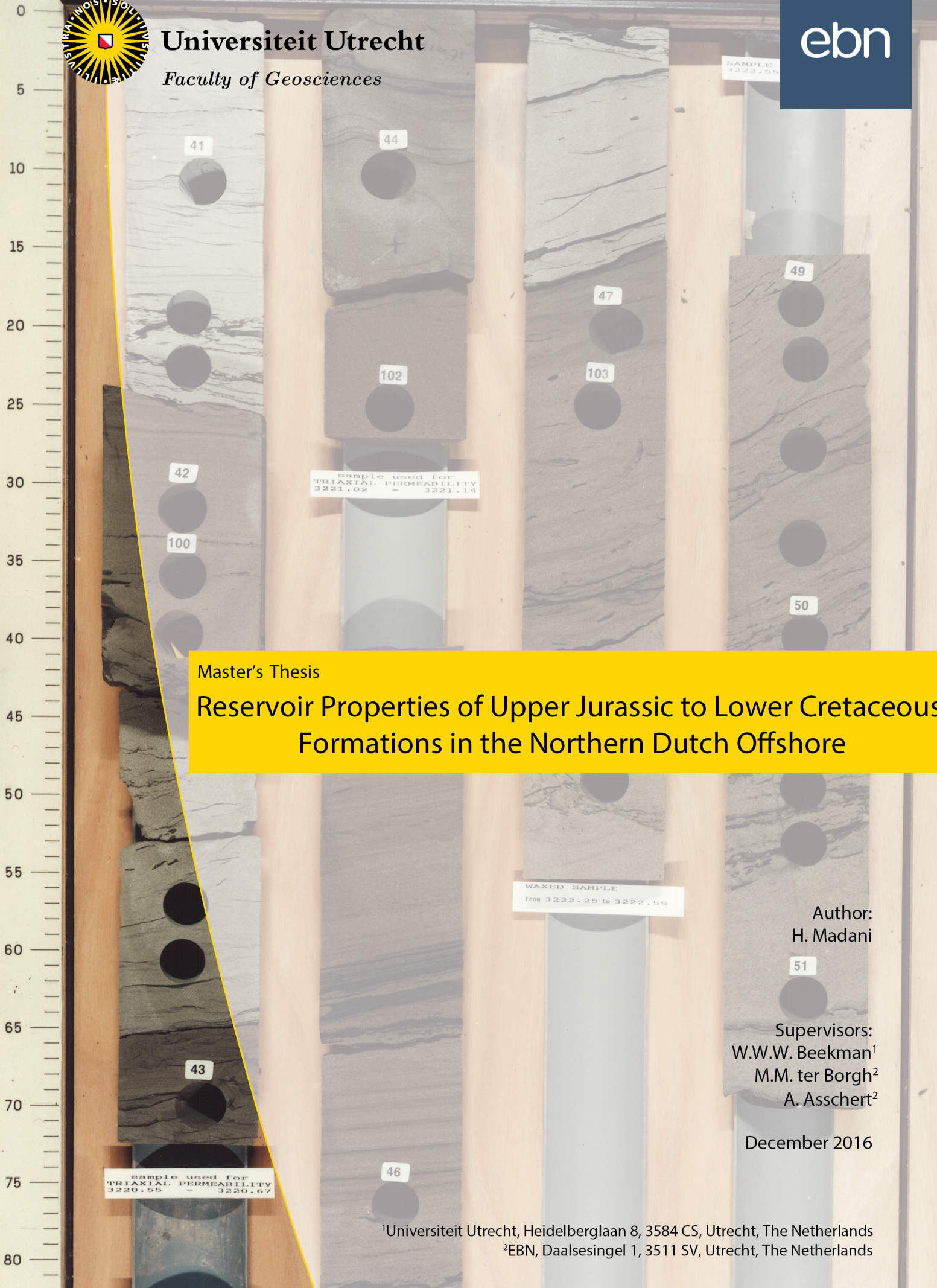
METRE

3219.84 3220.75 3221.65 3222.55



Universiteit Utrecht
Faculty of Geosciences

ebn



Master's Thesis

Reservoir Properties of Upper Jurassic to Lower Cretaceous Formations in the Northern Dutch Offshore

Author:
H. Madani

Supervisors:
W.W.W. Beekman¹
M.M. ter Borgh²
A. Asschert²

December 2016

sample used for
TRIAXIAL PERMEABILITY
3220.55 - 3220.67

Sample used for
TRIAXIAL PERMEABILITY
3221.02 - 3221.14

WAXED SAMPLE
from 3222.25 to 3222.55

46

¹Universiteit Utrecht, Heidelberglaan 8, 3584 CS, Utrecht, The Netherlands

²EBN, Daalsesingel 1, 3511 SV, Utrecht, The Netherlands

Frontispiece

Photograph from a core cut from the Lower Graben Formation in well F03-FB-101. As typically with cores, it was cut lengthwise and in pieces of 1 m long. Plug samples taken from the core leave the round-shaped holes as can be seen in the photo. The brownish, fine to very fine-grained well-sorted sandstones are interpreted as distributary channel deposits. The greyish claystones with bioturbated, fine to very fine-grained sandstones are interpreted as inter-distributary bay deposits.

Abstract

In the northern Dutch offshore, Upper Jurassic to Lower Cretaceous formations form an important target for hydrocarbon exploration. Late Jurassic to Early Cretaceous rifting in the Southern North Sea accommodated the deposition of three transgressive mega-sequences, which reflect a general change in energy conditions from proximal towards distal facies. The reservoir sands vary widely in presence, thickness, and reservoir quality, a factor which is still poorly understood. Because of renewed successes in Upper Jurassic to Lower Cretaceous reservoir sands, a study was performed of reservoir properties with the aim of constraining the main processes controlling reservoir quality. Core data was used from 45 exploration, appraisal, and production wells containing a total of 1426 m of core length including 4066 plug sample measurements on porosity, permeability, grain density. Additional data included petrographic data such as thin sections and Scanning Electron Microscope images. All cores were cut in the Lower Graben Subgroup and the Scruff Group, located in the Dutch Central Graben, Terschelling Basin, and Schill Grund Platform. Correlating facies data with plug sample data show clear differences in reservoir quality due to different depositional environments (eogenesis), the progression of these environments through time, and the combined effects of burial diagenesis (mesogenesis) on different lithologies. The most important factor determining reservoir quality is the environment of deposition, which controls energy conditions that influence clay content. The Friese Front Formation has the best reservoir quality in clean, well-sorted channel sands that indicate high energy conditions, which lead to lower clay content. Alluvial fan deposits in the Friese Front Formation show good reservoir quality. Other reservoir sands with good quality were deposited in marginal marine settings such as beach-barrier complexes as encountered in the Terschelling Sandstone Member, and tidal channel sands in the Lower Graben Formation in the F03-FB field. Marginal marine sands of the Middle and Upper Graben formations also have good reservoir quality. The shallow marine Noordvaarder Member has good reservoir quality with potential as it can be correlated with similar sands in the UK, Danish, and probably also the German section of the Central Graben. Depositional settings with low energy conditions lead to high clay content and a poor reservoir quality, as seen in the brackish lagoon/bay deposits of the Lower Graben Formation. Lower shoreface sands of the Scruff Greensand Formation have good permeability, and good porosity due to the dissolution of sponge spicules. Lithologies consisting of primarily clay such as the Kimmeridge Clay Formation and the Lutine Formation show a poor reservoir quality. Processes related to burial diagenesis significantly influence reservoir quality after initial deposition. Mechanical compaction and burial cementation cause a linear loss of porosity with depth. Permeability shows no clear trend with depth. However, core data from the F03-FB field show rapid losses of porosity and permeability at depths greater than 3100 m, which suggests chemical diagenesis as the dominant control on reservoir quality. Permeability losses at depths greater than 3100 m are in 1 to 2 orders of magnitude, which is attributed to chemical diagenesis due to the precipitation of clays such as illite at increased pressures and temperatures.

Acknowledgements

This research would not have been possible without the help of others. Therefore, I would like to express my gratitude to those who contributed to my research process.

First, I would like to thank EBN for providing the facilitating this project and providing a fantastic working environment. From EBN I would like to thank Marten Ter Borgh and Annemiek Asschert for their outstanding support in this project. Without their valuable feedback and suggestions, this result would not have been possible. Also, special thanks to Peter Bange for his help in fine-tuning the database, Walter Eikelenboom for helping with QGIS, and Tom Leeftink for his support with Spotfire.

From Utrecht University I would like to thank my supervisor Fred Beekman for his time, valuable feedback and suggestions.

I would like to thank TNO for constructing the database, and from TNO Roel Verreussel for providing feedback and suggestions in the early part of the project.

Finally, I would like to thank my colleague-interns for their help and contributing to a vibrant atmosphere with countless of interesting discussions and good laughs.

Table of contents

1. Introduction	1
2. Background	3
2.1 Tectonic evolution of the study area within the context of the regional southern North Sea during the Mesozoic	3
2.1.1 Early Triassic	5
2.1.2 Middle Triassic	6
2.1.3 Late Triassic	6
2.1.4 Early Jurassic	7
2.1.5 Middle Jurassic	9
2.1.6 Late Jurassic to Early Cretaceous	10
2.1.7 Mid- to Late Cretaceous	12
2.2 Structural elements in the northern Dutch offshore	13
2.3 Stratigraphic framework	17
2.4 Updated Upper Jurassic – Lower Cretaceous lithostratigraphy and correlation with the UK and Danish sections of the Central Graben (Munsterman et al., 2012)	21
2.4.1 Sequence 1	21
2.4.2 Sequence 2	23
2.4.3 Sequence 3	25
3. Methods	31
3.1 Database	31
3.2 Depositional framework and facies correlation	36
4. Results – Analysis of Trends in Reservoir Properties	39
4.1 Lower Graben Formation (SLCL)	42
4.2 Middle Graben Formation (SLCM)	48
4.3 Upper Graben Formation (SLCU)	50
4.4 Friese Front Formation (SLCF)	52
4.5 Skylge Formation (SGSK)	57
4.6 Kimmeridge Clay Formation (SGKI)	61
4.7 Scruff Greensand Formation (SGGS)	63
4.8 Lutine Formation (SGLU)	67
5. Results – Controls on Reservoir Properties	69
5.1 Main findings and uncertainties	69
5.2 Applicability of the revised lithostratigraphic scheme	71
5.3 Lithology and Depositional Environment	72
5.3.1 Lower, Middle, and Upper Graben formations: marginal marine sands	72
5.3.2 Friese Front Formation: alluvial fan deposits and fluvial channel sands	73
5.3.3 Skylge Formation – Terschelling Sandstone Member: marginal marine sands	73
5.3.4 Skylge Formation – Noordvaarder Member: shallow marine sands and mass-flow sandstones of the Brae Formation in the UK	74

5.3.5	Scruff Greensand Formation: lower shoreface sands and enhanced porosity due to dissolution of sponge spicules.....	76
5.3.6	Kimmeridge Clay Formation and Lutine Formation: open marine clay-rich sediments.....	77
5.4	Mineralogy.....	79
5.5	Diagenesis.....	79
5.5.1	Mechanical Compaction.....	80
6.	Discussion.....	82
6.1	Chemical Compaction.....	82
6.2	Dissolution of framework grains.....	83
6.3	Grain Coating.....	84
6.4	Allochthonous Salt.....	84
6.5	Overpressure.....	85
6.6	Early Hydrocarbon Emplacement.....	85
6.7	Provenance.....	86
6.8	Inversion.....	86
7.	Conclusions.....	87
8.	Appendices.....	89
8.1	Appendix A – Raw data per well.....	89
8.2	Appendix B – Late Jurassic to Early Cretaceous time slices of the facies distribution in the northern Dutch offshore through time. (Munsterman et al., 2012).....	96
9.	References.....	97

1. Introduction

In the whole North Sea area, about one fifth of the hydrocarbon reserves is contained in Upper Jurassic to Lower Cretaceous sediments (Fraser et al., 2003). For the Upper Jurassic – Lower Cretaceous play in the Netherlands this share is much lower – about 1/15 for total hydrocarbon reserves when excluding the Groningen field – as the Slochteren Formation of the Upper Rotliegend Group forms the main hydrocarbon reservoir (De Jager & Geluk, 2007). However, at present-day, it is still an important target for further exploration and may hold significant quantities of remaining reserves located in either structural or stratigraphic traps (Boldy & Fraser, 1999; Johnson & Fisher, 2009). In the Netherlands, recent successes such as the M07-B gas field led to renewed interest in this interval, with new research published and additional studies expected (Lott et al., 2010).

Upper Jurassic to Lower Cretaceous reservoir sediments are rather unevenly distributed throughout the southern North Sea. In addition, significant regional variations exist with respect to thickness and reservoir quality. This is a direct result of the complex and diachronous tectonic history, in which the tectonic regime changed at various points in time during the Mesozoic to Cenozoic. Older, Paleozoic faults were repeatedly reactivated during Late Jurassic to Early Cretaceous extension and subsequent inversion in the Late Cretaceous, which resulted in an extensive network of basins, platforms and highs (Ziegler, 1990a; Ziegler 1990b; De Jager, 2007). In addition, movement of the Zechstein salt in the southern North Sea further complicated the tectonic evolution. This halokinesis led to the development of piercing salt diapirs, resulting in the deposition of sediments in the rim synclines adjacent to the salt domes. Finally, differences in stratigraphic nomenclature between countries bordering the southern North Sea (UK, Germany, Denmark, and Norway) make correlating genetic sequences a challenging task.

Because of the remaining potential for the Upper Jurassic – Lower Cretaceous play in the Netherlands, a thorough understanding of the depositional history is essential to understand the regional variability of reservoir quality. In the northern Dutch offshore, the southern North Sea basin evolution during the Late Jurassic to Early Cretaceous can be subdivided into three distinct events: (1) rifting affecting only a narrow area of the Central Graben axis, (2) the subsequent opening of the peripheral basins, and (3) the flooding of the adjacent platforms and highs. During these three tectonic phases, repeated periods of transgression led to the formation of four major stratigraphic sequences (Herngreen et al., 2003; Abbink et al., 2006). The identification of these genetic mega-sequences led to a revised stratigraphic framework for the Late Jurassic – Early Cretaceous in the northern Dutch offshore (Munsterman et al., 2012). The overall nomenclature was simplified by changes based on consistent lithologic differences and improved dating methods, leading to a clearer distinction between marine and non-marine conditions. In addition, detailed sedimentary facies analyses were provided, with correlations with the updated Upper Jurassic – Lower Cretaceous strata in the Dutch offshore.

The underlying causes for the regional variations in reservoir properties of Upper Jurassic – Lower Cretaceous rocks have not yet been fully studied. Therefore, this study aims to focus on the distribution of reservoir properties in Upper Jurassic – Lower Cretaceous sediments in the northern Dutch offshore, and the factors essential in controlling reservoir quality. Also, the new lithostratigraphic framework will be tested and evaluated on its ability to correlate with other sections of the southern North Sea,

particularly in the UK and Danish sections of the southern Central Graben. Therefore, the primary aim of this study is to investigate the reservoir properties of Upper Jurassic – Lower Cretaceous rocks in the northern Dutch offshore and determine the main controls on the regional distribution of porosity and permeability in the reservoir sands. As such, this study will aim to answer the following research questions:

- What factors control reservoir properties of Upper Jurassic – Lower Cretaceous rocks in the northern Dutch offshore?
- What are the trends and outliers in these reservoir properties?
- Can we explain these trends and outliers as a function of depositional environment, diagenesis, tectonics, or salt movement?
- What combination of circumstances is responsible for producing the most favorable reservoir properties?
- Does the new lithostratigraphic framework for the Upper Jurassic to Lower Cretaceous successions help in predicting reservoir properties?

To answer these questions, this study will be subdivided into the following parts:

1. Database setup containing core data and plug measurements of relevant wells within the area of interest. Depending on the amount of data, the study area will be defined.
2. Mapping of the presence of relevant reservoirs and their relevant depositional settings in the Late Jurassic to Early Cretaceous time interval.
3. Identifying the regional distribution of trends and outliers in porosity and permeability. In addition, the potential role will be determined of processes such as tectonics, diagenesis, and salt movement.
4. Integrating the results to predict which parts of the northern Dutch offshore contain the most favorable reservoir properties by extrapolating the extent of the various controls on porosity and permeability.

2. Background

This chapter provides the relevant geological background information on the study area within the context of the larger, regional picture of the southern North Sea. First, an overview is given of the tectonic evolution of the North Sea region through time, with emphasis on the southern part of the North Sea and the structural elements that define the northern Dutch offshore. The second section of this chapter will consider the stratigraphic framework and the range of depositional environments associated with the three mega-sequences of the Late Jurassic – Early Cretaceous lithostratigraphy. The revised stratigraphic scheme is presented, containing descriptions of the individual stratigraphic units and their depositional environments. In the context of this study, correlation of genetically similar deposits results in an Upper Jurassic – Lower Cretaceous lithostratigraphy calibrated with a latest Middle Jurassic to earliest Cretaceous chronostratigraphy (Callovian – Ryazanian).

2.1 Tectonic evolution of the study area within the context of the regional southern North Sea during the Mesozoic

The northern Dutch offshore forms a small part of the larger southern North Sea, which in turn is the northwestern component of the Southern Permian Basin. The southern North Sea Basin was shaped by the following main tectonic events: 1) the assembly of Pangaea during the Paleozoic Caledonian and Variscan orogenies, 2) Rifting during the Mesozoic and the resulting break-up of Pangaea, and 3) compressional tectonics due to inversion caused by the Alpine orogeny resulting from the collision of the African and Eurasian plates during Late Cretaceous and Early Tertiary times, subsequently closing the Tethys Ocean (De Jager, 2007). The general idea behind the tectonic evolution is that pre-existing basement faults were repeatedly reactivated and hence controlled the development of the structural framework, even though the tectonic regime and stress direction changed over time (De Jager, 2007). In addition, the widespread presence of thick Permian Zechstein salt triggered halokinesis, which caused decoupling of extensional and transpressional faulting above the salt from sub-salt faulting (De Jager, 2007).

Thermal subsidence controlled the development of the Northern and Southern Permian basins during Late Permian to Mid-Triassic times (Pharaoh et al., 2010). During the Triassic and Jurassic, the Southern Permian Basin underwent a gradual change from a large, single basin into a series of smaller, fault-bounded basins and highs (De Jager, 2007). This transition into a multi-basinal configuration was related to the break-up of Pangaea (Ziegler, 1990a), which occurred during four phases of extensional tectonics: Hardegsen (Scythian), Early Cimmerian (Anisian – Carnian), Mid-Cimmerian (Aalenian – Callovian /Oxfordian), and Late Cimmerian (Kimmeridgian-Ryazanian) (Figure 1) (Wong, 2007). These phases were separated by intervals during which thermal subsidence was dominant.

A step-wise overview of the structural and tectonic evolution during the Mesozoic is summarized below, in which the study area is placed into the context of the broader picture of the southern North Sea Basin.

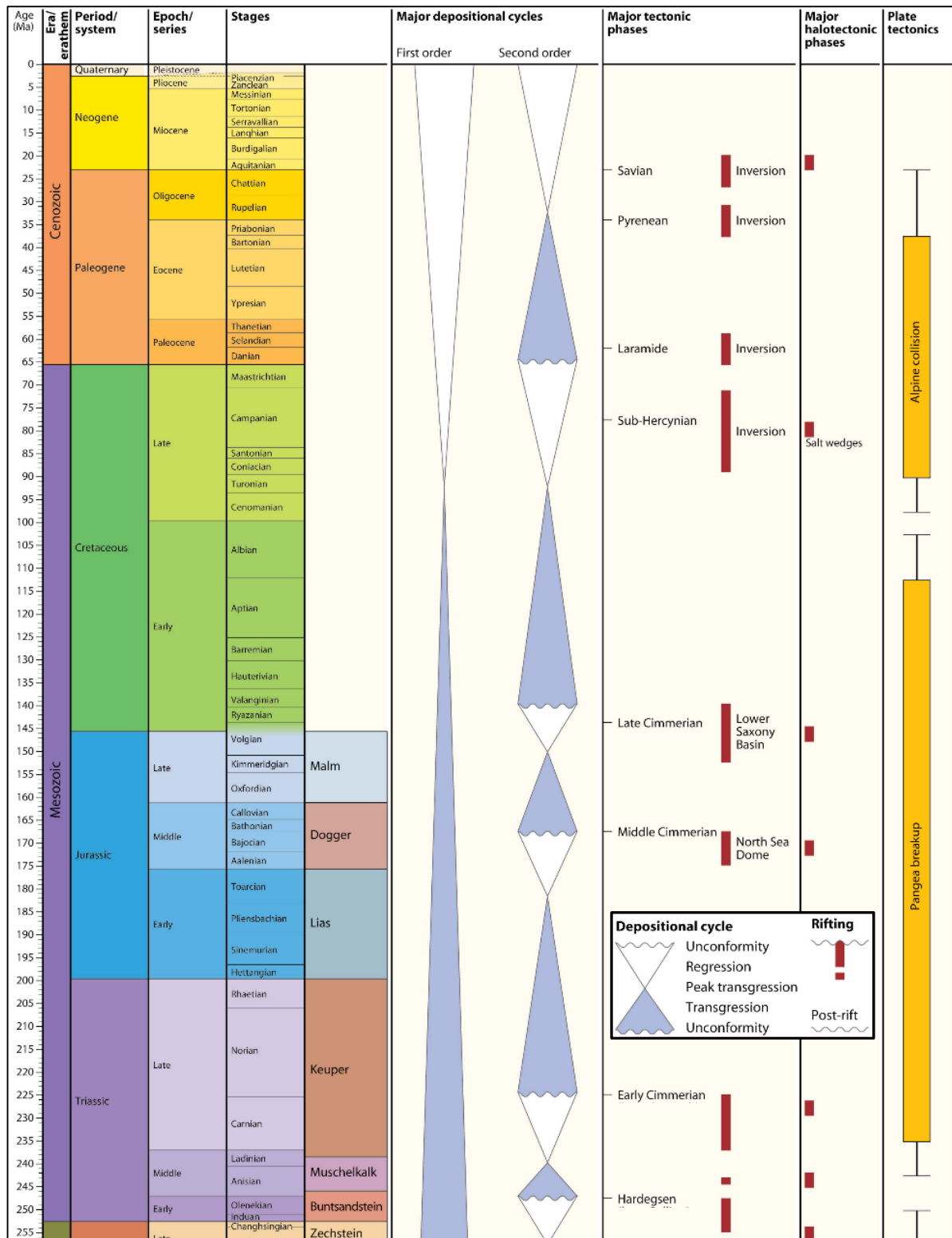


Figure 1. Mesozoic – Cenozoic timescale with major depositional cycles, tectonic phases and halokinetic episodes in the Southern Permian Basin (Pharaoh et al. (2010)).

2.1.1 Early Triassic

In the Early Triassic the break-up of Pangaea resulted in the start of rifting in the North Atlantic between Greenland and the Baltic Shield (Figure 2) (Lott et al., 2010). The rift system propagated southward into the Mid North Sea–Ringkøbing-Fyn High, although extensional faulting was more pronounced in the northern North Sea compared to the southern North Sea (Ziegler, 1990a; Ziegler, 1990b; Roberts et al., 1995; Coward et al., 2003).

The southern North Sea underwent uniform thermal subsidence. The Dutch Central Graben subsided faster than the surrounding platforms, areas that would later become the Terschelling and Vlieland basins (Ziegler, 1990a; Ziegler, 1990b; Geluk, 2007).

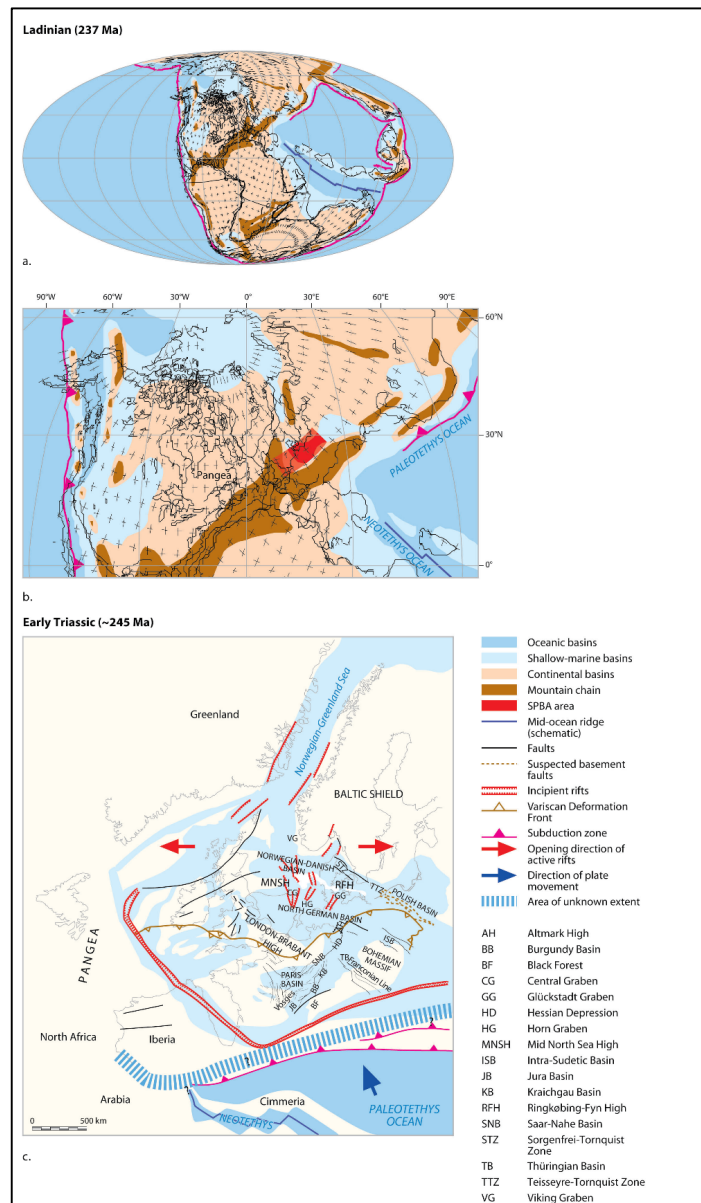


Figure 2. Early to Mid-Triassic tectonic evolution: a) Paleogeographic world map for the Early Triassic (Ladinian, 237 Ma); b) Detailed Ladinian paleogeographic map; c) Early Triassic structural overview map (~245 Ma) (Pharaoh et al., 2010).

2.1.2 Middle Triassic

During the Middle Triassic, thermal subsidence continued, and Triassic formations become thicker into the recently formed Dutch Central Graben and the Broad Fourteens Basin, which were the only areas with fault activity (Guterch et al., 2010). Mobilization of the Zechstein salt was triggered, which later during the Late Triassic resulted in salt domes piercing the overlying strata and the subsequent development of rim-synclines (De Jager, 2007). The presence of salt is an important parameter that can be used to distinguish between the northern North Sea (no salt), the central and southern North Sea (abundant salt). The mobility and lateral extent of the Zechstein salt led to differential sedimentation, erosion, and structural changes that significantly influenced the evolution of not only Triassic strata, but also the deposition of Jurassic sediments in the southern North Sea Basin (Goldsmith et al., 2003).

2.1.3 Late Triassic

In the Late Triassic, the southern North Sea area experienced E-W rifting as a branch of the North Atlantic rift system extended southward into the Central Atlantic area (Figure 3) (Pharaoh et al., 2010). In the northern Dutch offshore, the Zechstein underwent differential loading by increased sedimentation, which triggered the piercing of salt diapirs and the subsequent development of mini-basins by the formation of rim-synclines (Pharaoh et al., 2010). During the latest Triassic, the erosion and collapse of the Variscan orogeny caused an increasingly humid climate in northwestern Europe, resulting in a rapid change from red to grey beds characteristic for Early to Mid-Jurassic sediments (Roberts et al., 1999).

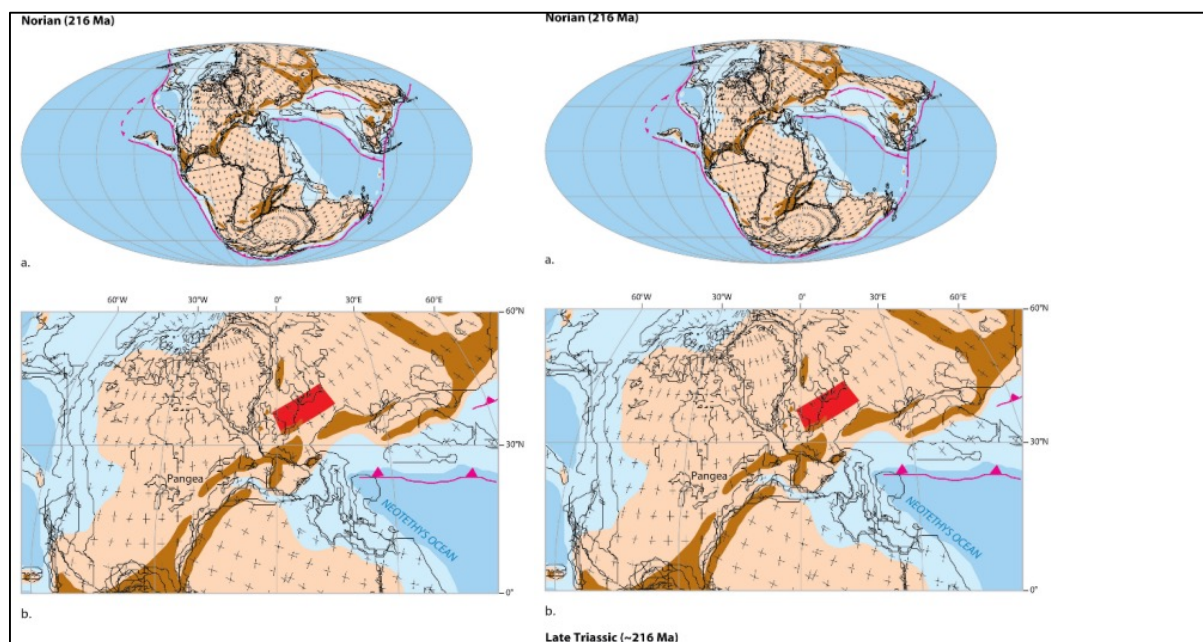


Figure 3. Late Triassic tectonic evolution: a) Paleogeographic world map for the Norian (216 Ma); b) Detailed paleogeographic map for the Norian; c) Late Triassic structural overview map (~216 Ma) (Pharaoh et al., 2010).

2.1.5 Early Jurassic

During the Early Jurassic, the North Sea rift system remained active, as shown by evidence of activity in the Viking Graben and Dutch Central Graben. The Northern and Southern Permian basins underwent steady regional thermal subsidence coupled with a eustatic sea-level rise during the Rhaetian and Hettangian, resulting in the formation of an extensive, open-marine basin (Figure 4) (Guterch et al., 2010). While the basin was regionally subsiding, clastic sediments were transported from the Baltic Shield, East European Platform and Bohemian Massif into the basin (Guterch et al., 2010). During the Toarcian, stagnant-water stratification triggered the deposition of the anoxic shales belonging to the Posidonia Shale Formation, the main oil source rock of the southern North Sea and northern Germany (Ziegler, 1990a).

In the central North Sea, Lower to Middle Jurassic deposits are thin or missing due to deep truncation during Mid- to Late Jurassic times (Pharaoh et al., 2010). However, the Early Jurassic was a period of relative tectonic quiescence, with faulting mostly occurring in Dutch Central Graben and the Broad Fourteens Basin (Guterch et al., 2010). During most of the Early Jurassic, the Cleaver Bank Platform, Ameland Platform, and Schill Grund Platform remained stable platforms that accumulated thick sediment deposits estimated to be hundreds of meters thick (Pharaoh et al., 2010).

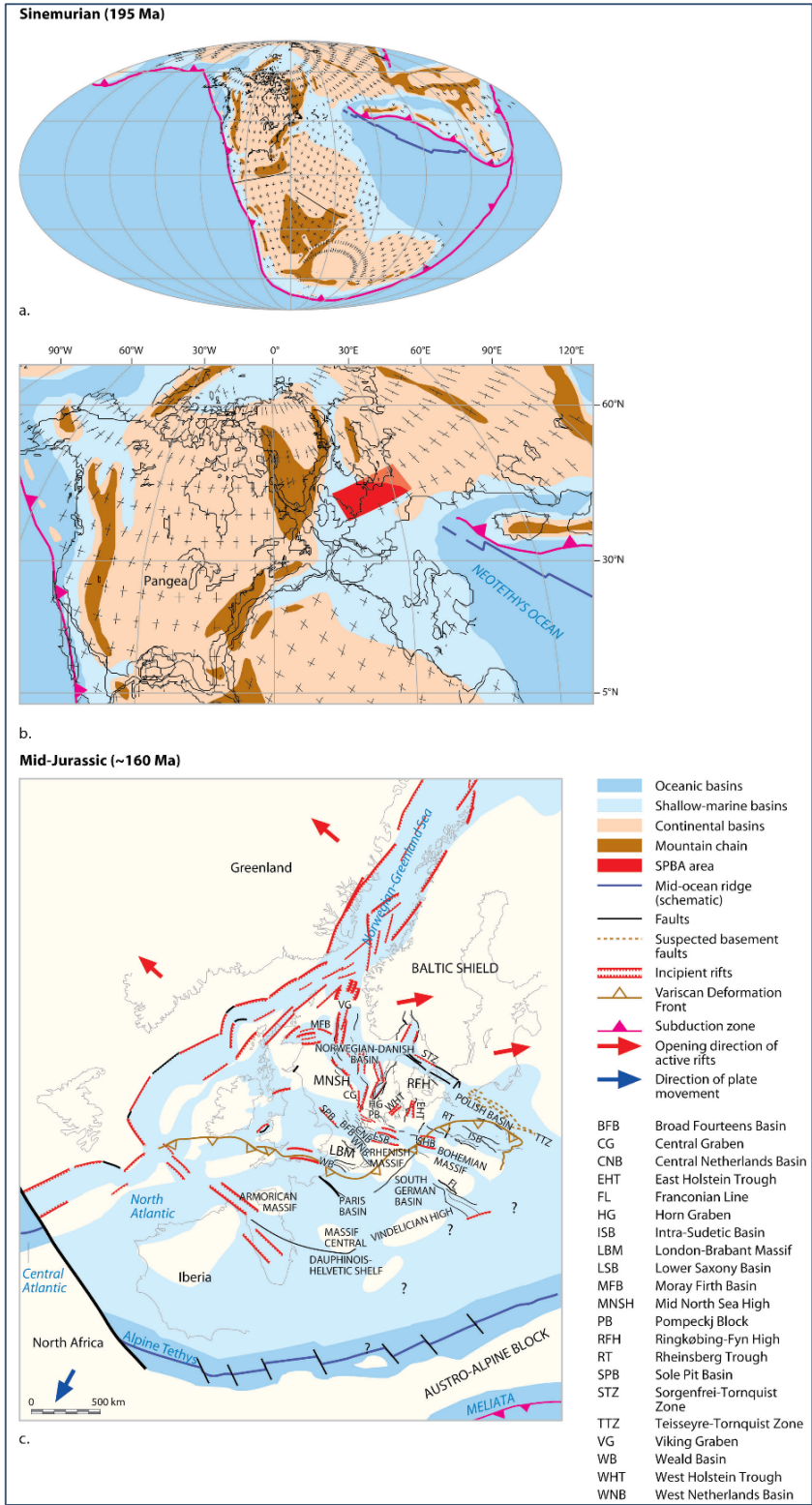


Figure 4. Early to Mid-Jurassic tectonic evolution: a) Paleogeographic world map for the Sinemurian (195 Ma); b) Detailed Sinemurian paleogeographic map; c) Structural overview map for the Mid-Jurassic (~160 Ma) (Pharaoh et al., 2010).

2.1.6 Middle Jurassic

At the end of the Aalenian the central North Sea area underwent extensive uplift, which continued throughout the Bajocian and Bathonian stages (Ziegler, 1990a; Surlyk & Ineson 2003). One theory that could explain this uplift is the impingement of a transient mantle plume (Underhill & Partington, 1993). This theory postulates a critical event in the Middle Jurassic that led to the development of a large thermal dome (700 x 1000 km) in the central North Sea area. This caused deep truncation of Lower Jurassic and even Triassic strata, leading to the formation of a stratigraphic hiatus, also known as the Mid-Cimmerian Unconformity. This caused blocking of the existing connection between the Arctic seas and the Tethys and Central Atlantic oceans (Ziegler, 1988; Ziegler, 1990a). During uplift of this thermal dome crustal extension continued across the North Sea rift system as indicated by 1) continued fault-controlled subsidence of the Viking Graben, 2) the subsidence of deep half-grabens containing continental deposits in the Central Graben, and 3) the ongoing tectonic activity in transtensional basins along the southern margin of the Southern Permian Basin (Ziegler, 1990a). At the end of the Middle Jurassic the thermal dome had sufficiently subsided and open-marine conditions returned in the southern North Sea.

While the northern part of the Southern Permian Basin was uplifted and subjected to erosion, the south experienced essentially continuous sedimentation (Pharaoh et al., 2010). In the areas uplifted during Mid-Jurassic times, sedimentation resumed variably during the Callovian or Late Jurassic (Ziegler 1990a).

Uplift also occurred in the London-Brabant Massif, resulting in the removal of Triassic and Upper Paleozoic strata, thereby exposing the underlying Lower Carboniferous and older Paleozoic rocks. Fission-track data suggest that a thickness of up to 3000 m of sediments was removed (Van den Haute & Vercoetere, 1990).

In the Dutch offshore the Mid-Cimmerian thermal doming event also led to widespread uplift and erosion (Ziegler, 1982; Ziegler, 1990a). The Step Graben and Terschelling Basin were eroded down to Lower Jurassic and Triassic strata, while in the north adjacent to the Dutch Central Graben the Cleaver Bank Platform was eroded by up to 2000 m with locally exposing the Carboniferous (Glennie, 1986; Pharaoh et al., 2010). The Step Graben and Terschelling Basin underwent subsidence later and at a slower rate than the Dutch Central Graben, resulting in thinner deposits of Sequence 1 during the Late Jurassic. This changed in the Late Cimmerian phase, during which renewed subsidence in the Terschelling Basin led to accumulations of Sequence 2 and 3 reaching a thickness of more than 2000 m. On the Elbow Spit High in well A17-01 even Devonian strata were exposed under Upper Cretaceous rocks. For the Mid North Sea High, Ringkøbing-Fyn High, and Schill Grund Platform, no data is available on erosion. During the Callovian, the central North Sea thermal dome began to subside and from then on rifting accelerated in the North Sea rift system including the Central Graben (Pharaoh et al., 2010).

Three major rift systems were active in the Netherlands during Mid to Late Jurassic times: 1) the N-S oriented Dutch Central Graben-Vlieland Basin system (including the Terschelling Basin), 2) the E-W oriented Lower Saxony Basin system extending into Germany, and 3) the NW-SE oriented block-

faulted transtensional system of the Ruhr Valley Graben, West and Central Netherlands Basins, and Broad Fourteens Basin, which extended into the Sole Pit Basin in the UK (Wong, 2007).

2.1.7 Late Jurassic to Early Cretaceous

During the Late Jurassic and Early Cretaceous, transtensional subsidence occurred of NW-SE oriented basins at the southern end of the North Sea rift system, and transpressional uplift of narrow highs along the southern margin of the Southern Permian Basin (Figure 5) (Pharaoh et al., 2010). During the transition towards the Late Cretaceous epoch, the North Sea rift became deactivated and thermal sag became the main control on subsidence throughout the rest of times (Ziegler, 1990a; Scheck-Wenderoth et al., 2008).

A eustatic sea-level lowstand at the Jurassic-Cretaceous transition, combined with stress-induced deflation of the lithosphere, led to earliest Cretaceous emergence and erosion of large parts of Western and Central Europe (Ziegler, 1990a). Across the North Sea rift system, crustal extension gradually decreased during the Early Cretaceous and essentially ended during the Aptian to Albian (Ziegler, 1990a; Torsvik et al., 2002; Coward et al., 2003).

The Late Cimmerian rift pulses in Late Jurassic to Early Cretaceous times led to the development of the main tectonic elements in the Dutch subsurface (Pharaoh et al., 2010). The Dutch Central Graben underwent E-W rifting, as extensional faulting and subsidence accelerated and progressed in time from north to south (Heybroek, 1975; Schroot 1991).

Upper Jurassic and Lower Cretaceous rocks in the graben are characterized by thick fluvio-lacustrine to shallow-marine sequences (Figure 6) (Pharaoh et al., 2010). In the northern part of the Central Graben, the Volgian to Ryazanian shales of the Kimmeridge Clay Formation are kerogenous (Herngreen & Wong, 1989). Uplift of the Cleaver Bank Platform-Broad Fourteens High during the Callovian provided the clastic sediments in the southern part of the graben. Simultaneously, adjacent highs such as the Friesland High also experienced uplift and erosion (Pharaoh et al., 2010). On the eastern flank of the Dutch Central Graben, a stable platform area was formed by the Schill Grund Platform.

Salt walls developed in the Dutch Central Graben, some of which along major bounding faults. Uplift of the Friesland Platform during the Late Jurassic caused erosion down to Lower Triassic and, locally, to Zechstein levels (TNO-NITG, 2004). Basin-controlling faults accommodated east-west extension as seen in the Central Graben. However, due to the complex reactivation history, unambiguous evidence of dextral transtensional displacement is only available locally, e.g. in the Rifgronden Fault Zone between the Terschelling Basin and the Schill Grund Platform (De Jager, 2007).

The uplift of structural highs such as the Elbow Spit Platform, Cleaverbank Platform, and Schill Grund Platform during the Callovian to Oxfordian time interval led to deposition of clastic sediments into the adjacent rapidly subsiding basins. During the Late Cimmerian rifting phase, the Zuidwal volcanic complex developed. Tectonic events in the Terschelling Basin and the Dutch Central Graben did take not place at the same time; uplift in the Terschelling Basin occurred before the end of the Mid-

Jurassic and a thick younger Upper Jurassic sequence covers the Triassic here, while the Lower Cretaceous sequence is thicker than in the Central Graben (Pharaoh et al., 2010).

The Cleaverbank Platform, Ameland Platform, and Schill Grund Platform were platforms during most of the Triassic to Early Jurassic times and were uplifted and eroded during the Mid- to Late Cimmerian rifting phases. Upper Jurassic and Lower Cretaceous syn-rift strata are missing from these highs, where thin post-rift Lower Cretaceous and thick Upper Cretaceous sequences unconformably cover the Triassic and Permian successions (De Jager, 2007). Estimations of the total amount of sediments removed from these highs reach up to hundreds of meters for Triassic to Middle Jurassic strata. The Rijnland Group (latest Ryazanian to Albian) succession, comprising mainly fine-grained clastics, was subsequently deposited across a large open-marine basin (Pharaoh et al., 2010).

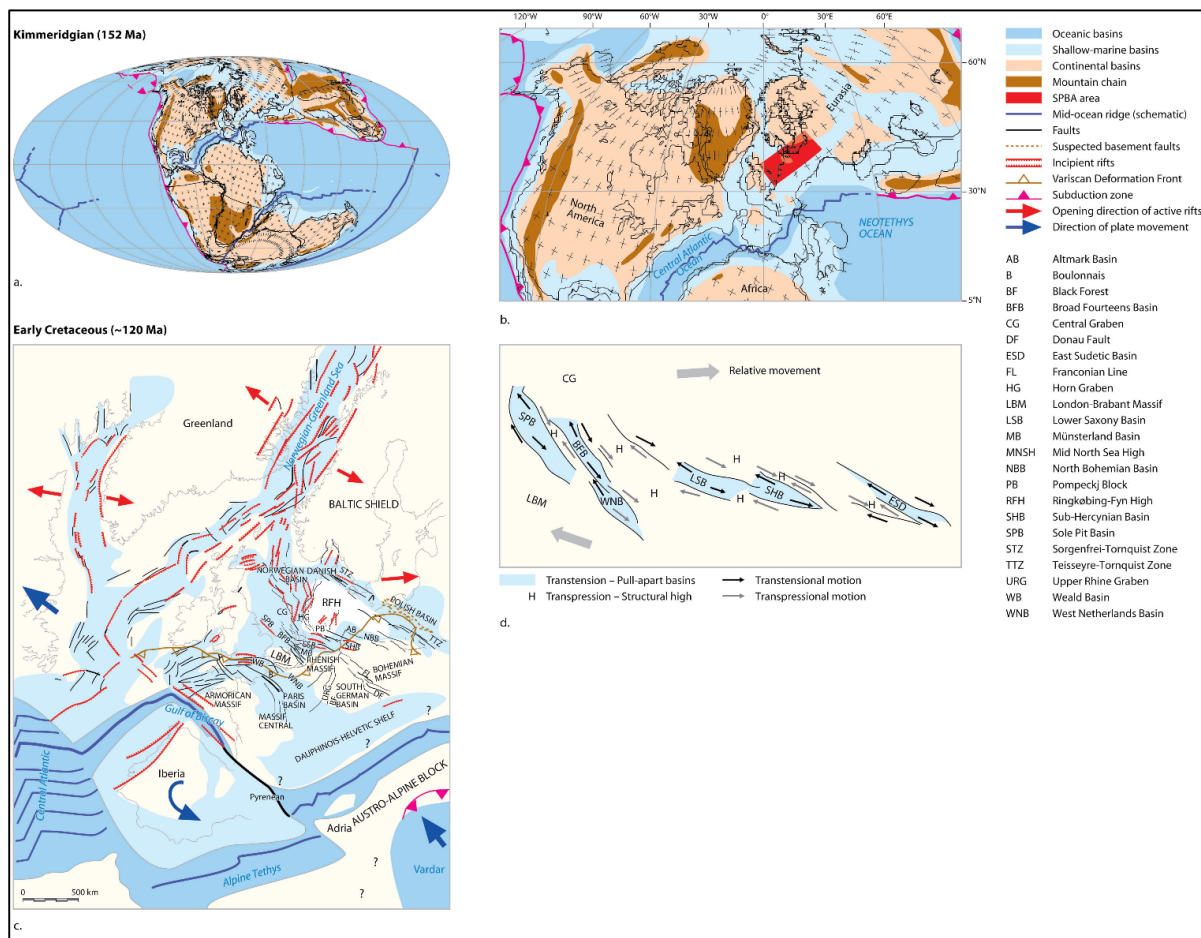


Figure 5. Late Jurassic – Early Cretaceous tectonic evolution: a) Paleogeographic map for the Kimmeridgian (152 Ma); b) Detailed Kimmeridgian paleogeographic map; c) Structural overview map for the Early Cretaceous (~120 Ma); d) Effect of transpression and transtension on the marginal basins (Pharaoh et al., 2010).

2.1.8 Mid- to Late Cretaceous

Crustal separation was completed in the North Atlantic at the end of the Early Cretaceous, while rifting started to concentrate on the area in the Norwegian and Greenland seas (Ziegler 1988; Ziegler, 1990a). Rifting in the Netherlands essentially stopped by this time. The Neo-Tethys Ocean opened to the south of Europe during the Mid-Cretaceous and started to close during the Late Cretaceous due to the convergence of the African and Eurasian plates (Ziegler, 1990a).

Regional thermal subsidence of the North Sea Basin started during the Hauterivian and Barremian in combination with gradually rising seas, and by Aptian to Albian times the Southern Permian Basin was a vast shallow-marine basin. Transgression and thermal subsidence occurred during the Albian to Turonian. During the Late Cretaceous the Southern Permian Basin further expanded to reach its maximum extent in response to thermal subsidence and sea-level rise to about 100-200 m above the present-day level. The Upper Cretaceous to Lower Paleocene (Danian) Chalk series is up to 2000 m thick in the basin (Ziegler, 1990a).

In the Southern Permian Basin inversion tectonics due to the Alpine orogeny affected basement blocks during the late Turonian and intensified during the Senonian and the Paleocene (Ziegler, 1990a). This inversion was heterogeneous with strain localized in narrow zones separated by undeformed regions (Pharaoh et al., 2010). Inversion also produced decoupling on Zechstein salt and thin-skinned tectonics. The NW trend of early inverted basins and transpressional fault reactivation indicates N-S to NE-SW oriented compressional stresses (Kley & Voigt, 2008).

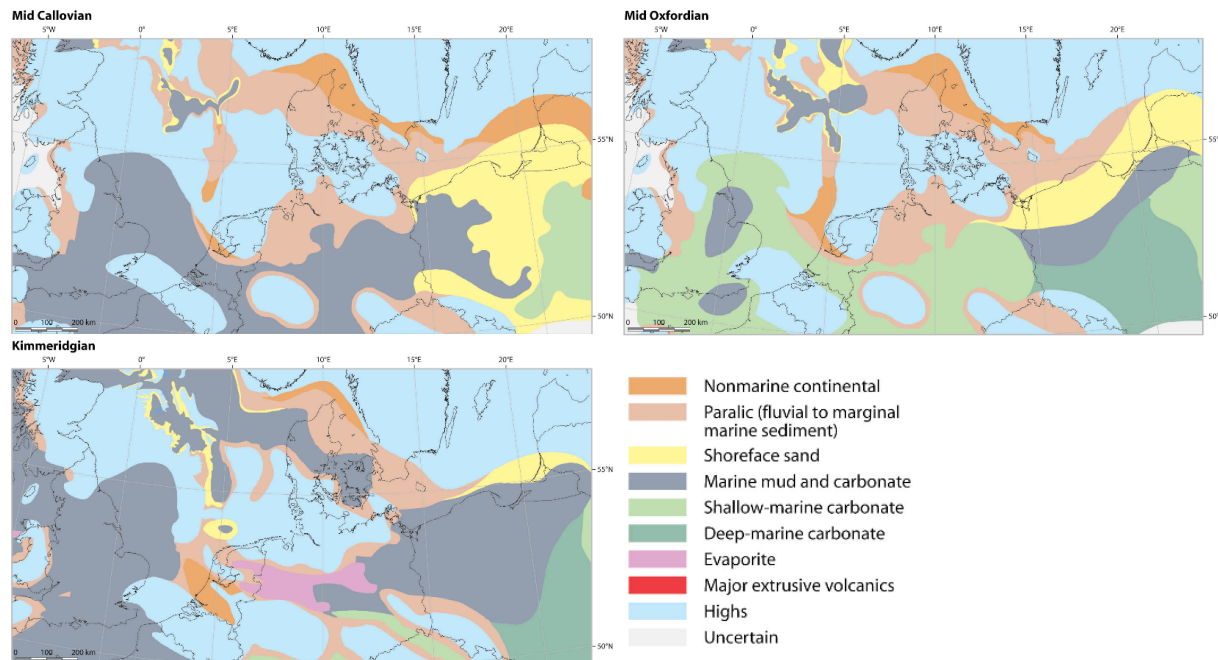


Figure 6. Paleogeographic evolution of the Netherlands during latest Mid-Jurassic to Late Jurassic times. (Lott et al., 2010).

2.2 Structural elements in the northern Dutch offshore

The overall structure of the subsurface in the Netherlands can be subdivided into smaller units called structural elements, which are named according to the structural style they represent. Recent updates and detailed mapping of the first structural elements map (Heybroek, 1974) was done by NAM & RGD (1980), Van Wijhe (1987), Duin et al. (2006), and Kombrink et al. (2012). Duin et al. (2006) described structural elements as “*regional structures with a uniform deformation history in terms of subsidence, faulting, uplift and erosion during a specific time interval*”. Three types of structural elements can be recognized in the northern Dutch offshore: basins (grabens), platforms, and highs. The term graben is applied to a basin bounded by major faults and containing sediments of at least Jurassic age (Duin et al., 2006; Kombrink et al., 2012). A high is an area that experienced significant non-deposition and erosion, resulting in deep truncation all the way down to Permian or even Carboniferous strata (Duin et al., 2006; Kombrink et al., 2012). When Lower and Upper Jurassic strata are absent due to Late Cretaceous uplift and erosion down to Triassic sequences, the term ‘platform’ is used (Duin et al., 2006; Kombrink et al., 2012). While basins accumulated thick syn-rift sequences, platforms and highs were uplifted and eroded during the Middle Jurassic and Early Cretaceous rifting phases (De Jager, 2007). Platforms are further subdivided into 1) areas where Cretaceous strata cover Triassic sediments, and 2) areas where Cretaceous rocks directly overlie Permian sediments (Duin et al., 2006; Kombrink et al., 2012). Because Jurassic basins in the Netherlands experienced differential inversion during the Late Cretaceous and Paleogene periods, they are further subdivided into 1) basins that underwent strong inversion and therefore lack Upper Cretaceous or older strata, and 2) basins that display a mild degree of inversion and contain Lower and Upper Cretaceous sequences (Figure 7) (Duin et al., 2006; Kombrink et al., 2012).

Most of the structural elements in the Dutch subsurface are bounded by fault systems that were formed by reactivation of existing Paleozoic faults in the Late Cimmerian rifting phase during Late Jurassic to Early Cretaceous times (De Jager, 2007). These Paleozoic faults were part of a large-scale NW-SE fault trend that possibly dates back to collision of the Laurentian with Avalonian plates, resulting in the formation of the Caledonian orogen (De Jager, 2007). The individual structural elements therefore reflect the complex history of deposition and subsequent deformation due to subsidence, faulting, uplift and erosion; a testimony to the different structural styles that play an essential role in the formation and development of the greater North Sea region. Below, a summary is presented of the structural elements in the northern Dutch offshore relevant for this study and in the updated version as published by Kombrink et al. (2012).

Dutch Central Graben

The Dutch Central Graben is situated between the Step Graben in the west, the Schill Grund Platform in the east, and the Terschelling Basin in the southeast. It forms the southernmost extent of the Mesozoic North Sea rift system, and is defined by major north-south trending faults, a product of large-scale rifting during Late Jurassic to Early Cretaceous times (De Jager, 2007). There are indications that as early as the Late Devonian epoch the structural low of the Dutch Central Graben was present as a sea-way connected with Laurussia (Ziegler, 1990a), and that the north-south structural outline of the graben was defined at the start of the Permian (Ter Borgh et al., 2015). In the Triassic period, movement

along the major boundary faults triggered the development of extensive salt walls along the flanks of the Mesozoic rift basins in the northern part of the offshore (De Jager, 2007). Differential subsidence in the graben was controlled by faults and led to formation thickness differences during the Early and Middle Jurassic (Figure 8) (De Jager, 2007). Especially Middle Jurassic sequences are thicker in the northern part of the Dutch Central Graben (Heybroek, 1975). Main rifting during the Late Jurassic to Early Cretaceous reached the northern part before propagating further towards the south, and thick fluvial to shallow-marine sediments accumulated within the graben, while the surrounding platforms and highs experienced uplift and erosion (De Jager, 2007). Inversion during the Late Cretaceous and Paleogene led to the complete removal of the overlying Cretaceous strata in some areas (Kombrink et al., 2012). Different development of parts of the Dutch Central Graben require a subdivision into roughly three sub-basins: the northern, middle, and southern Dutch Central Graben (Verreussel et al., 2014). These sub-basins display different facies and thicknesses for Upper Jurassic – Early Cretaceous formations.

Step Graben

The Step Graben sits adjacent to the eastern Dutch Central Graben and the western Elbow Spit and Cleaverbank platforms. It is named after its terrace-like (stepwise) structure consisting of tilted half-grabens, in which accommodation space was created locally and therefore resulted in irregular distribution of Late Jurassic sediments (Kombrink et al., 2012). Early Jurassic strata are absent due to uplift and erosion during the Mid-Cimmerian thermal uplift. The Step Graben experienced mild inversion during the Late Cretaceous (Kombrink et al., 2012).

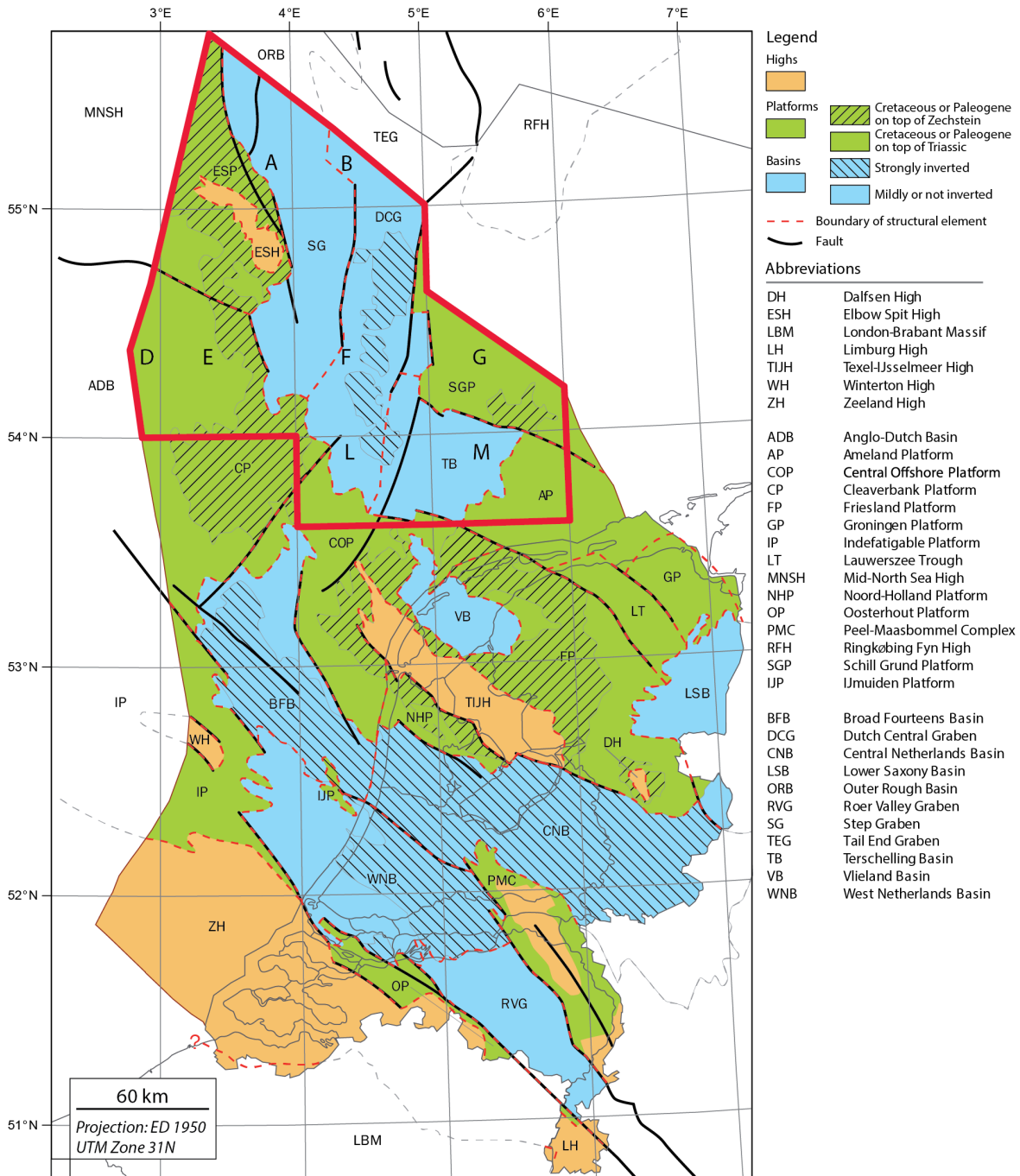


Figure 7. Late Jurassic – Early Cretaceous structural elements of the Netherlands. The study area is delineated in red, with relevant quadrants indicated with their corresponding letters. Different degrees of inversion are displayed within individual structural elements (Kombrink et al., 2012).

Terschelling Basin

The Terschelling Basin is confined by the Schill Grund Platform in the north, the Ameland Platform in the east, the Central Offshore Platform in the south, and the Dutch Central Graben in the west. Major faults form its boundaries: the ENE-WSW Rifgronden Fault in the north and the ENE-WSW Hantum Fault in the south. These pre-existing faults were reactivated as normal faults during the latest Jurassic. Like the Step Graben, the Mid-Cimmerian event caused uplift, which triggered erosion of Early

Jurassic and Triassic strata (De Jager, 2007). The Terschelling Basin subsided less and at later times than the Dutch Central Graben, resulting in a shallow basin with a thinner Upper Jurassic succession (De Jager et al., 2007). The Terschelling Basin underwent mild inversion, and Upper Cretaceous strata are still present (Kombrink et al., 2012).

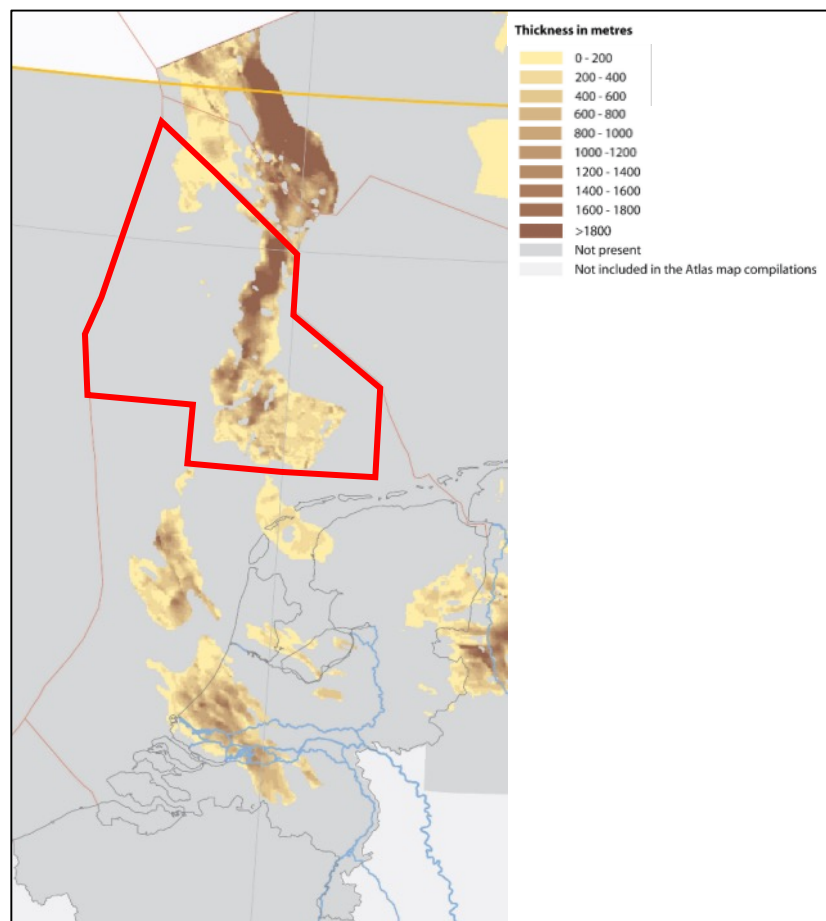


Figure 8. Thickness of the Upper Jurassic within the Southern Permian Basin as shown in the Dutch, German, and Danish offshore areas. Note the differences in thickness between the Dutch Central Graben and the Terschelling Basin. Thickness variations also exist within the Dutch Central Graben, which tends to thicken towards the north into the Danish Central Graben. The study area is delineated in red (Lott et al., 2010).

Ameland Platform

Similar to the Terschelling Basin across its western boundary, the Ameland Platform is sharply bounded by the Rifgronden and Hantum fault zones in the north and south, respectively. The Schill Grund Platform is located to the north, the Friesland Platform to the south. The Ameland Platform is characterized by Cretaceous and Cenozoic sediments directly overlying Triassic strata.

Cleaverbank Platform

The Cleaverbank Platform is bordered by the Elbow Spit Platform and the Step Graben in the north, the Dutch Central Graben and Central Offshore Platform in the east, and the Anglo-Dutch Basin in the south and the west. The northern boundary with the Elbow Spit Platform forms a poorly constrained contact, across which the Rotliegend and the Zechstein intervals display a sudden change in depth

(Kombrink et al., 2012). The southern boundary is delineated by a fault, which has a NE-SW orientation and extends from the Dutch Central Graben into the Broad Fourteens Basin.

Elbow Spit Platform and Elbow Spit High

Situated to the west of the Step Graben and to the north of the Cleaverbank Platform, the Elbow Spit Platform and Elbow Spit High form the southeastern extension of the Mid-North Sea High. The difference with the Elbow Spit High is that the Elbow Spit Platform contains not only Cretaceous sediments, but also Triassic strata covering Permian sequences in the south (Kombrink et al., 2012). Normal faults form the eastern boundary with the Step Graben. The depth of the Zechstein and Rotliegend increases significantly southward into the Cleaverbank Platform, although the boundary between both structural elements is poorly constrained (Kombrink et al., 2012).

The Elbow Spit High is characterized by an area with partly erosion or non-deposition of the Carboniferous, and where Lower and Upper Cretaceous sediments cover Devonian or Carboniferous strata. The Rotliegend is only partly present and very thin. Jurassic and Triassic successions are completely eroded due to thermal uplift triggered by the Mid-Cimmerian rifting event (Kombrink et al., 2012). Its buoyant structure is possibly explained by magmatic activity during the Late Devonian, which also generated similar features in the UK sector (Donato et al., 1983).

Schill Grund Platform

The Schill Grund Platform is bordered by the Dutch Central Graben in the west, the Terschelling Basin and the Ameland Platform in the south; both boundaries are delineated by faults. In the north and the east, the Schill Grund Platform extends into the Germany offshore area. Because Cretaceous sediments directly overlie Triassic and Permian strata, this structural element is characterized as a platform (Kombrink et al., 2012).

2.3 Stratigraphic framework

This section contains an overview of the current stratigraphy of the Upper Jurassic – Lower Cretaceous sequences, using the updated classification by Munsterman et al. (2012) for the northern Dutch offshore. Four groups characterize the Late Jurassic to Early Cretaceous time interval in the Netherlands: the Schieland, Scruff, Niedersachsen, and Rijnland groups. The Niedersachsen Group and the Delfland Subgroup (part of the Schieland Group) are absent in the study area and will therefore not be considered here. Out of the other three groups remaining, the Schieland and Scruff are the most important in this study. Both groups were deposited on top of the Lower to Middle Jurassic Altena Group, which consists primarily of marine argillaceous sediments with some intercalations of calcareous strata. The most important of these argillaceous units is the Posidonia Shale Formation source rock, its deposition triggered by basin-wide restricted circulation during the Toarcian stage (Lott et al., 2010).

Deposition of Upper Jurassic – Lower Cretaceous sediments in the basins and grabens was primarily controlled by the existing structural elements and their evolution through time. Subsequent uplift and erosion in the Late Cretaceous period due to inversion led to the removal of large parts of the Jurassic stratigraphic record in the northern Dutch offshore. Upper Jurassic – Lower Cretaceous sediments

therefore tend to be preserved primarily in the Dutch Central Graben and the Terschelling Basin (Figure 10, Figure 11).

In the central and northern North Sea, preservation of Upper Jurassic – Lower Cretaceous rocks is also highest in the areas defined by the grabens, where thicknesses of 3000 m are reached and with the top of the Upper Jurassic interval commonly situated between 2500 – 5000 m below sea level (Fraser et al., 2003). In the northern Dutch offshore, southern North Sea, thicknesses in the Dutch Central Graben may reach up to 2000 m for the Central Graben Subgroup, and the Scruff Group can reach a thickness of 2000 m in the Terschelling Basin.

Sequence 1

Sediments from Sequence 1 were deposited when rifting resumed during Mid-Callovia to Early Kimmeridgian times. E-W oriented rifting affected the Dutch Central Graben and the southwestern Broad Fourteens Basin. In the study area, these strata are referred to as the Central Graben Subgroup (part of the Schieland Group), consisting of the Lower Graben, Middle Graben, Upper Graben, Frieze Front, and Puzzle Hole formations. In the Broad Fourteens Basin, deposits from similar age are classified as the Delfland Subgroup.

Sequence 1 deposits are mostly non-marine and characterized by an alternation of sandstones, silty to argillaceous sandstones, with occasional intercalations of coal or calcareous layers that are restricted to the Dutch Central Graben and Terschelling Basin (Abbink et al., 2006; Munsterman et al., 2012).

Sequence 2

The Kimmeridgian stage signaled an important change in tectonic regime, in which the direction of rifting shifted from E-W to NE-SW (Zanella & Coward, 2003). This caused reactivation of pre-existing NW-SE oriented faults and structures, which triggered the opening of the surrounding basins (e.g. the Step Graben and Terschelling Basin). In the Dutch Central Graben, however, some areas experienced uplift and erosion, most of which occurred due to movement of salt. The removal of salt from rim synclines eventually creates turtle structures, whereas the addition of salt in other areas creates uplift due to formation of salt pillows that may develop into piercing salt diapirs. Abbink et al. (2006) referred to this interval as Sequence 2, which is characterized by siliciclastic sediments of the shallow- to open-marine Scruff Group. The peripheral basins contain deposits of both Sequence 2 and 3, with thicknesses of up to 2000 m in the Terschelling Basin (Munsterman et al., 2012).

Sequence 3

This phase marked the onset of flooding of adjacent platforms and highs such as the Schill Grund Platform and the Cleaver Bank Platform. Abbink et al. (2006) referred to this phase as Sequence 3, which consists of sediments deposited around the Jurassic-Cretaceous boundary. Sequences 2 and 3 are thicker in the peripheral basins (e.g. Terschelling Basin) than in the Dutch Central Graben, where Late Cretaceous inversion caused extensive uplift and erosion, particularly in the middle part of the graben.

Rifting essentially stopped in the Early Cretaceous at the beginning of the Valanginian (end of Ryazanian). While fault activity in the Central Graben area gradually ceased, thermal subsidence took over as dominant control on tectonics of the study area and the rest of the southern North Sea. Marine sandstones and shales of the Early Cretaceous Rijnland Group began to cover the grabens, platforms, and highs in the northern Dutch offshore. This phase is referred to as Sequence 4 and consists of the Vlieland Sandstone and Vlieland Claystone formations (Abbink et al., 2006). Sequence 4 will not be considered in this study.

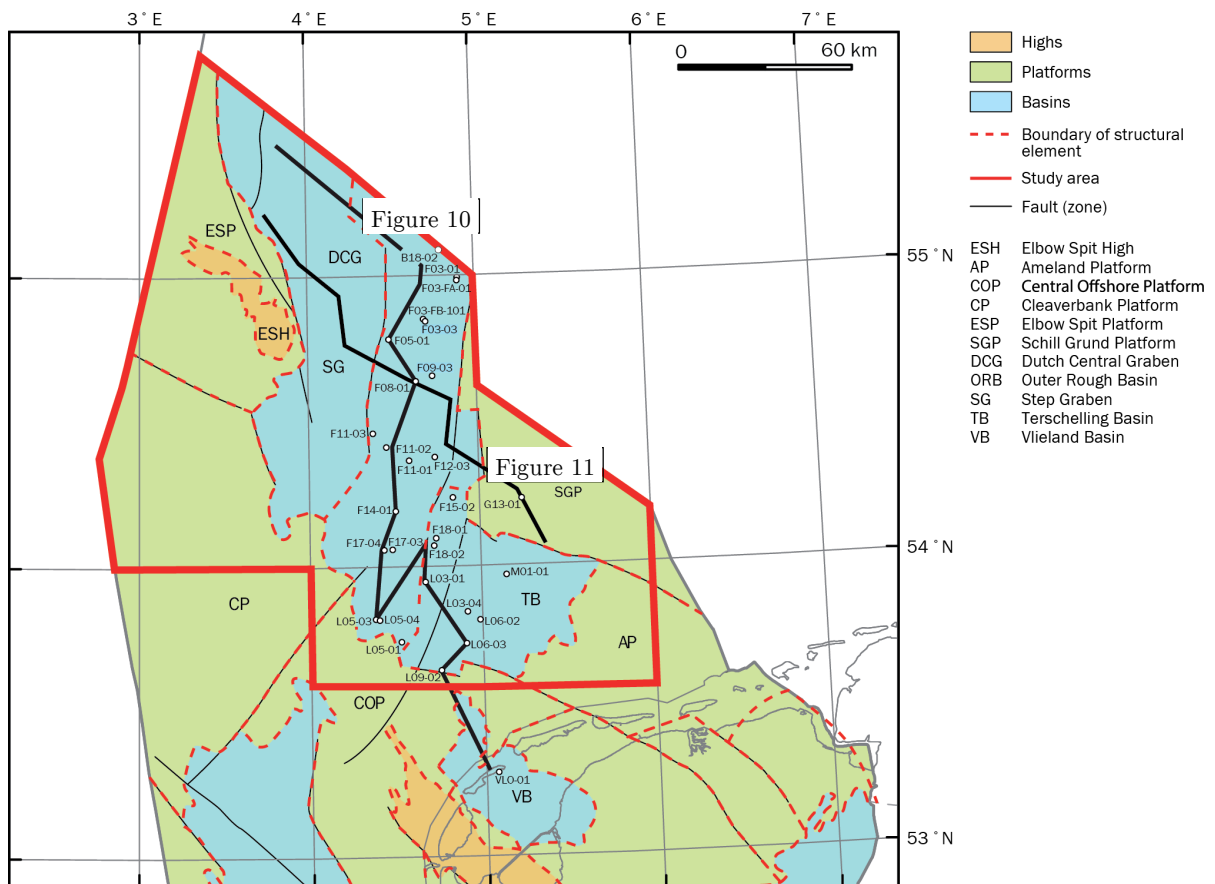


Figure 9. Map showing the lithostratigraphic cross-sections of Figure 10 and Figure 11 with the Mesozoic structural elements as updated by Kombrink et al. (2012).

2.4 Updated Upper Jurassic – Lower Cretaceous lithostratigraphy and correlation with the UK and Danish sections of the Central Graben (Munsterman et al., 2012)

What follows is an overview of the revised lithostratigraphy and depositional environments as performed by Munsterman et al. (2012). In addition, if possible, formations are correlated with equivalent units in the UK and Danish sections of the Central Graben in the southern North Sea. Due to a lack of publicly available information, no correlation was possible with the German sector of the southern North Sea, also known as the Entenschnabel. A description is given of the individual lithostratigraphic units, which are organized according to the sequence they belong to. Abbreviations are given next to the unit names.

Visualizations of the lithostratigraphic overview, along with the correlations across other sections of the Central Graben, can be seen in Figure 12. Cross-sections across the Central Graben are shown in Figure 14, Figure 15, and Figure 16. For detailed time slices showing the distribution of facies in the northern Dutch offshore through time, see Appendix B.

2.4.1 Sequence 1

- **Central Graben Subgroup (SLC)**
 - **Lithology:** mainly non-marine sediments consisting of claystones, silty to argillaceous sandstones. Presence of intercalations of distinct coal layers or calcareous layers.
 - **Distribution:** mainly developed in the Dutch Central Graben. The youngest part of the subgroup (uppermost Friese Front Formation) is not only present in the southernmost part of the Central Graben, but also in the Terschelling Basin.
 - **Depositional environment:** mostly non-marine coastal to delta plain deposits, with intermittent marine sediments, deposited during transgressions.

- **Lower Graben Formation (SLCL)**
 - **Lithology:** the formation is characterized by greyish brown, very fine to fine-grained, well-sorted sandstones, occurring in beds generally less than 10 m thick, with intercalations of thin greyish brown silty to sandy claystones. The formation is overall carbonaceous, although some distinct coal layers exist. The individual sandstone layers show a restricted lateral extent.
 - **Distribution:** the formation is restricted to the northern-central part of the Dutch Central Graben. Its thickness varies widely: 40-562 m, with the thickest accumulation in the fault-bounded southwestern corner of block F03.
 - **Depositional environment:** fluvio-deltaic and coastal plain.
 - **Correlation:** strata with equivalent lithology are found in the Danish part of the Central Graben and are referred to as the Bryne Formation (Herngreen & Wong, 1989; Michelsen & Wong, 1991; Michelsen et al., 2003).

- **Middle Graben Formation (SLCM)**
 - **Lithology:** grey, locally very silty, carbonaceous claystones. In the northern part of the F-quadrant one thick or locally two sandstone beds may be intercalated. At the base of the formation three thin but distinct coal seams occur. These coal layers are laterally extensive and form important lithostratigraphic markers.
 - **Distribution:** area of distribution is smaller than the Lower Graben Formation: in the northern and central parts of the Dutch Central Graben.
 - **Depositional environment:** lacustrine to marginal marine embayment.
 - **Correlation:** the Middle Graben Formation is also present in the Danish Central Graben, where it bears the same name.

- **Upper Graben Formation (SLCU)**
 - **Lithology:** the formation consists of two units of greyish brown, fine-grained, carbonaceous sandstones, separated by a silty clay succession.
 - **Distribution:** the formation is present in the northern part of the Dutch Central Graben. The general depositional trend is N-S directed.
 - **Depositional environment:** marginal marine barrier-island system.
 - **Correlation:** direct correlation is not possible. However, in the Danish Central Graben, the younger Lulu Formation is equivalent in lithology and was deposited in a similar setting. A time-equivalent unit is the Danish Lola Formation, which was deposited during Early Oxfordian to Late Kimmeridgian times and consists of dark olive-grey to grey claystones, with organic material of mainly terrestrial origin (Michelsen et al., 2003). This overlaps the time of deposition of the Upper Graben Formation (Late Oxfordian). The depositional setting of the Lola Formation was a low energy, offshore open-marine environment, and likely reflects the deeper part of the Central Graben with respect of the Dutch Central Graben at the time.

- **Puzzle Hole Formation (SLCP)**
 - **Lithology:** light brownish-grey carbonaceous claystones with intercalations of siltstones, thin sandstones, and frequent coal seams (10-20 seams per 100 m interval). The sandstones, particularly in the south, show a fining-upward character.
 - **Distribution:** deposition of the Puzzle Hole Formation is in the central part of the Dutch Central Graben, the southern parts of blocks F05 and F06, and blocks F08, F09, F11, F12, and F14.
 - **Depositional environment:** lower delta plain; lagoonal tidal flats, estuary and tidal channels, bay head deltas and mouthbars.
 - **Correlation:** no direct correlation possible with other countries. To the north, the formation grades into the marginal marine Upper Graben Formation at the southern margin of blocks F05-F08 (Herngreen & Wong, 1989). The formation can therefore be considered a (partial) time-equivalent unit of the Upper Graben Formation and open-marine the Lola Formation.

- **Friese Front Formation (SLCF)**
 - **Lithology:** alternating claystones, siltstones, sandstones, and minor coal. The siltstones and claystones vary in color but are mostly grey and becoming increasingly red towards the south in the L blocks. Siderite spherulites and concretions are common. The sands have been described as sheets, isolated, and amalgamated channels (Van Adrichem Boogaert & Kouwe, 1993-1997).
 - **Distribution:** the Friese Front Formation is present in the southern part of the southern Dutch Central Graben and Terschelling Basin. The upper part of the formation intercalates with the marine Scruff Group.
 - **Depositional environment:** non-marine (coastal) delta plain to lagoonal deposits.
 - **Correlation:** the formation is a time-equivalent of the Lower, Middle Graben, and the Puzzle Hole formations in the northern part of the Central Graben. It is therefore also a time-equivalent of the shallow-marine to paralic Lulu and open-marine Lola formations in the Danish Central Graben.

- **Friese Front Formation – Rifgronden Member (SLCFR)**
 - **Lithology:** dark-grey, carbonaceous, locally silty to sandy claystone, with thin intercalated beds of well-sorted, very fine to fine-grained sandstone, dolomite and coal.
 - **Distribution:** the Rifgronden Member is restricted to the southern Dutch Central Graben (blocks F17-L05).
 - **Depositional environment:** lagoonal.
 - **Correlation:** this member is time-equivalent of the lowermost part of the Middle Graben Formation and the uppermost part of the Lower Graben Formation to the north. It is also time-equivalent to the Middle Graben, Lulu and Bryne formations in the Danish Central Graben.

2.4.2 Sequence 2

- **Scruff Group (SG)**
 - **Lithology:** this group of formations consists of a succession of locally bituminous claystones with thin intercalated carbonate beds, and fine- to coarse-grained sandstone, which contain glauconite and are sometimes argillaceous.
 - **Distribution:** presence in the Step Graben, Central Graben, Schill Grund Platform, Terschelling Basin and in the northern part of the Vlieland Basin.
 - **Depositional environment:** Late Jurassic to earliest Cretaceous marine environments, from restricted (lagoonal) to open-marine (outer shelf) conditions.

- **Kimmeridge Clay Formation (SGKI)**
 - **Lithology:** olive-grey, generally silty claystones with thin streaks of dolomite. Dolomite presence increases to the north, while in the south the claystones become increasingly silty to sandy and the carbonate streaks and olive color disappear gradually.

- **Distribution:** occurrence of the formation is restricted to the northern part of the Central Graben and locally to the Step Graben. It is associated with a transgression from north to south.
 - **Depositional environment:** outer shelf setting. Dolomitic beds and structureless organic matter (SOM) indicate times of decreased clastic input and stagnant water conditions with a stratified water column. The higher frequency of dolomitic beds and SOM in the north reflects a slightly deeper environment.
 - **Correlation:** direct correlation of the Kimmeridge Clay Formation is possible with other countries in the Central Graben: in the UK sector, it bears the same name; in the Danish Central Graben, its lithological equivalents are the open-marine Lola and Farsund formations; the Norwegian lithological equivalent is the Mandal Formation (Michelsen & Wong, 1991).
- **Skylge Formation (SGSK)**
 - **Lithology:** alternating slightly silty to sandy claystones, argillaceous and/or non-argillaceous glauconitic sandstones. Sediments are often bioturbated. Local presence of pyrite, lignite, and/or shell fragments.
 - **Distribution:** presence at the fringes of the Central Graben, the Terschelling and Vlieland basins.
 - **Depositional environment:** restricted to shallow marine conditions.
 - **Correlation:** direct correlation of the formation is not possible. However, individual members do have time- and lithological equivalents. The Danish Heno Formation consists of the Gert and Ravn members, which are equivalent in time and lithology to the Terschelling and Noordvaarder members, respectively. The Gert Member was deposited in a back-barrier and marine shoreface environment, which is similar to the Terschelling Member. Sediments of the Ravn Member were deposited in a marine shoreface environment, which is similar to the Noordvaarder Member. In the northern part of the Central Graben the open-marine Kimmeridge Clay Formation is the time-equivalent of the restricted to shallow marine Skylge Formation. It is also time-equivalent to the Danish Lola and Farsund formations, the UK Kimmeridge Clay Formation, and the Norwegian Mandal Formation.
- **Skylge Formation – Oyster Ground Member (SGSKO)**
 - **Lithology:** brown-grey claystones, sometimes slightly silty. Some limestone beds are found. Thick sand beds, characteristic for the main Friese Front Formation, are absent. Along the basin margins the lithology may change into a sandier subfacies, like in the southern Terschelling Basin. The member is different from the Kimmeridge Clay Formation due to its marginal marine depositional environment and geographical setting.
 - **Distribution:** presence of the member is restricted to the southern Dutch Central Graben and Terschelling Basin.
 - **Depositional environment:** lithology, fossils, lignite, and regional paleogeography indicate restricted lagoon-like conditions with washover deposits.

- **Skylge Formation – Terschelling Sandstone Member (SGSKT)**
 - **Lithology:** fine- to medium-grained sandstone (occasionally up to coarse sand and gravel), well to poorly sorted. Carbonate cement, glauconite, and lignite are common. Deposition primarily in the form of sheets and channels, separated by thin intervals of claystones.
 - **Distribution:** deposition in the Terschelling Basin and the southeastern part of the Dutch Central Graben.
 - **Depositional environment:** barrier island complex, including shoreface to foreshore and washover fans, protecting the restricted marine (lagoonal) setting of the Oyster Ground Member.

- **Skylge Formation – Noordvaarder Member (SGSKN)**
 - **Lithology:** well-sorted, greenish-grey, slightly argillaceous, occasionally calcite cemented, glauconitic sandstones. Presence of bioturbation, local pyrite, lignite, and shell debris.
 - **Distribution:** member found at the fringes of the Central Graben and in the northwestern Terschelling Basin.
 - **Depositional environment:** shallow marine, ranging from offshore to lower shoreface.

- **Skylge Formation – Lies Member (SGSKL)**
 - **Lithology:** bioturbated silty to sandy claystones, with locally containing glauconite, pyrite, and carbonate streaks.
 - **Distribution:** deposition in the Terschelling and Vlieland basins, and in the southeastern part of the Dutch Central Graben.
 - **Depositional environment:** deposition in an offshore-shelf environment.

2.4.3 Sequence 3

- **Scruff Greensand Formation (SGGS)**
 - **Lithology:** grey-green fine-grained sandstones that have often undergone intense bioturbation. Glauconite content is high and spiculites are locally abundant at the base of the formation. The sandstones can be slightly argillaceous and/or calcareous.
 - **Distribution:** discontinuous presence in the Central Graben, Schill Grund Platform, Step Graben, and Terschelling Basin. In the northern part of the Dutch Central Graben the formation covers the salt dome of the F03-Fa field, where it forms a gas reservoir. The middle part of the Dutch Central Graben contains no well-developed sand successions. However, along the fringes of the graben, local sections of sand are observed.
 - **Depositional environment:** deposition in a near coastal and shoreface to offshore setting.

- **Correlation:** the Scruff Greensand Formation is roughly time-equivalent to the ‘hot’ shale Bo Member, which is present in the Danish Central Graben. The shaly Bo Member corresponds to the deeper part of the basin, whereas the sandy Scruff Greensand Formation represents the relatively shallower edge with more sand input. The British sector of the Central Graben contains the Fulmar Formation, which consists of offshore to shelf deposited sands, the deposition of which took place as a reaction due to salt movement. This environment and mechanisms of deposition of the Fulmar Formation are remarkably similar to the Scruff Greensand.
- **Scruff Greensand Formation – Scruff Spiculite Member (SGGSP)**
 - **Lithology:** light green-grey, fine-grained, glauconitic, and slightly argillaceous intensely bioturbated sandstones. No primary sedimentary structures. The bulk of the framework is made up of spicules, which are skeletal remains of sponges, thus forming a bioclastic sandstone.
 - **Distribution:** developed in the southern Dutch Central Graben and in the Terschelling Basin.
 - **Depositional environment:** near coastal deposition in a shoreface environment. Facies change laterally from relatively clean ‘bioclastic’ sandstone to an argillaceous sandstone reflecting the position of the depositional area on the basin floor topography (Abbink et al., 2006). This resembles a semi-enclosed shallow marine environment.
- **Scruff Greensand Formation – Stortemelk Member (SGGSS)**
 - **Lithology:** fine- to very fine-grained, argillaceous sandstones with intense bioturbation. The sands are often slightly calcareous, glauconitic, with thin streaks of lignite. Cores show some intercalations of up to coarse, glauconitic, and sometimes argillaceous sandstone.
 - **Distribution:** the Stortemelk Member is found in the southern Dutch Central Graben and in the Terschelling Basin. In the north it shales out into the Schill Grund Member.
 - **Depositional environment:** shoreface to offshore setting.
- **Lutine Formation (SGLU)**
 - **Lithology:** in the northern part of the Dutch Central Graben the formation is characterized by grey-brown to black bituminous claystones (Clay Deep Member). South of blocks F11/F12 the color changes into olive-grey to grey-brown and the clays become more silty to very fine sandy and less bituminous (Schill Grund Member).
 - **Distribution:** widely present in the Central Graben, Step Graben, Schill Grund Platform, and Terschelling Basin.
 - **Depositional environment:** stagnation of basin circulation in the northernmost part of the basin resulted in dysoxic to anoxyic basin-floor conditions and in the deposition and preservation of bituminous claystones. The southern part of the basin is characterized by relatively shallower, open-marine conditions with (near) normal basin-floor ventilation. This led to deposition of more finely sandy to silty, slightly bituminous claystones.

- **Correlation:** in the Danish sector of the Central Graben, the lithological and time-equivalent of the Lutine Formation is the Bo Member of the Farsund Formation. The Bo Member correlates especially well with the Clay Deep Member. In the Norwegian sector, the lithological and time-equivalent is the Mandal Formation (Michelsen & Wong, 1991).
- **Lutine Formation – Clay Deep Member (SGLUC)**
 - **Lithology:** grey-brown to black bituminous claystones. The base of the interval is usually siltier.
 - **Distribution:** deposition restricted to the northern part of the Dutch Central Graben and Step Graben. The organic matter decreases to the south, where the member grades into the Schill Grund Member.
 - **Depositional environment:** shelf environment. Stagnation of basin circulation triggered dysoxic to anoxic basin-floor conditions, resulting in deposition of bituminous claystones.
- **Lutine Formation – Schill Grund Member (SGLUS)**
 - **Lithology:** olive-grey to grey-brown claystones. The claystones are non- to slightly calcareous, silty to very fine sandy, locally slightly bituminous, micaceous, and pyritic.
 - **Distribution:** limited to the southern part of the Dutch Central Graben, Schill Grund Platform and Terschelling Basin. The member is partially a lateral time equivalent of the Stortemelk Member along the southern margin of the Central Graben.
 - **Depositional environment:** open-marine shelf conditions. The slightly or non-bituminous nature of the sediments indicate conditions reflecting a nearly oxygenated basin-floor.

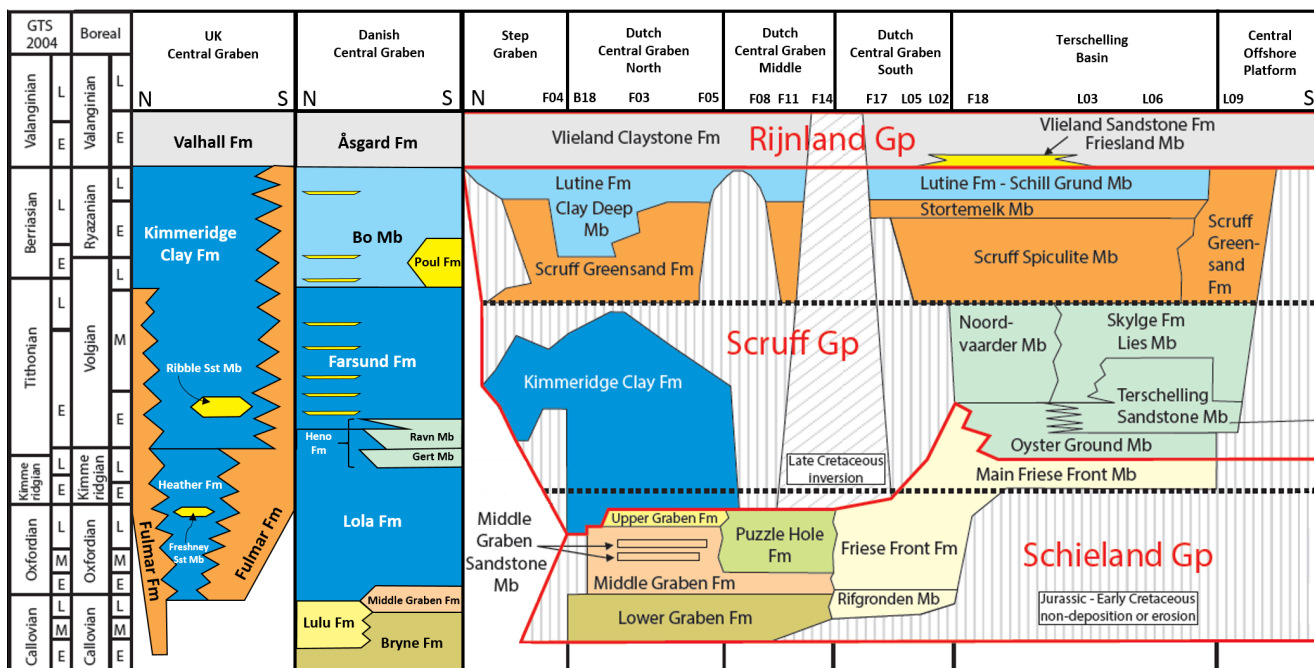


Figure 12. North-south oriented Upper Jurassic to Lower Cretaceous lithostratigraphy and correlation with the UK and Danish sectors of the Central Graben. Equivalent colors indicate a comparable lithology due to corresponding depositional environments (after Michelsen et al., 2003; Johnson et al., 2005; Munsterman et al., 2012).

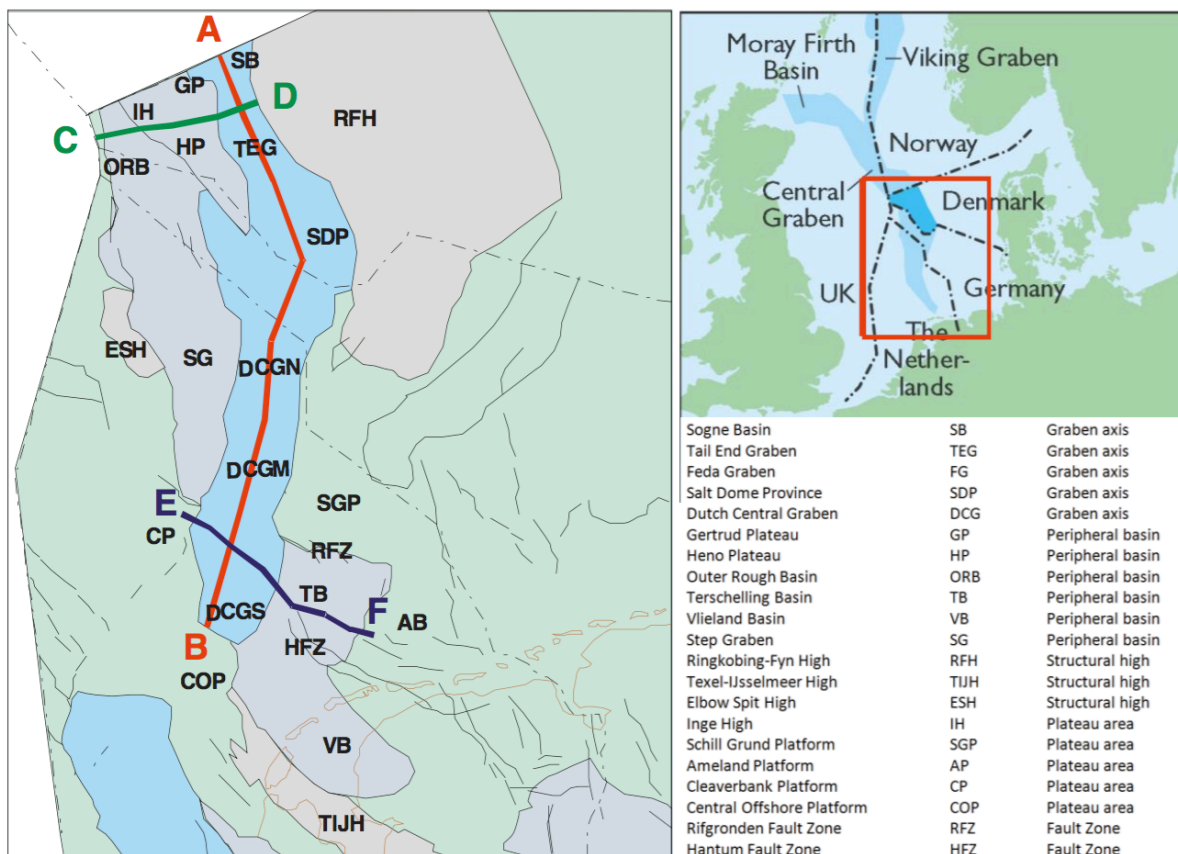


Figure 13. Map showing the Danish, German, and Dutch sectors of the Central Graben system. Three cross-sections are indicated, with A-B along the graben axis, C-D across the peripheral basins and the Tail End Graben in Denmark, and E-F across the Dutch Central Graben South and the Terschelling Basin. The graben axis is colored in blue, the peripheral basins are colored in greyish-blue, the platform areas are in green, and the structural highs are in greyish orange (Verreussel et al., 2014).

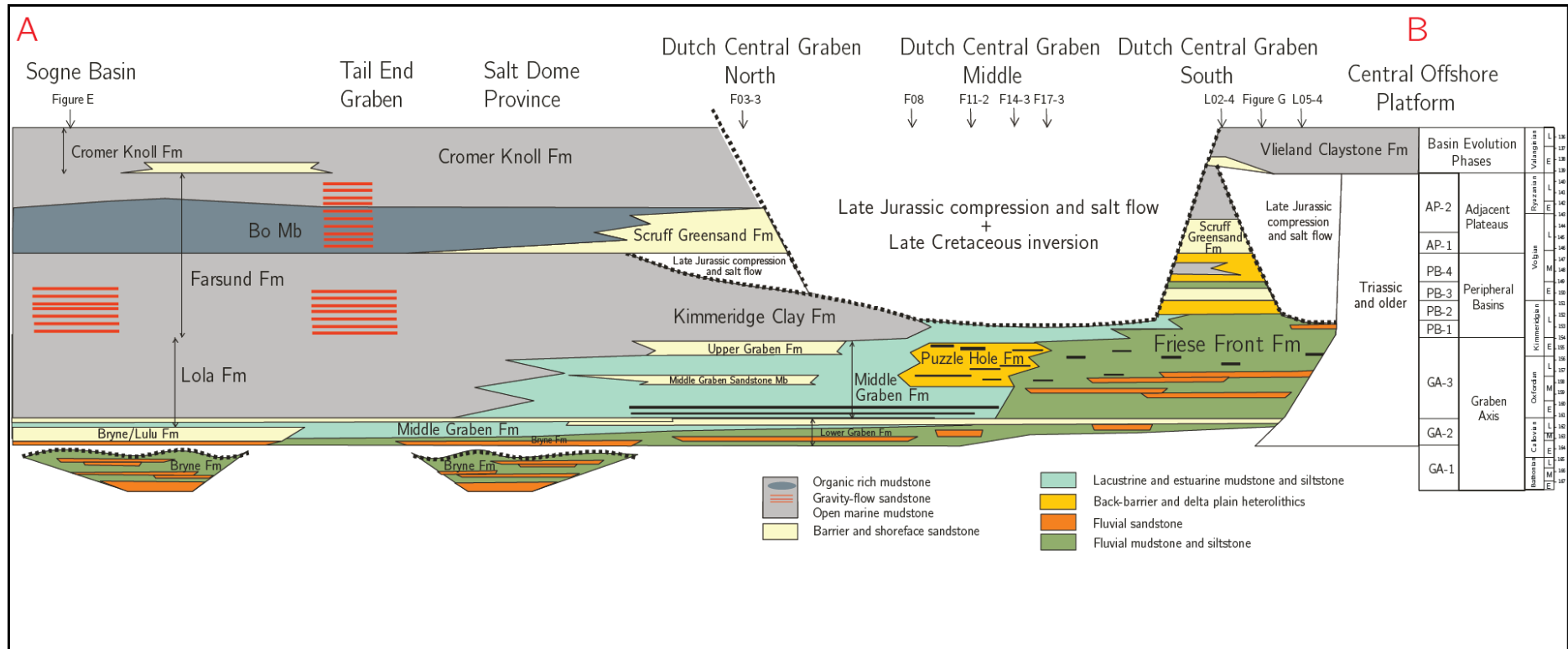


Figure 14. Cross-section A-B with a roughly N-S orientation along the graben axis from the Danish sector towards the Dutch sector. The trend in facies development towards continental settings is clearly visible from north to south (after Verreussel et al., 2014).

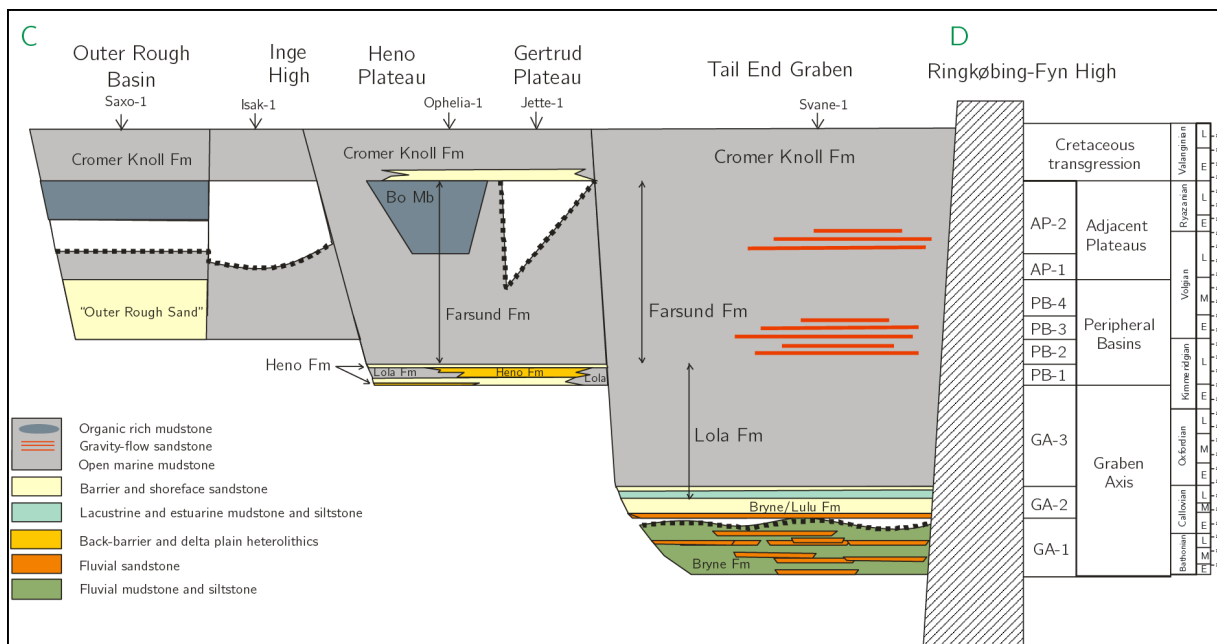


Figure 15. Cross-section C-D with a W-E orientation from the Outer Rough Basin across the graben axis up to the Ringkøbing-Fyn High showing the basin evolution and facies distribution (after Verreussel et al., 2014).

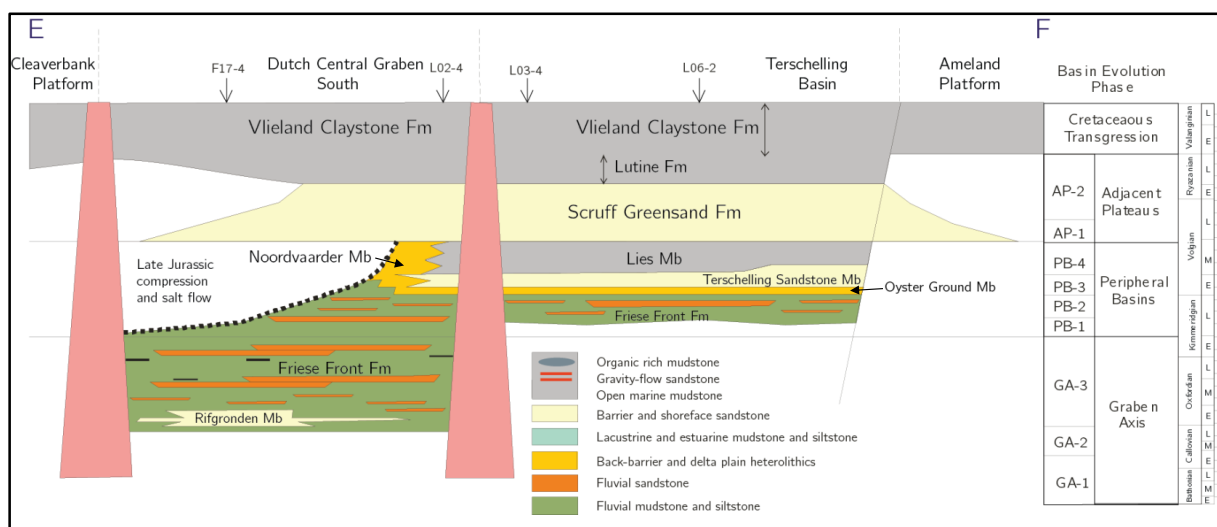


Figure 16. Cross-section E-F oriented NW-SE from the Dutch Central Graben South to the Terschelling Basin (after Verreussel et al., 2014).

3. Methods

This section provides an overview of the available data and the analytical techniques used to arrive to the final results. For individual results per well, see Appendix A.

3.1 Database

All well and core analysis data were derived from NLOG, a website containing all publicly available data on the Dutch subsurface and a joint project between TNO and the Ministry of Economic Affairs of the Netherlands. With collaboration of TNO, a database was constructed containing all publicly available core analysis data from the Dutch subsurface. The database was then narrowed down to a total of 45 exploration, appraisal, and production wells containing 4066 plug sample measurements taken in cores from Upper Jurassic and Lower Cretaceous rocks in the northern Dutch offshore, notably from quadrants A, B, D, E, F, G, L (blocks 01-09), and M (blocks 01-09) (Table 1, Figure 17, Figure 18). Combined length of all cores amounted to 1426 m. Typical data on plug samples contained measurements on porosity, permeability (horizontal and vertical), density, and the coordinates of the well and core. The database was further extended by including data on variables such as borehole name, analysis number, depth along hole, true vertical depth (using deviation data), lithostratigraphic unit (group, formation, member).

The plug sample database was then imported into Spotfire (EBN in-house software) to allow for practical visualization of the data. Using different filters, continuous immediate visualization of the data was possible, resulting in identification of trends and outliers on the spot. Spatial information on fields and structural elements were added to Spotfire to assist in analyzing trends within these features. Furthermore, using the available core analysis reports from the various operators, facies data was extracted and added to the database, resulting in a link between plug sample data and environment of deposition. Specifically, core data from wells within fields were analyzed to identify the favorable circumstances allowing for good reservoir rock (Table 2).

Additional information from NLOG on the cored intervals was studied, the material of which consisted of analyzing composite logs, mud logs, and sedimentological, petrophysical and petrographical reports containing thin-sections and electron microscope photos. As this study considered only the properties of reservoir rocks, volume-specific parameters such as the net-to-gross ratio were not taken into account.

Porosity can be measured and defined differently by using various methods. In this study, when referring to porosity, only effective porosity is considered, which includes the void space of all interconnected pores using an oven-dried analysis and helium to saturate the sample. This means that isolated pores and intragranular porosity were not considered. When referring to permeability, only horizontal permeability is considered.

Although porosity can always be measured accurately, measuring permeability is far from perfect, especially in samples with poor reservoir quality. Plug samples with poor reservoir quality generally have a poor permeability that cannot be measured accurately, as the lower boundary of the measuring

device, the detection limit, is reached. This significantly distorts subsequent statistical calculations, and therefore these measurements were not included in the statistical analysis. This resulted in the removal of all measurements with a permeability of <0.1 millidarcy (mD), as well as detection limit values of 0.3, 0.304, 0.4 and 0.5 mD.

One of the problems with using the depth in core data is that differences may arise between the depth at which the logs were taken (logger's depth) and the depth at which the core was originally drilled (driller's depth). Depth from wireline logging is generally considered more reliable than driller's depth. This difference can normally be adjusted for by matching the core log with a wireline log, also known as a 'core shift', which is especially useful when the focus is on relatively small-scale differences. This depth shift generally accounts for a relatively small (2 – 3 m) change in depth, which are values in the order of magnitude that are not significant in the regional scope of this study. The choice was therefore made to exclude this procedure. However, in order to identify possible outliers in the data resulting e.g. from a core taken on the transition between two contrasting layers, an extra feature was built in by adding two columns to the database denoting 1) the depth below the top of the formation, and 2) the depth above the bottom of the formation. This allowed for relative simple and straightforward identification of plug samples that were taken from depths close to the boundary separating two different lithostratigraphic units, as resulted by e.g. a core-depth shift.

Table 1. Characteristics of wells used in this project. An overview is given of the cored formations (up to member level if possible), core length, and depth interval. If applicable, the corresponding field is specified. Measured Depth (MD) refers to depth along hole; True Vertical Depth (TVD) refers to depth below Kelly Bushing. The rightmost column specifies whether the plug samples were taken from a dry (water-bearing) interval, or from a hydrocarbon-bearing interval within an existing field.

Quadrant	Well	Cored Formation	Cored Member	Number of Plugs	Core Length (m MD)	Depth Interval (m TVD)	Cored Interval Dry or in Field
B	B13-02	SGSK	SGSKN	35	8.8	2266.7 - 2275.5	Dry
	B14-01	SGKI		61	17.9	2207.5 - 2225.3	Dry
	B18-03	SGGS		48	15.8	2412.1 - 2427.9	Dry
F	F02-01-S1	SLCL		83	29.8	3166.8 - 3196.6	F03-FB
	F03-01	SGGS		36	10.5	2359.8 - 2370.3	F03-FA
	F03-04	SLCU		53	17.3	2902.7 - 2919.9	F03-FA
	F03-05-S1	SLCL		57	20.4	2755.1 - 2775.5	Dry
	F03-06	SLCL		416	134.1	3167.1 - 3300.8	F03-FB
	F03-07	SGGS		359	113.9	3156.1 - 3269.7	F03-FB
	F03-08	SLCM		73	18.8	2476.5 - 2495.3	F03-FC
	F03-FB-101	SLCL		18	5.1	2920.9 - 2925.9	Dry
	F03-FB-105-S3	SLCM	SLCMS	33	14.1	2835.6 - 2849.7	F03-FA
	F03-FB-107	SGKI		116	26.7	3105.5 - 3132.1	F03-FB
	F06-01	SLCM		66	14.3	2952.8 - 2964.4	F03-FB
	F11-01	SLCL		17	4.3	2542.3 - 2546.4	Dry
	F15-02-S1	SGGS	SGGSP	201	62.9	2546.7 - 2606.0	F03-FB
	F15-06	SLCF		14	8.9	3205.5 - 3214.4	Dry
	F15-A-01	SGGS	SGGSS	344	101.3	3214.7 - 3316.0	F03-FB
	F16-04	SGGS	SGGSP	59	17.9	2261.6 - 2279.5	Dry
	F17-04	SLCF	SLCFM	3	0.6	2501.7 - 2502.3	Dry
	F17-06	SLCF	SLCFR	69	8.6	3042.2 - 3050.8	Dry
	F18-01	SGGS	SGGSP	72	18.3	3248.0 - 3266.3	Dry
	F18-02	SLCF	SLCFM	55	49.2	2482.5 - 2531.7	Dry
	F18-05	SGSK	SGSK	52	12.7	2558.8 - 2571.4	Dry
	F18-07	SLCF	SLCFM	58	6.6	2576.7 - 2583.4	Dry
	F18-09-S1	SLCF	SLCFM	15	72.5	3248.8 - 3321.1	Dry
	F18-10-S1	SGGS	SGGSS	28	8.7	2451.9 - 2460.5	F17-FB
	F18-10-S2	SLCF	SLCFM	27	18.4	2536.2 - 2554.5	F17-FB
	G16-03	SGGS	SGGSP	10	9.8	1646.2 - 1656.0	Dry
	G16-06-S1	SLCF	SLCFM	50	14.7	2200.9 - 2215.6	Dry
L02-04	SGSK	SGSKT	10	5.3	2561.7 - 2567.0	F18-FA	
L02-FA-102	SLCF	SLCFM	45	29.2	2436.5 - 2465.6	F18-FA	
L03-01	SGGS	SGGSP	11	3.0	2445.5 - 2448.4	F18-FA	
L05-01	SLCF	SLCFM	27	7.8	2508.1 - 2515.9	F18-FA	
L05-02	SGGS	SGGSS	34	24.9	2662.2 - 2687.1	Dry	
L05-04	SLCF	SLCFM	30	8.8	2080.7 - 2087.1	Dry	
L05-05	SLCF	SLCFM	20	5.9	2492.8 - 2497.3	F18-FA	
L06-02	SGGS	SGGSP	11	2.5	2494.4 - 2496.5	G16-FA	
L06-03	SGSK	SGSKT	41	13.5	2504.4 - 2515.7	G16-FA	
L09-02	SGGS	SGGSS	5	1.1	2560.9 - 2561.7	G16-FA	
M01-01	SGSK	SGSKT	79	52.4	2561.9 - 2597.3	G16-FA	
M04-02	SLCF	SLCFM	33	16.4	2099.4 - 2115.8	Dry	
M07-03	SGLU	SGLUS	22	6.3	2204.6 - 2210.9	Dry	
M07-07	SGGS	SGGSP	8	1.8	2039.8 - 2041.6	Dry	
			72	24.0	1996.8 - 2020.8	Dry	
			25	8.2	2546.8 - 2555.0	Dry	
			59	18.0	2784.8 - 2802.7	Dry	
			16	4.5	2883.0 - 2887.5	Dry	
			59	17.4	2482.4 - 2499.8	Dry	
			57	36.4	2638.0 - 2674.4	Dry	
			5	1.2	2715.1 - 2716.3	Dry	
			19	8.1	2751.7 - 2759.8	Dry	
			10	3.0	2804.7 - 2807.7	Dry	
			4	1.7	2821.8 - 2823.5	Dry	
			15	4.1	2703.9 - 2708.0	L05a-E	
			128	36.0	2226.7 - 2262.7	Dry	
			112	45.6	2463.3 - 2508.9	L06-FA	
			53	17.2	2026.8 - 2043.9	Dry	
			50	15.7	2094.4 - 2110.1	Dry	
			25	14.6	2253.9 - 2268.4	Dry	
			53	18.1	2302.9 - 2321.0	Dry	
			90	27.4	2927.9 - 2955.3	Dry	
			27	8.1	2287.2 - 2295.2	Dry	
			52	14.0	2636.5 - 2650.4	Dry	
			6	2.0	2824.7 - 2826.7	Dry	
			25	6.0	2725.0 - 2731.0	Dry	
			189	49.2	~2835 - ~2865	M07-B	

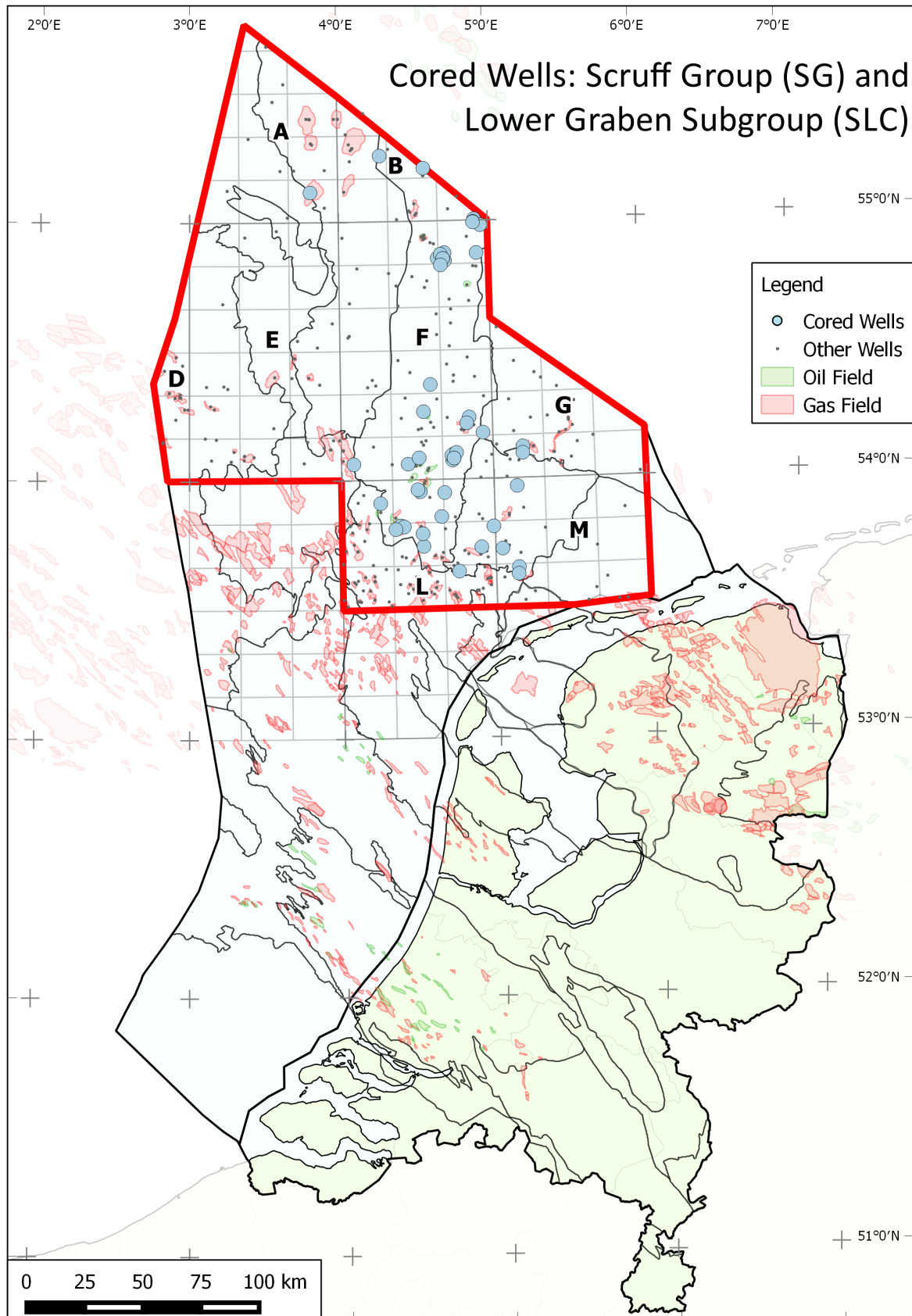


Figure 17. Base map showing the study area in the context of the Netherlands. Structural elements, quadrants, blocks, fields, and wells are displayed. Wells with cores within Upper Jurassic to Early Cretaceous intervals that have been used in this study are highlighted in light blue.

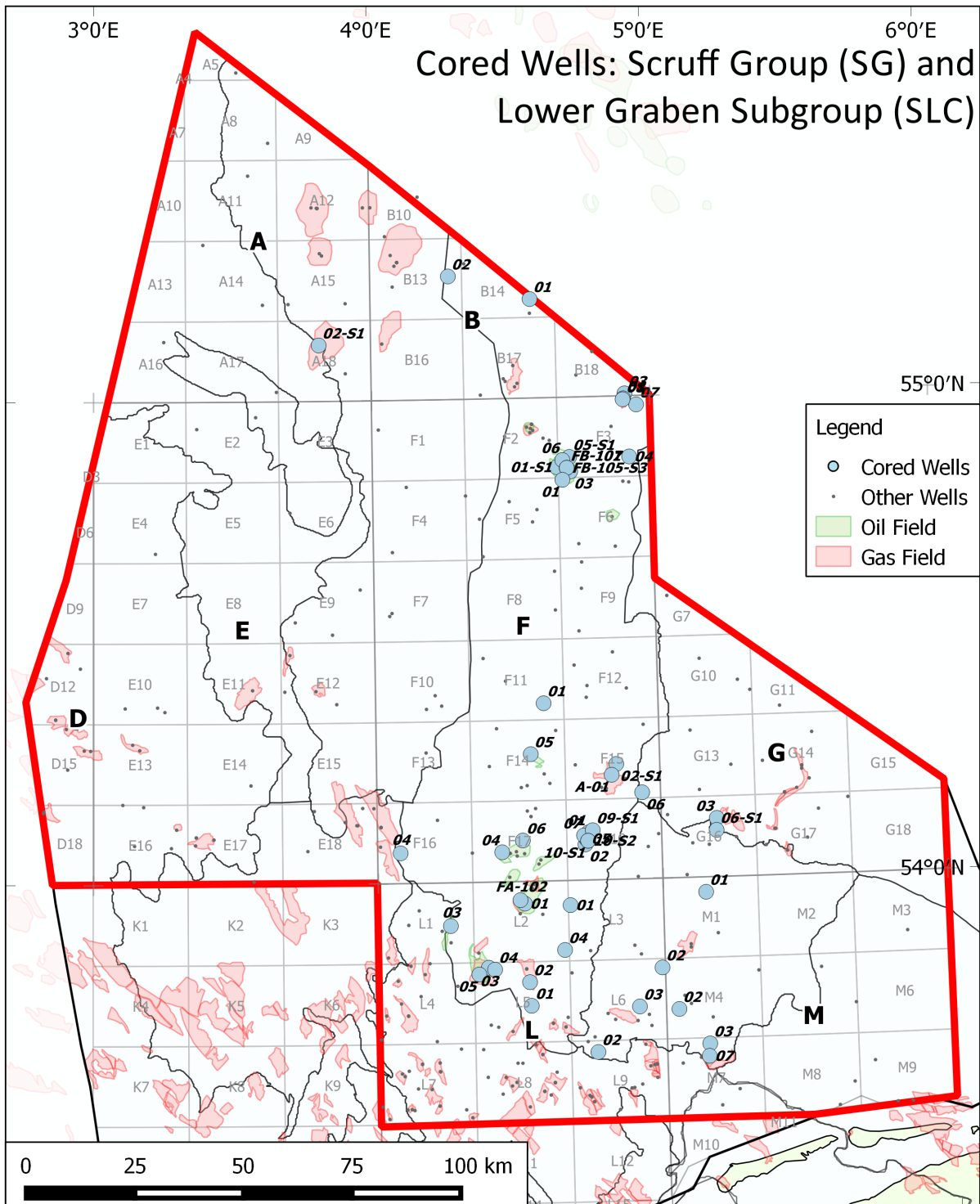


Figure 18. Detailed base map of the study area in the northern Dutch offshore. Structural elements, quadrants, blocks, fields, and wells are displayed. Wells with cores within Upper Jurassic to Early Cretaceous intervals that have been used in this study are highlighted in light blue.

Table 2. List of Upper Jurassic to Lower Cretaceous oil and gas fields and the corresponding lithostratigraphic units that have been drilled.

Field	Hydrocarbon	Discovery well	Discovery year	Lithostratigraphic unit	Sequence
B18-FA	Oil	B18-03	1982	Lower Graben Formation (SLCL)	1
F03-FA	Gas	F03-01	1971	Scruff Greensand Formation (SGGS) /Central Graben Subgroup (SLC)	3,1
F03-FB	Oil and Gas	F03-03	1974	Upper Graben Formation (SLCU) /Central Graben Subgroup (SLC)	1
F03-FC	Oil	F03-07	1981	Scruff Greensand Formation (SGGS)	3
F14-A	Oil	F14-05	1986	Lower Graben Formation (SLCL)	1
F15-B	Gas	F15-A-04-S3	1998	Scruff Spiculite Member (SGGSP)	3
F17-FB	Oil	F17-04	1982	Friese Front Formation (SLCF)	1
F17-FA	Oil	F17-03	1982	Friese Front Formation (SLCF)	1
F18-FA	Oil	F18-01	1970	Friese Front Formation (SLCF) /Skylge Formation (SGSK)	2,3
G16-FA	Gas	G16-01	1985	Scruff Greensand Formation (SGGS)/Friese Front Formation /Zechstein caprock	3,1
L01-FB	Oil	L01-03	1985	Central Graben Subgroup (SLC)	1
L05a-E	Oil	L05-03	1983	Friese Front Formation (SLCF)	1
L06-FA	Gas	L06-02	1990	Scuff Greensand Formation (SGGS) /Terschelling Sandstone Member (SGSKT)	2
M07-B	Gas	M07-05-S1	1996	Terschelling Sandstone Member (SGSKT) /Scruff Greensand Formation	2

3.2 Depositional framework and facies correlation

Munsterman et al. (2012) provided a comprehensive overview of the general depositional settings and the corresponding depositional environments resulting from palynological and biostratigraphic data. This model was used as a framework for comparison with the interpretations in the available core reports of the studied wells. As the wells considered in this study have been drilled during the past 50 years, some differences exist in the nomenclature used in core analysis and interpretation of depositional environments. Over the years, terminology has evolved and recently drilled wells may therefore contain different interpretations than older wells, which in turn may contain now obsolete definitions. In addition, operators may apply different practices in analyzing and interpreting core data. The differences between operators and the evolution in time of the terminology as applied in assigning depositional settings provides a challenge finding a uniform approach, in which all the different interpretations have a seamless fit with the updated depositional framework. In order to arrive at a best approximation of such an approach, correlating an operator's interpretation with the schematic model was done by identifying the common denominator in the defined facies. In most cases, straight one-on-one correlation of old with new terminology was possible. The operator's interpretation was matched with the interpretation in the depositional framework by Munsterman, after which this definition was applied in the subsequent input that linked the facies to the correct plug samples in the database.

Facies were separated across a range of environments or settings, from relatively low energy to higher energy conditions. Environments with low energy conditions range from open marine to shallow

marine (lower shoreface), to restricted marine settings such as a brackish lagoon or inter-distributary bay, to continental settings such as swamps. Higher energy conditions range from marginal marine settings such as an upper shoreface, foreshore, or beach, towards estuarine, tidal shoal/channel settings. Continental facies with relatively higher energy include alluvial fans. To avoid complication, some subfacies were grouped together: estuarine, tidal shoal/channel deposits were joined together; upper shoreface, foreshore and beach deposits were joined into one category; brackish lagoon and (inter-distributary) bay deposits were also grouped together and include sediments deposited in environments of varying salinity (brackish and freshwater), which may also be fluvial in origin. This resulted in the classification of 8 groups of facies.

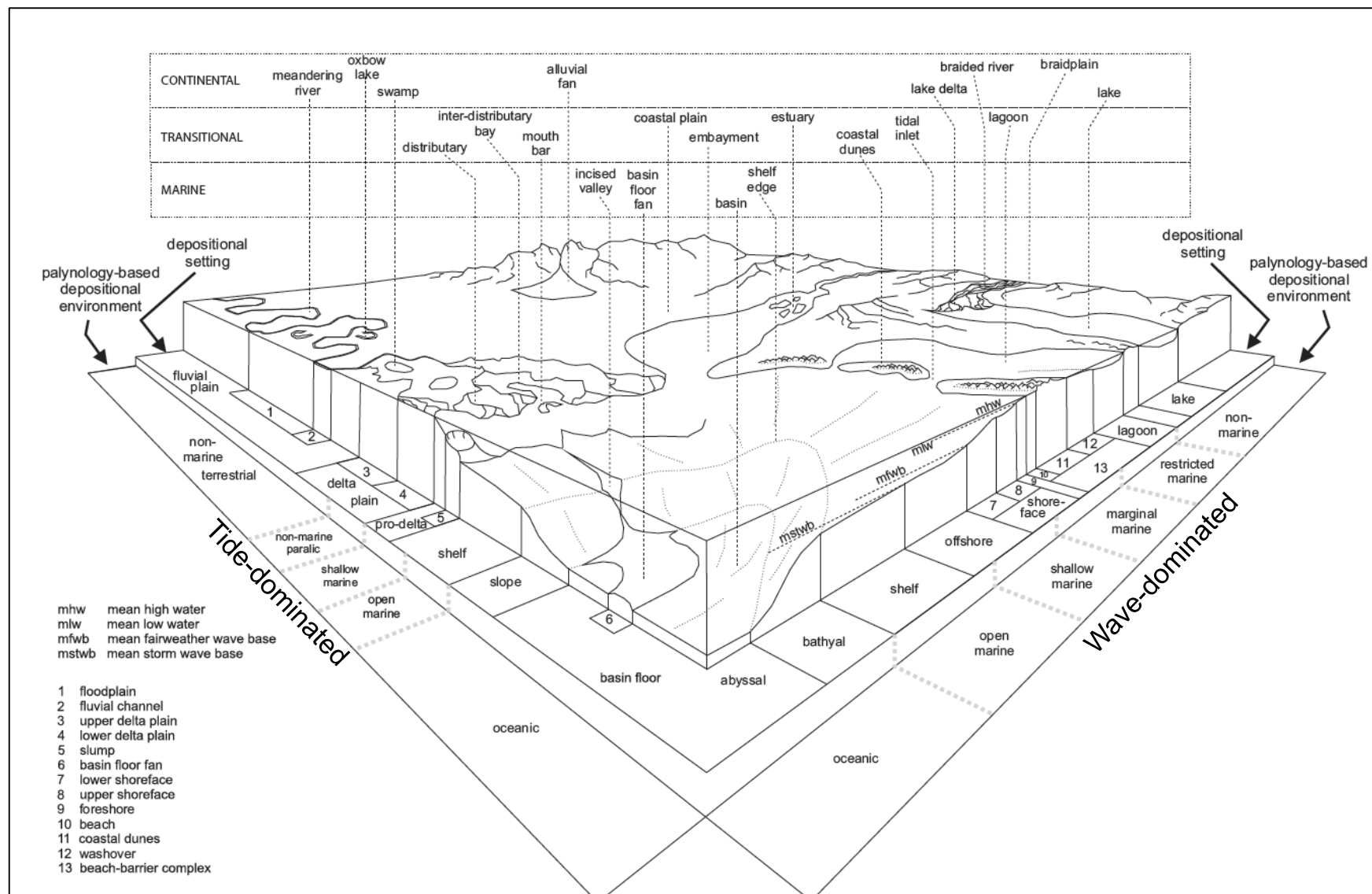


Figure 19. Schematic overview of typical depositional settings within their corresponding depositional environments, specified for tide- and wave-dominated regimes (Munsterman et al., 2012).

4. Results – Analysis of Trends in Reservoir Properties

Plug sample data from all wells that cored Upper Jurassic – Lower Cretaceous formations were plotted in the following diagrams: porosity vs permeability, porosity vs depth, and permeability vs depth. These diagrams were constructed for the following lithostratigraphic units: Lower Graben Formation, Middle Graben Formation, Upper Graben Formation, Friese Front Formation, Skylge Formation, Kimmeridge Clay Formation, Scruff Greensand Formation, and Lutine Formation. No core data was available for the Puzzle Hole Formation in the study area. Data on facies was found for 2066 plug samples and subsequently visualized in the diagrams. From Figure 23 up to Figure 48, cores are displayed as a pie chart, with each slice representing the total share of plug samples corresponding to each depositional setting as interpreted from the core itself. By establishing the main trends, it was possible to identify outliers representing anomalously high or low porosity-permeability relations.

Generally, the data is distributed over a wide range of porosities and permeabilities. However, this changes when facies data is correlated with the core plug samples and subsequently highlighted. The result is the tendency of core plug data belonging to a certain depositional environment to occupy a specific area or range in the porosity vs permeability plot (Figure 20). The depositional environments that have relatively low energy conditions, such as open marine, swamp, and brackish lagoon/bay settings, tend to have the lowest reservoir quality. Depositional environments with relatively high energy conditions such as estuarine, tidal shoal/channel, and upper shoreface, foreshore, and beach settings, tend to have higher reservoir quality.

Excellent reservoir quality is found in the Lower, Middle, and Upper Graben formations, as well as the Friese Front and Skylge formations. These formations contain well-sorted, clean sands, which tend to have excellent porosity and permeability. These sands are deposited in estuarine, tidal shoal, and tidal channel settings, as well as upper shoreface, foreshore, and beach settings. To a lesser extent, some lower shoreface sands in the Scruff Greensand Formation may contain excellent porosity and moderate to good permeability.

Interpreting the porosity/depth and permeability/depth relations proved challenging. Generally, for all formations, porosity loss showed two approximately linear trends: one trend up to depths of 3000 m, and one trend from 3100 – 3300 m (Figure 21). Permeability loss is not observable in depths of up to 3000 m. However, permeability shows rapid losses with depth in the 3100 – 3300 m depth interval. Interpretation of the grain density vs depth relation shows no clear link between increased burial depth and a higher density, although there is more spreading towards higher densities in the 3100 – 3300 m depth interval (Figure 22).

The available data show that certain facies associations are specific for each of the three Upper Jurassic to Lower Cretaceous mega-sequences. Therefore, these facies are present only at certain depth intervals. For example, restricted marine settings (brackish lagoon/bay) are present in the Lower Graben Formation but not in the Scruff Greensand Formation, which is dominated by lower shoreface and open marine settings. Most of the core data from the Lower Graben Formation was taken from depths below 3100 m. At shallower depths, available data becomes limited. Other formations show the same facies/depth dependency. Due to this phenomenon and due to some formations having limited

core data, the porosity/depth and permeability/depth relations of only two formations could be accurately interpreted.

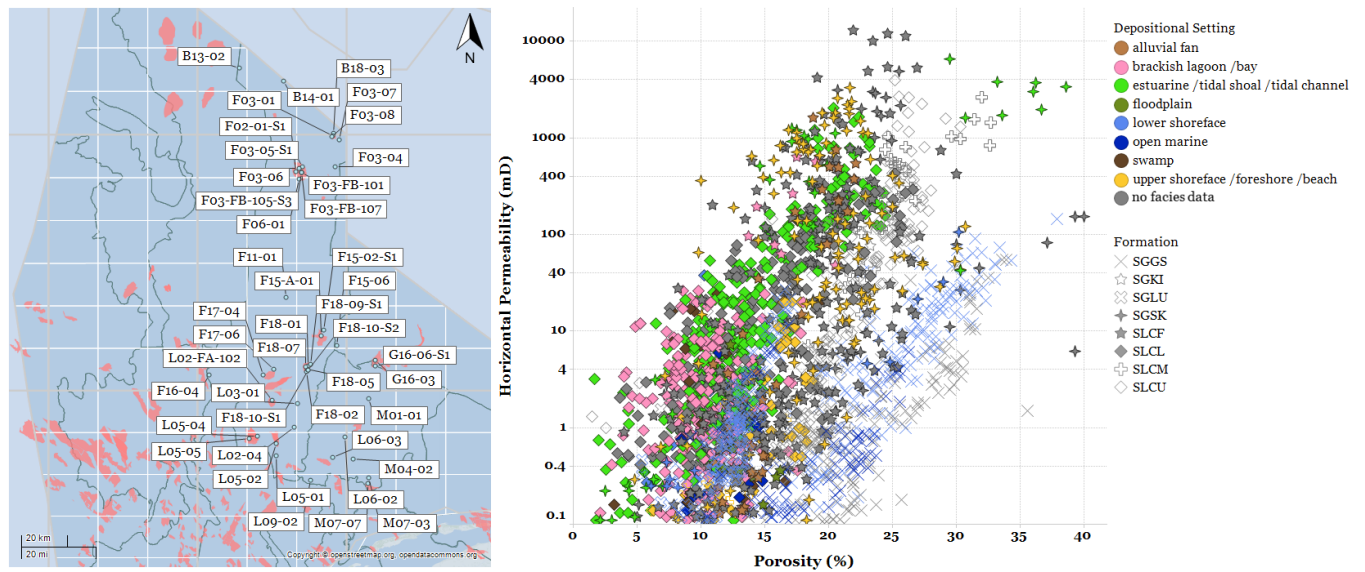


Figure 20. Left: geographical map chart with an overview of the locations of all wells with core plug measurements used in this study. Right: graphic visualization of the plug sample data in a plot of porosity vs permeability. Individual formations and wells are specified in color and shape, respectively. Note that different facies display different trends.

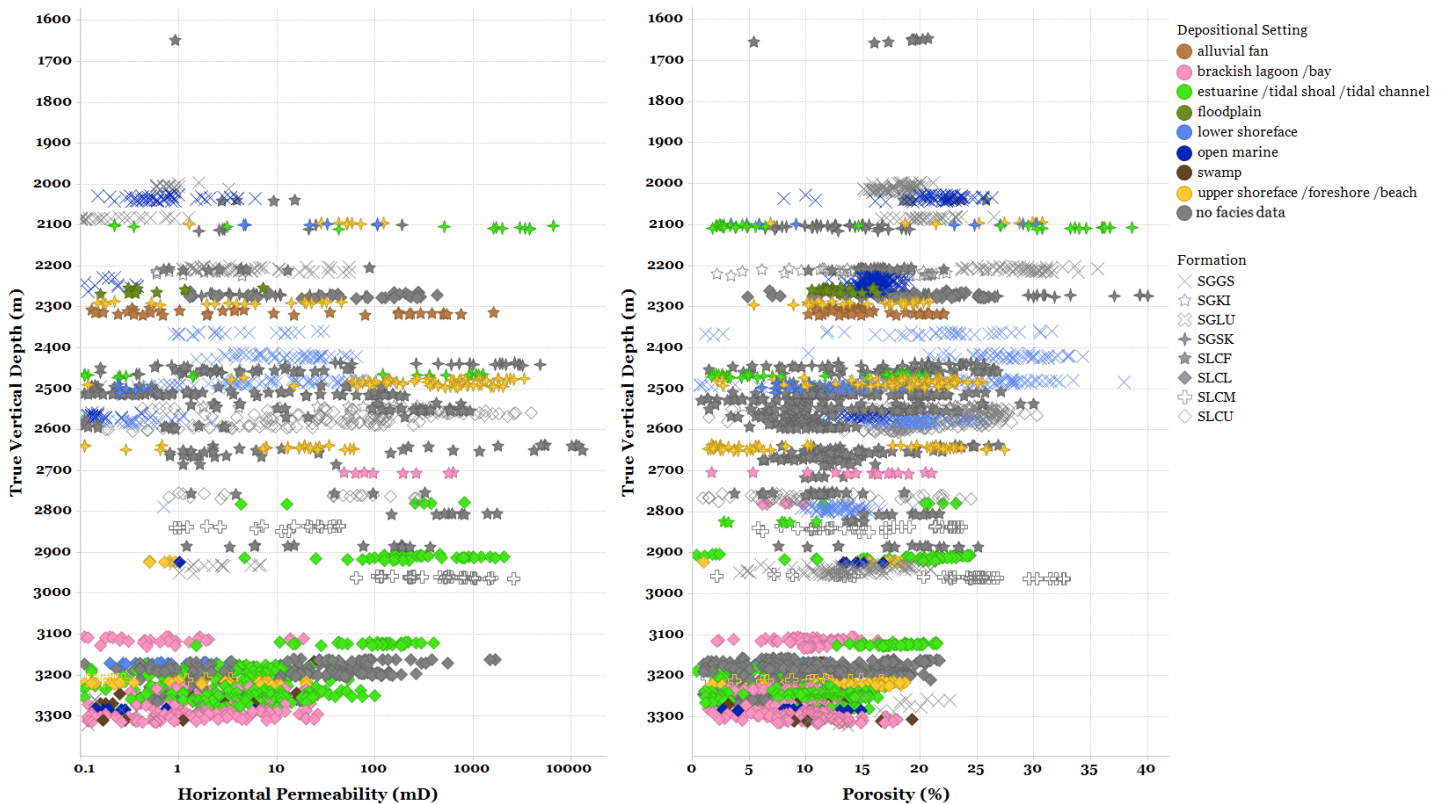


Figure 21. Graphic visualization of all core plug sample data in a permeability vs depth plot (left) and a porosity vs depth plot (right). Individual facies and wells are specified in color and shape, respectively. Note the roughly linear loss of porosity with increased depth, and the different trend for the 3100 – 3300 m depth interval as compared to the trend for depths up to 3000 m. Permeability shows a similar trend for the 3100 – 3300 m depth interval, but there does not appear to be a clear, linear trend in permeability loss for depths up to 3000 m.

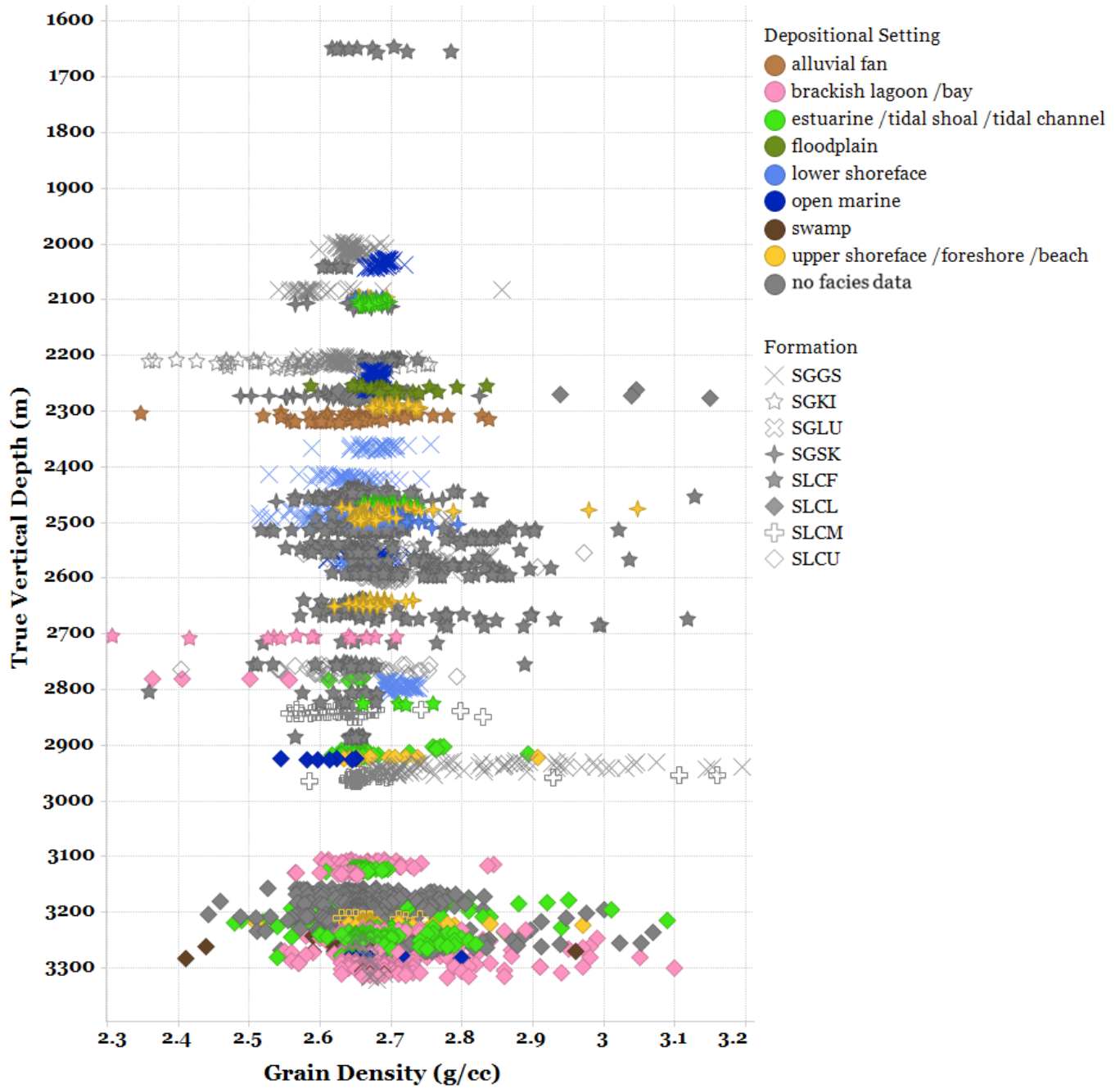


Figure 22. Graphic visualization of all core plug sample data in a grain density vs depth plot. Individual facies and formations are specified in color and shape, respectively. Note the wide spread in grain density for some formations such as the Lower Graben Formation between 3100 – 3300 m, and the Scruff Greensand Formation between 2900 – 3000 m. There is no clear increase of grain density with increasing depth, and therefore no relationship can be interpreted.

4.1 Lower Graben Formation (SLCL)

A total amount of 1462 plug samples was taken from nine wells that cut a total of 451 m of core length from the Lower Graben Formation (Table 3). Removal of core plug data below the detection limit resulted in 1262 porosity and 884 permeability measurements (Figure 23). Overall, core data from the Lower Graben Formation displays the widest variety in sedimentary facies of all formations. Depositional environments range from mostly marginal marine (estuarine and tidal shoal/channel settings), to less abundant shallower, upper shoreface settings, and traces of open marine influences.

A total of 958 plug samples was correlated with facies data of the Lower Graben Formation. The dominant environment of deposition is marginal to restricted marine, with 452 samples representing sediments deposited in an estuarine, tidal shoal/channel setting (Figure 24). The relatively higher energy conditions present in such a system caused deposition of coarser sediments with higher porosity and permeability in wells such as B18-03, F03-01, and F03-FB-101. Sediments deposited in a brackish lagoon or bay setting account for 369 samples, and, due to the lower energy conditions present in the system, led to deposition of finer sediments, which display relatively lower porosity and permeability. Upper shoreface, foreshore, and beach settings account for a significantly lower share of the formation. Continental facies (swamps), and open marine settings are even less abundant. Seven wells found the Lower Graben Formation to be hydrocarbon-bearing within three fields: B18-FA, F03-FA, and F03-FB. The longest cores were cut from wells that drilled the F03-FB field: F03-05-S1, F03-06, F06-01, F03-FB-101, and F03-01-S1. Plug sample measurements show a wide range in reservoir quality within the Lower Graben Formation, with excellent porosity of up to 26.6% (average 11.9%) and excellent permeability of up to 2048 mD, average 49 mD).

When looking at individual depositional environments, the estuarine and tidal shoal/channel settings display the best, but variable, reservoir quality (Figure 25). Porosity within these sediments ranges between 1.7 – 24.4%, with an average of 13.3%. Permeability averages 84 mD, with a maximum value measured at 2048 mD. Samples from well F03-01 show significantly higher porosities and permeabilities than wells containing samples deposited in the same setting but buried at greater depth, such as in wells F03-FB-101 and F06-01. This could be related to differences in diagenesis by either mechanical compaction or chemical compaction due to replacement clays caused by illitization at depths greater than 3000 m.

Brackish lagoon/bay deposits display a mostly poor to moderate reservoir quality. Porosity ranges between 2.1 – 18.0%, with an average of 10.1%. Permeability has a maximum of 26 mD, with an average of 3.7 mD. In well F03-FB-101, claystones with bioturbated, fine to very fine-grained sandstones are interpreted as inter-distributary bays and swamp deposits. There is also a 9.5 m thick erosive based sandstone unit consisting of wavy/irregular bedded, deformed, fine to very fine-grained well-sorted sandstones interpreted as distributary channel deposits (Figure 26, Figure 27) (NAM, 1994). Some samples in F03-FB-101 display a higher porosity and permeability compared with samples from F06-01, both of which were deposited in the same setting. This difference is interpreted to be related to the increased burial depth resulting in either mechanical or chemical compaction within the sandstones of well F06-01. Scanning electron microscope images of well F03-FB-101 show pore-clogging of kaolinite and quartz overgrowths, which could significantly have degraded overall reservoir quality (Figure 28).

Upper shoreface, foreshore, and beach settings display a poor to moderate reservoir quality. Porosity ranges between 6.3 – 18.7%, with an average of 14.9%. Permeability displays a maximum value of 20.0 mD, with an average of 4.3 mD. Porosity is higher than in brackish lagoon/bay settings, while permeability is comparable. Lower shoreface sediments display a poor reservoir quality, with a porosity of 5.8 – 11.1% (average 9.6%), and a permeability of up to 38.0 mD (average 3.3 mD). Swamp deposits display a poor reservoir quality, with porosity ranging between 3.2 – 19.3% (average 10.5%) and a permeability of up to 24.0 mD (average 6.0 mD). Open marine sediments display a poor reservoir quality, with a porosity between 8.5 – 14.8% (average 11.3%) and a permeability of up to 5.9 mD (average 0.9 mD).

When considering the porosity/depth relation, there are two different depth intervals, each of which with its own gradient. For depths up to 3100 m, the loss of porosity with depth is significantly less than compared with depths exceeding 3100 m. The exact ‘boundary’ between the two trends cannot be pinpointed due to the lack of data between 2900 – 3000 m. The cause for the increased loss of porosity in the 3100 – 3300 m depth interval can be explained by diagenesis due to chemical compaction picking up at elevated pressures and temperatures below 3100 m. However, this trend is mostly seen for estuarine and tidal shoal/channel settings. Brackish lagoon/bay settings seem to ignore this trend. Interpretation of the permeability/depth relation reveals linear permeability loss below a depth of 3100 m, but not a distinct trend at depths shallower than 3100 m (Figure 29).

It must be noted that there is significantly more data for the 3100 – 3300 m depth interval than for depths up to 3100 m. Furthermore, most of the data for the Lower Graben Formation comes from the F03-FB field, therefore any regional interpretation will mostly represent this part of the Dutch Central Graben.

Table 3. Characteristics of wells that cored the Lower Graben Formation (SLCL). Nine wells cored this interval, resulting in 1462 plug samples taken from 451 m of core length. Measured Depth (MD) refers to depth along hole; True Vertical Depth (TVD) refers to depth below Kelly Bushing.

Well	Cored Formation	Cored Member	Number of Plugs	Core Length (m MD)	Depth Interval (m TVD)	Cored Interval Dry or in Field
B18-03	SLCL		11	3.9	2778.8 - 2782.6	B18-FA
F02-01-S1	SLCL		83	29.8	3166.8 - 3196.6	F03-FB
F03-01	SLCL		53	17.3	2902.7 - 2919.9	F03-FA
F03-05-S1	SLCL		416	134.1	3167.1 - 3300.8	F03-FB
F03-06	SLCL		359	113.9	3156.1 - 3269.7	F03-FB
F03-07	SLCL		18	5.1	2920.9 - 2925.9	Dry
F03-FB-101	SLCL		116	26.7	3105.5 - 3132.1	F03-FB
F06-01	SLCL		344	101.3	3214.7 - 3316.0	F03-FB
F11-01	SLCL		59	17.9	2261.6 - 2279.5	Dry
			3	0.6	2501.7 - 2502.3	Dry

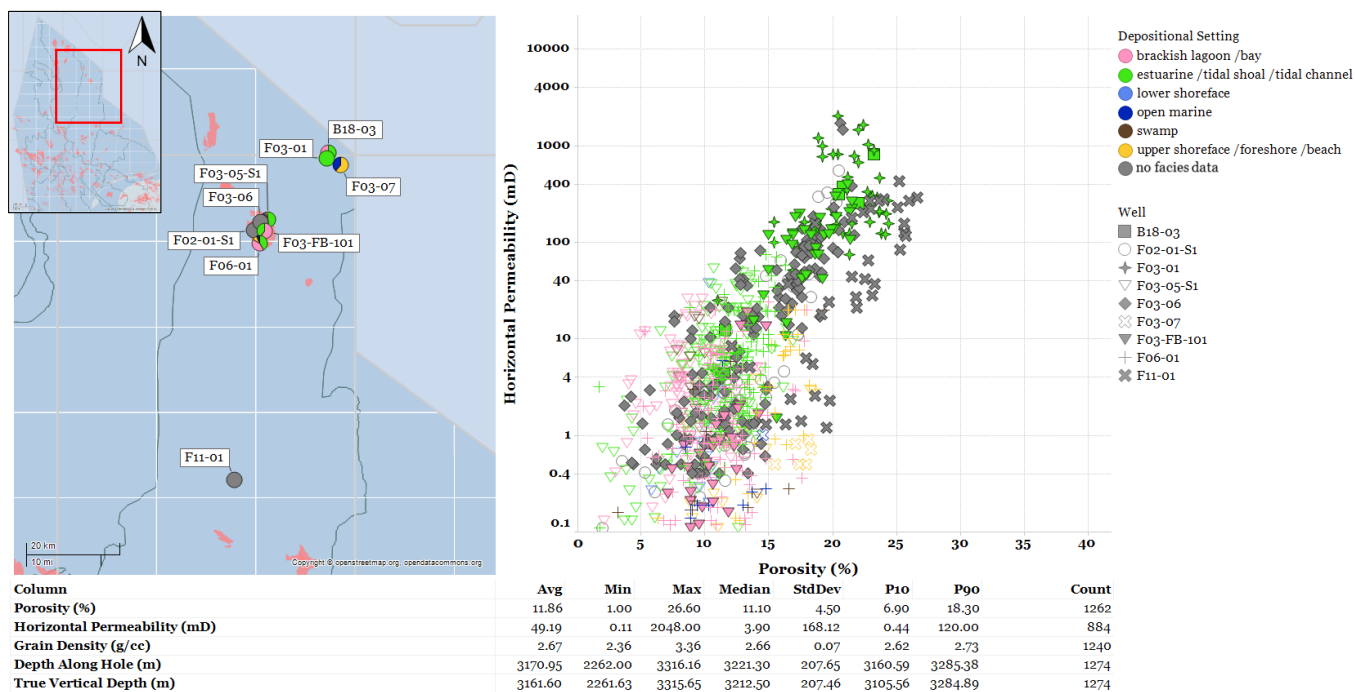


Figure 23. Left: geographical map chart with the locations of all wells that cored the Lower Graben Formation. Right: graphic visualization of the plug sample data in a porosity vs permeability plot. Bottom: statistical results of the relevant parameters, where Avg: average, and StdDev: standard deviation. Note the distinct trend of each depositional setting as displayed by the data. Facies correlation with plug sample data clearly show a predominant marginal to restricted marine environment.

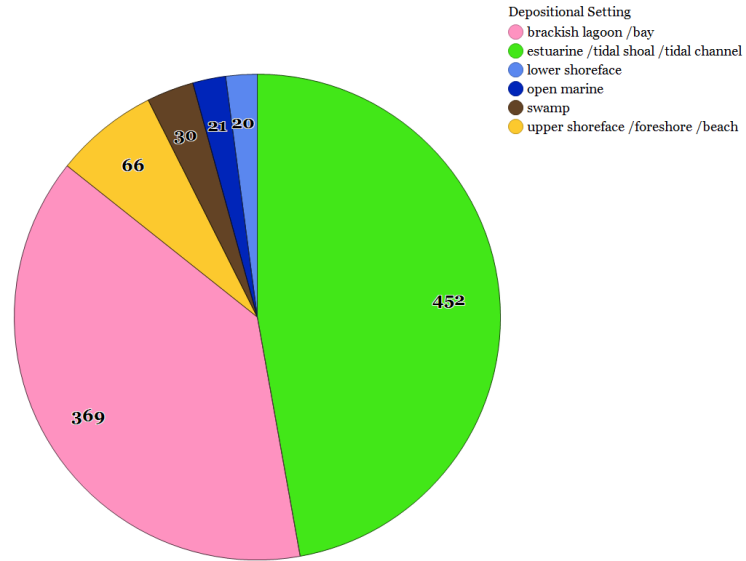


Figure 24. Total amount of plug samples in the Lower Graben Formation distributed per facies. Note that most of the data reflect a marginal to restricted marine environment of deposition.

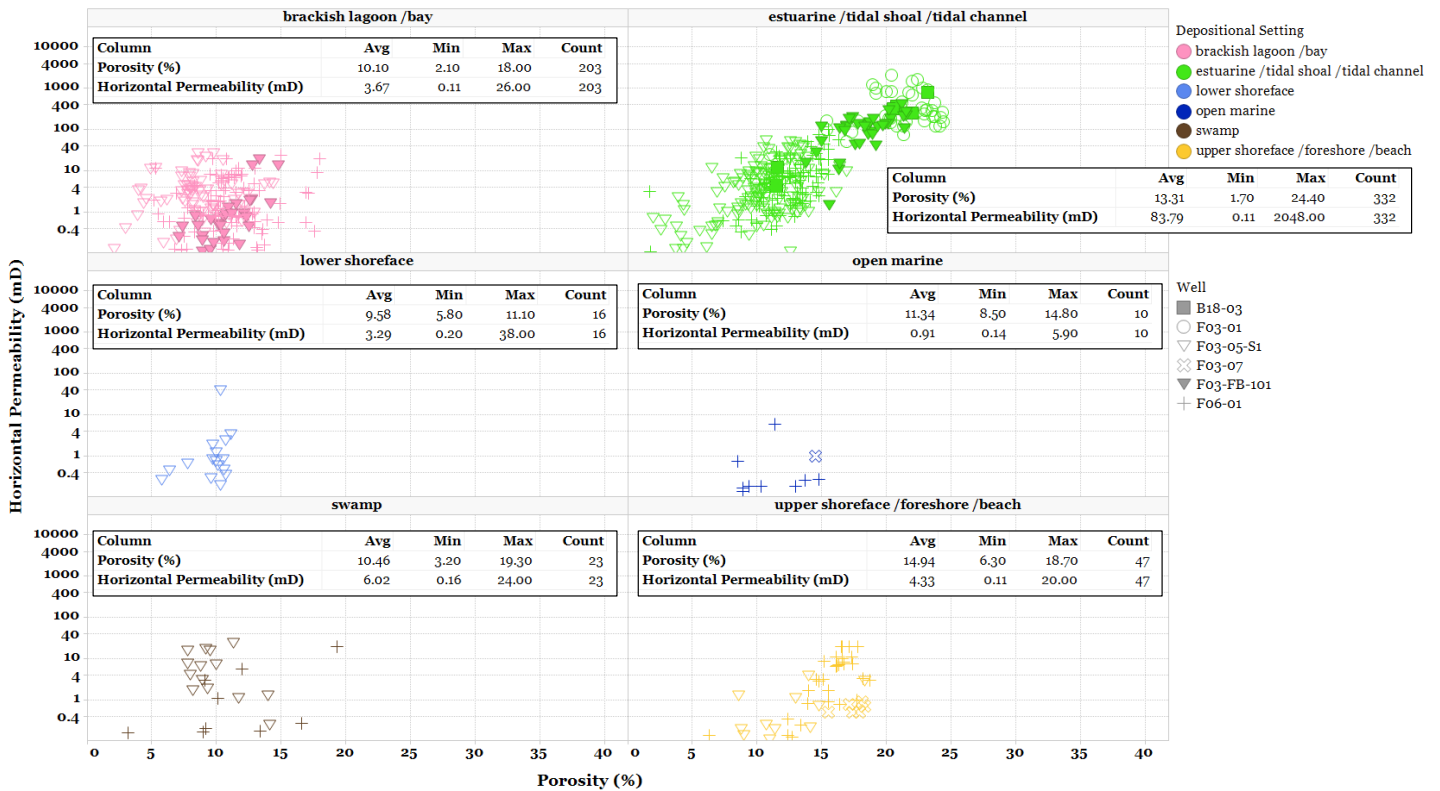


Figure 25. Trellis view of the Lower Graben Formation, in which each panel represents a porosity/permeability plot of the total amount of plug samples per facies. Results for the individual facies are shown in the corresponding tables.

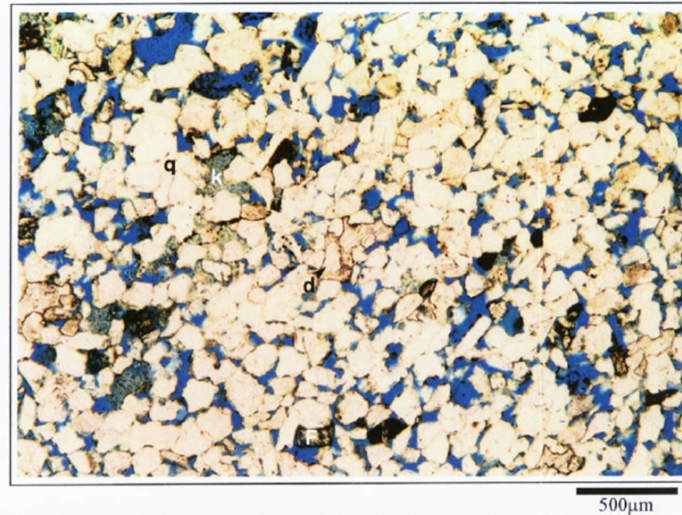


Figure 27. Thin section of sample number 60 (depth 3225.95 m) from well F03-FB-101, showing well-sorted, texturally mature, fine-grained sandstone. Magnification: $\times 45$, depth: 3225.95 m, porosity: 17.8%, permeability: 133.31 mD, grain density: 2.655 g/cc. Primary intergranular pores are moderately to well interconnected. Note abundant quartz (q) and dolomite cement replacing grains (d). Leaching of detrital grains such as feldspar (F) has created intragranular pores and mouldic pores. Oversized pores are locally filled with kaolinite (k). Point and long grain contacts indicate weak to moderate compaction (NAM 1994).

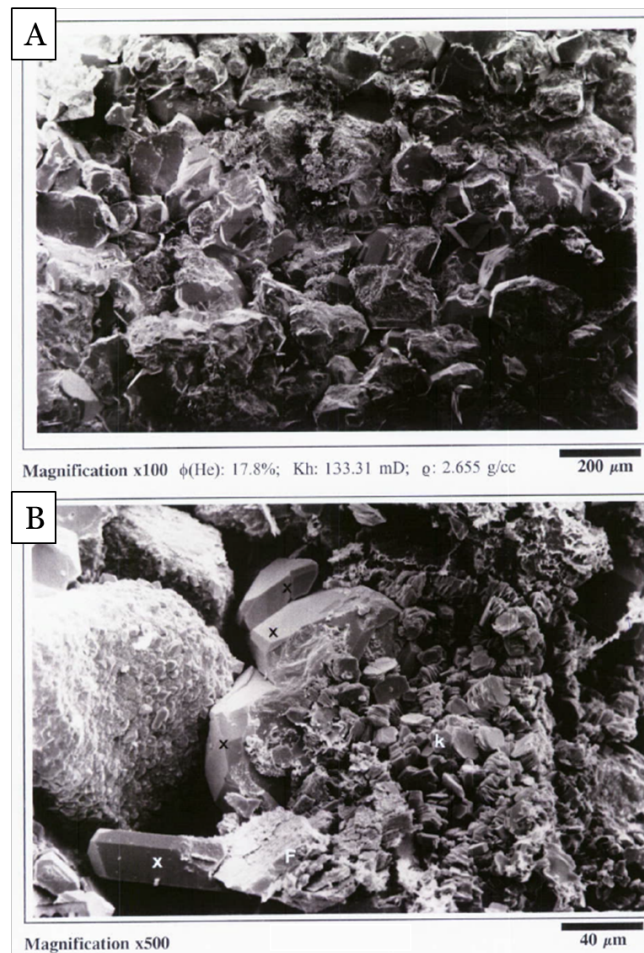


Figure 28. A general view of the sandstone from sample number 60, revealing mainly primary intergranular pores, which are commonly reduced by quartz cement and locally filled with authigenic clay. B: Close-up view of kaolinite "booklets" (k) adjacent to decomposed feldspar (F). Authigenic quartz overgrowths (x) developed on the host and authigenic clay (NAM, 1994).

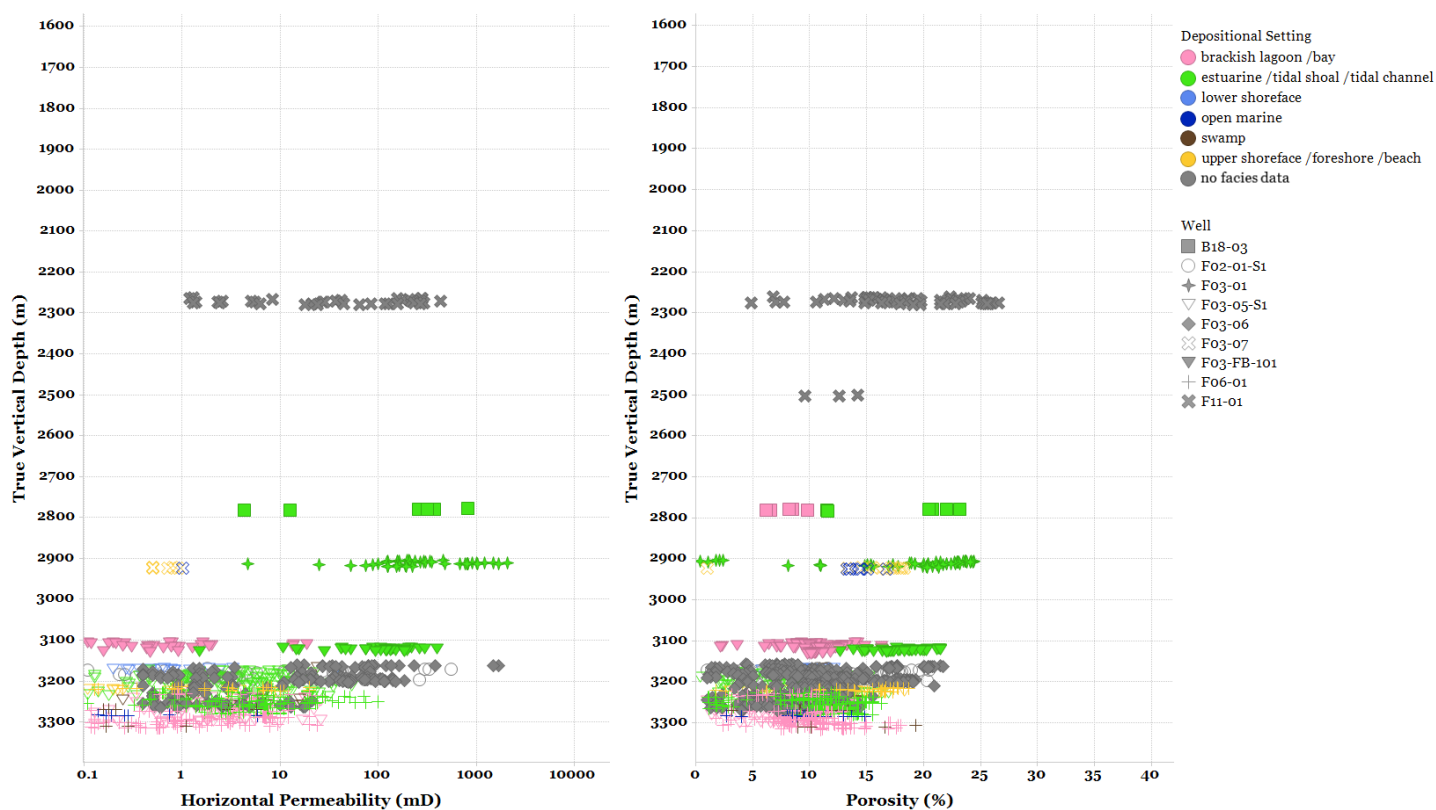


Figure 29. Plug sample data from the Lower Graben Formation visualized in a permeability vs depth plot (left) and porosity vs depth plot (right). Individual facies and wells are specified in color and shape, respectively. Note the increased porosity loss at the 3100 – 3300 m depth interval compared with porosity loss at depths up to 3100 m. Permeability loss displays a similar trend in the 3100 – 3300 m depth interval, but there is no clear loss of permeability with depths up to 3100 m.

4.2 Middle Graben Formation (SLCM)

The Middle Graben Formation was cored in three wells, with 113 plug samples from 37 m of core length (Table 4). Removal of core plug data below the detection limit resulted in 107 porosity and 85 permeability measurements (Figure 30). Two wells drilled and cored two Upper Jurassic – Lower Cretaceous fields: F03-FA and F03-FB. In well F03-FB-105-S3, the formation consists of fine to very fine bioturbated sandstone, while in F03-08 and F06-01 the formation consists more of claystone and coal beds.

Overall, the core data indicate a wide range in reservoir quality, with poor to excellent porosity and permeability. Porosities ranges between 1.3 – 32.7%, with an average of 19.5%. Permeability averages 374 mD, with a maximum measured value at 2615 mD. Plug samples of the F06-01 well were correlated with facies data, resulting in a marginal marine environment of deposition, consisting of upper shoreface, foreshore, and beach settings. Well F06-01 contains a much lower reservoir quality than expected for such an environment of deposition. Especially compared to core data from well F03-FB-105-S3, which show porosity ranging between 20.3 – 32.7% (average 26.2%), while permeability averages 629 mD, with a maximum value of 2614 mD. This difference is most likely explained by a difference in lithology of the formation in well F06-01, which consists mostly of coal and claystone. Core data from F03-08 display

a low to moderate reservoir quality. This is also interpreted as a difference in lithology of the cored formation, which is situated directly below a 5 m thick sandstone interval and consists of primarily argillaceous sediments with only thin sand streaks at the top of the core. The sandy streaks have a relatively higher reservoir quality, with porosity in the order of 15 – 20% and a permeability of 10 – 40 mD. The rest of the plug samples show a poor reservoir quality as similar to well F06-01. Due to the lack of sufficient and uniformly distributed data throughout the investigated depth range, no clear relationship could be derived for the porosity vs depth or permeability vs depth relation (Figure 31).

Table 4. Characteristics of wells that cored the Middle Graben Formation (SLCM). A total amount of 113 plug samples was taken from 37 m of core length. Measured Depth (MD) refers to depth along hole; True Vertical Depth (TVD) refers to depth below Kelly Bushing. Only three wells cored this interval.

Well	Cored Formation	Cored Member	Number of Plugs	Core Length (m MD)	Depth Interval (m TVD)	Cored Interval Dry or in Field
F03-08	SLCM		33	14.1	2835.6 - 2849.7	F03-FA
F03-FB-105-S3	SLCM	SLCMS	66	14.3	2952.8 - 2964.4	F03-FB
F06-01	SLCM		14	8.9	3205.5 - 3214.4	Dry

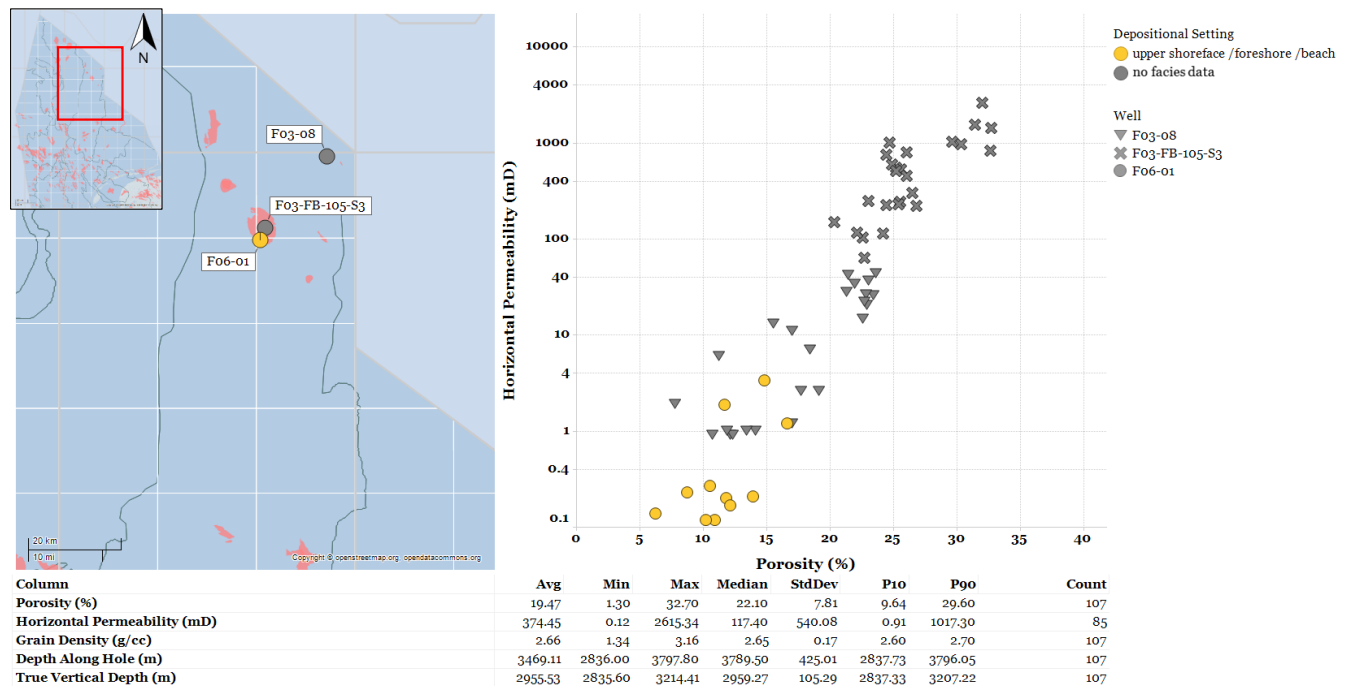


Figure 30. Left: geographical map chart with the locations of all wells that cored the Middle Graben Formation. Right: graphic visualization of the plug sample data in a porosity vs permeability plot. Bottom: statistical results of the relevant parameters, where Avg: average, and StdDev: standard deviation. Facies correlation with plug sample data from F06-01 show a marginal marine depositional environment for the Middle Graben Formation.

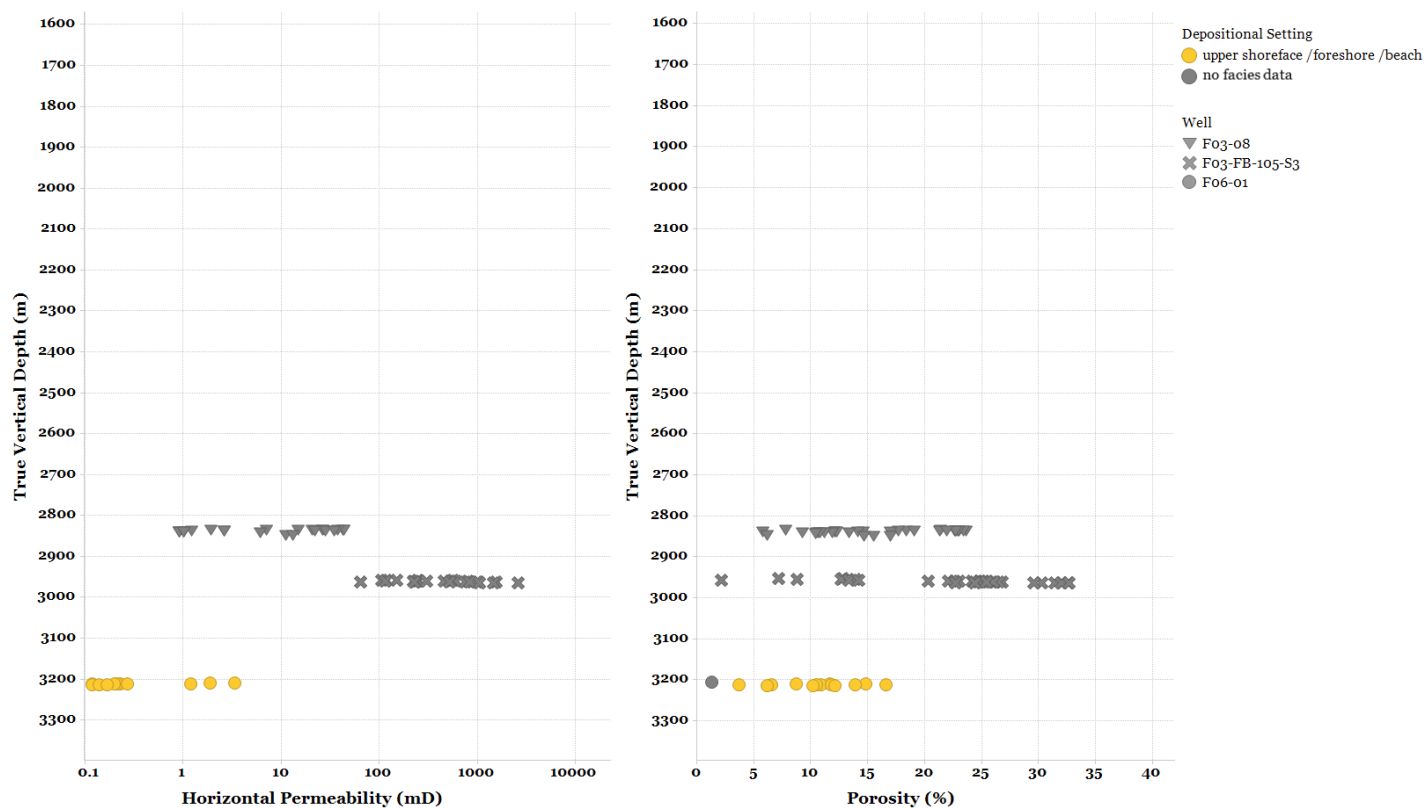


Figure 31. Plug sample data from the Middle Graben Formation visualized in a permeability vs depth plot (left) and a porosity vs depth plot (right). Individual facies and wells are specified in color and shape, respectively. Due to the lack of sufficient data, no clear interpretation was possible of the porosity/depth or permeability/depth relation.

4.3 Upper Graben Formation (SLCU)

The Upper Graben Formation was cored in two wells, with 258 plug sample measurements from a total core length of 83 m (Table 5). Removal of core plug data below the detection limit resulted in 233 porosity and 158 permeability measurements (Figure 32). Well F03-FB-107 drilled the formation as part of the F03-FB field.

Overall, the formation has a reservoir quality varying from poor to good in well F03-04, and poor to excellent in well F03-FB-107. Porosity ranges between 1.5 – 30.3%, with an average of 20.0%. Permeability averages at 218 mD, with a maximum value measured at 3949 mD. Correlation of facies with plug samples was not possible due to the lack of facies data. The formation was only cored in the northern part of the Dutch Central Graben in block F03-03. In both wells, intervals with increased clay content have a relatively lower reservoir quality compared with the more sandy intervals, suggesting a relation between reservoir quality and clay content. For well F03-FB-107, an excellent reservoir quality is likely related to the presence of cleaner sandstone with less clay content.

Interpretation of the porosity vs depth or permeability vs depth relation was not possible due to the lack of sufficient data on different depth intervals (Figure 33).

Table 5. Characteristics of wells that cored the Upper Graben Formation (SLCU). A total amount of 258 plug samples was taken from 83 m of core length. Measured Depth (MD) refers to depth along hole; True Vertical Depth (TVD) refers to depth below Kelly Bushing. Only two wells cored this interval.

Well	Cored Formation	Cored Member	Number of Plugs	Core Length (m MD)	Depth Interval (m TVD)	Cored Interval Dry or in Field
F03-04	SLCU		57	20.4	2755.1 - 2775.5	Dry
F03-FB-107	SLCU		201	62.9	2546.7 - 2606.0	F03-FB

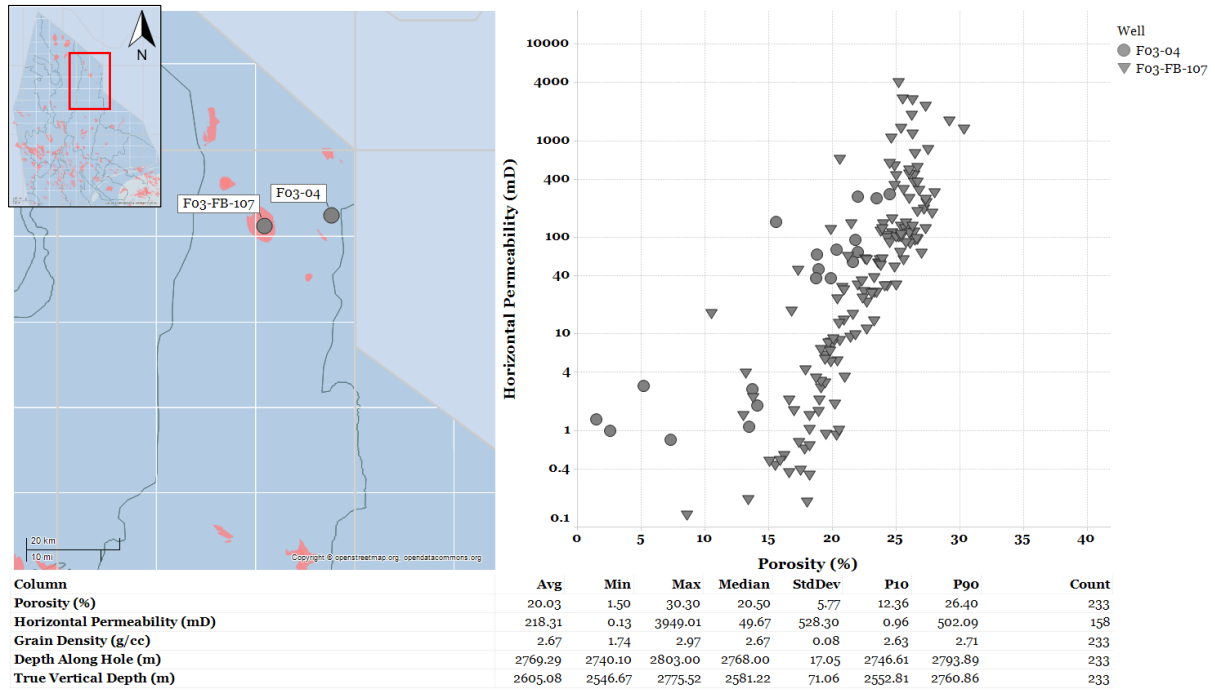


Figure 32. Left: geographical map chart with the locations of all wells that cored the Upper Graben Formation. Right: graphic visualization of the plug sample data in a porosity vs permeability plot. Bottom: statistical results of the relevant parameters, where Avg: average, and StdDev: standard deviation. No facies data was available for correlation.

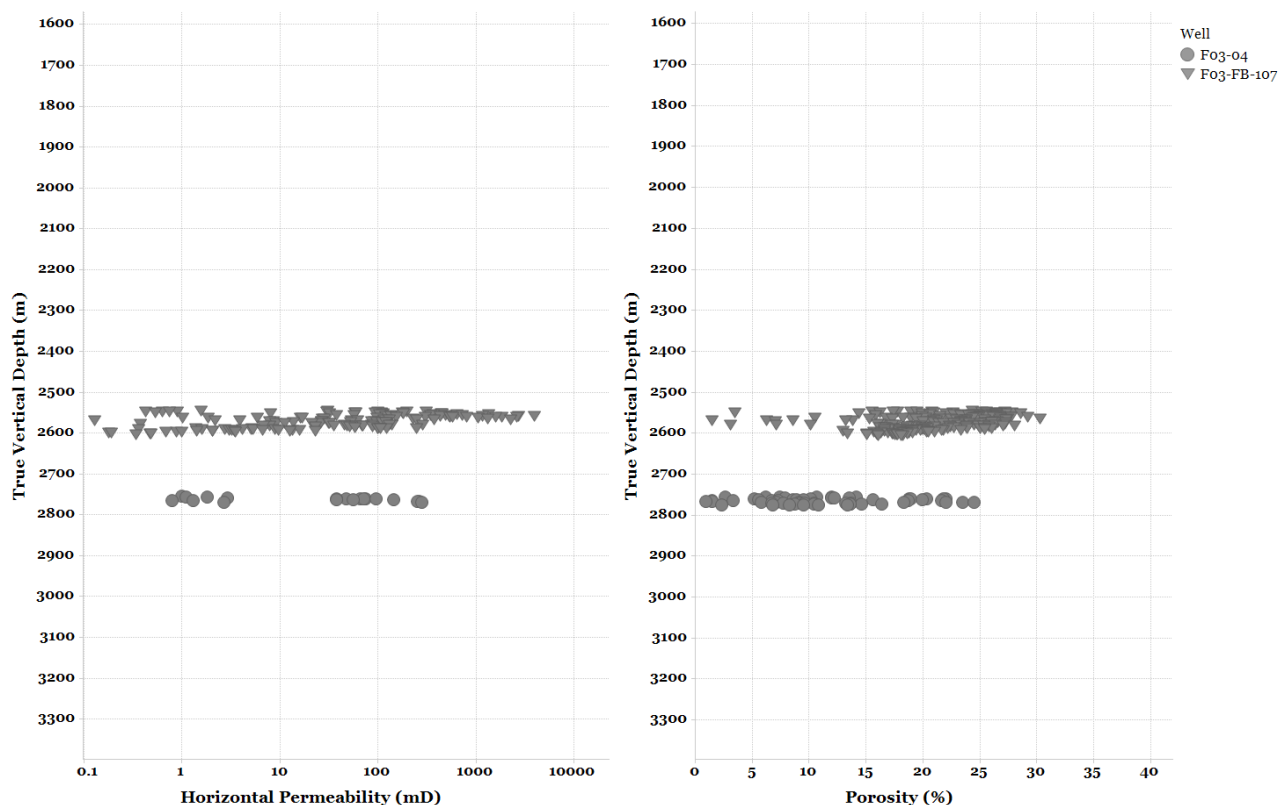


Figure 33. Plug sample data from the Upper Graben Formation visualized in a permeability vs depth plot (left) and porosity vs depth plot (right). Individual wells are specified in shape. Interpretation of the porosity/depth or permeability/depth relation was not possible due to lack of sufficient data.

4.4 Friese Front Formation (SLCF)

The Friese Front Formation was cored in 17 wells, with 607 plug samples taken from a total core length of 309 m (Table 6). Removal of core plug data below the detection limit resulted in 517 porosity and 292 permeability measurements (Figure 34). At member level, the Main Friese Front Member was cored in 12 wells, while the Rifgronden Member was cored in only two wells. The formation in the remaining wells was not defined at member level. Hydrocarbon-bearing intervals within the Friese Front Formation that are part of a field were cored in nine wells, with four wells located in the F18-FA field. Other fields include F17-FB, G16-FA, and L05a-E.

Overall, the reservoir quality of the Friese Front Formation has a wide variety, with poor to excellent porosity and permeability. Porosity ranges between 0.8 – 30%, with an average of 14.4%. Permeability displays an average of 342 mD, with a maximum of 12984 mD, the highest permeability in this study. The overall environment of deposition is continental, as most samples were deposited in either an alluvial fan or floodplain setting (Figure 35). To a lesser extent the depositional environment is also restricted marine due to the presence of brackish lagoon/bay, estuarine, and tidal shoal/channel settings. Estuarine, tidal shoal/channel settings are only present in well M04-02 and have poor porosity and no detectable permeability.

Sediments from an alluvial fan setting display a remarkably wide range in reservoir quality, as core data from well L06-03 demonstrates (Figure 36). Porosity ranges between 11.0 – 22.1% (average 15.8%),

and permeability shows a maximum of 1603 mD (average 154 mD). Core photos show the relatively lower porosities and permeabilities to dominate in the darker parts of the formation, while higher values seem to be present in the lighter colored sediments. This difference is interpreted as a function of clay content.

Floodplain deposits from the Friese Front Formation display an overall lower porosity and permeability, which is as expected due to the silt-like nature of the sediments deposited in such a setting.

Well L05-05 found oil in cross-bedded channel sands, which form part of the reservoir of the L05a-E oil field. The depositional setting is interpreted as a fluvial channel, but salt water influence is not ruled out. The same channel sands can be correlated by means of log comparing with wells L05-04, and L05-01. In well L05-05, the sands have a good reservoir quality, with a porosity of 13.7 – 20.5%, and a permeability of up to 630 mD (average 242 mD). The equivalent sands in well L05-04 have a much better reservoir quality, especially in the 2638 – 2653 m and 2805 – 2808 m depth intervals, where porosity ranges between 3.7 – 26.9% (average 14.5%), and permeability has an average of 1819 mD, with a maximum of 12984 mD. Most of the variety in reservoir properties is likely due to increased clay content in some sections within the cored formation. However, the sands in the 2638 – 2653 m depth interval of well L05-04 are situated about 35 – 50 m below an unconformity, above which the Vlieland Claystone Formation was deposited. This indicates that some uplift and erosion has taken place, which could have played a role in enhancing especially permeability of the sands due to activity of surface processes such as meteoric water flow. In well L05-01, the Friese Front Formation is relatively sandier than in wells L05-04 and L05-05, which contain relatively more as well as thicker intervals with more clay content. Well F17-04 also displays a good reservoir quality, with porosity ranging between 10.1 – 30.0% (average 21.2%), and permeability of up to 746 mD (average 50 mD). Core data from well L03-01 displays an excellent reservoir quality. The cored formation consists of fining upward, clean, cross-bedded sandstones, which display a porosity of 5.2 – 23.3% (average 16.7%) and a permeability of up to 928 mD (average 359 mD). This trend is similar for the channel sands from wells L05-01, L05-04, and L05-05 as discussed previously.

The results from the rest of the core data are roughly similar throughout the southern part of the Dutch Central Graben. Core data from sandy intervals within the Friese Front Formation all display good to excellent reservoir quality, with high porosity and permeability, especially in wells F17-04, F18-07, F18-10-S2, and F15-06. Lower than expected reservoir quality was encountered in wells, which cored parts of the formation with increased clay content: L02-04, L02-FA-102, F17-06, F18-02, and F18-09-S1. When comparing the logs of all the wells that drilled the Friese Front Formation, the result is that they share the same characteristic trend in lithology. Overall, the lithology consists of intervals of sandstone alternating with more argillaceous strata and coal streaks. The trend shows that these sandstone intervals start out with a relatively small thickness of 2 – 5 m at the bottom of the formation, and increase to thicknesses of 5 – 10 m towards the top. In well F15-06, the thickness of the Friese Front Formation is only about 30 m, and the core data show an interval at 2514 – 2518 m TVD with a porosity of 18.2 – 22.5% (average 20.5%) and a permeability of up to 199 mD (average 121 mD).

Table 6. Characteristics of wells that cored the Friese Front Formation (SLCF). 17 wells cored this interval, resulting in 607 plug samples taken from 309 m of core length. Measured Depth (MD) refers to depth along hole; True Vertical Depth (TVD) refers to depth below Kelly Bushing.

Well	Cored Formation	Cored Member	Number of Plugs	Core Length (m MD)	Depth Interval (m TVD)	Cored Interval Dry or in Field
F15-06	SLCF		55	49.2	2482.5 - 2531.7	Dry
F17-04	SLCF	SLCFM	28	8.7	2451.9 - 2460.5	F17-FB
		SLCFR	27	18.4	2536.2 - 2554.5	F17-FB
F17-06	SLCF	SLCFM	10	9.8	1646.2 - 1656.0	Dry
F18-02	SLCF	SLCFM	10	5.3	2561.7 - 2567.0	F18-FA
F18-07	SLCF	SLCFM	11	3.0	2445.5 - 2448.4	F18-FA
			27	7.8	2508.1 - 2515.9	F18-FA
F18-09-S1	SLCF	SLCFM	34	24.9	2662.2 - 2687.1	Dry
F18-10-S2	SLCF		20	5.9	2492.8 - 2497.3	F18-FA
G16-03	SLCF		41	13.5	2504.4 - 2515.7	G16-FA
G16-06-S1	SLCF		79	52.4	2561.9 - 2597.3	G16-FA
L02-04	SLCF	SLCFM	22	6.3	2204.6 - 2210.9	Dry
L02-FA-102	SLCF	SLCFM	8	1.8	2039.8 - 2041.6	Dry
L03-01	SLCF		25	8.2	2546.8 - 2555.0	Dry
L05-01	SLCF	SLCFM	16	4.5	2883.0 - 2887.5	Dry
L05-04	SLCF	SLCFM	57	36.4	2638.0 - 2674.4	Dry
			5	1.2	2715.1 - 2716.3	Dry
			19	8.1	2751.7 - 2759.8	Dry
			10	3.0	2804.7 - 2807.7	Dry
		SLCFR	4	1.7	2821.8 - 2823.5	Dry
L05-05	SLCF	SLCFM	15	4.1	2703.9 - 2708.0	L05a-E
L06-03	SLCF	SLCFM	25	14.6	2253.9 - 2268.4	Dry
			53	18.1	2302.9 - 2321.0	Dry
M04-02	SLCF	SLCFM	6	2.0	2824.7 - 2826.7	Dry

Core data from the Friese Front Formation in the Terschelling Basin display a different environment of deposition, as the cross-bedded channel sands are substituted by predominantly alluvial fan and floodplains sediments in well L06-03. Towards the north of the Terschelling Basin, two wells were drilled on the fringe of the Schill Grund Platform: G16-03 and G16-06-S1. Both wells found hydrocarbon-bearing strata in the Friese Front Formation. The formation in well G16-03 consists of two sections, both of which consist of argillaceous sandstones, interpreted as coastal plain deposits, and medium to coarse-grained sandstone with varying proportions of intra- and extraclasts, interpreted as mudflows. The top section is of slightly better reservoir quality than the bottom section, with average porosity of 13% and permeability of up to 13.3 mD. The bottom section has an average porosity of 11% and a permeability of up to 0.74 mD. In well G16-06-S1, the Friese Front consists of a lower sandy interval and an upper, more silty section. The lower sandy part is composed of braided river conglomerate and thinly alternating sheetflood sandstones and lake claystones, which is interpreted as a fan-delta environment. The upper, silty interval contains thick soils and a meandering channel sandbody. The lower, braided river deposits lack intergranular porosity due to extensive matrix formation. The very fine-grained sheet floods have lost most intergranular porosity due to abundant clay content. Reservoir quality in sheetflood deposits is limited to the fine-grained sandstones, which

display up to 3.0 mD. The meandering river sandbody in the upper part of the Friese Front Formation contains a permeability of up to 201 mD. Overall, the sandstones in well G16-06-S1 are less clean than in well G16-03 due to the intercalation of layers with increased clay content. As a result, the sandstones found in well G16-03 display a higher reservoir quality than in well G16-06-S1.

When considering the porosity vs depth relation for the Friese Front Formation, no clear interpretation was possible due to the lack of sufficient uniformly distributed data (Figure 37). Permeability is independent of depth, and hence no clear interpretation was possible for the permeability/depth trend within the Friese Front Formation.

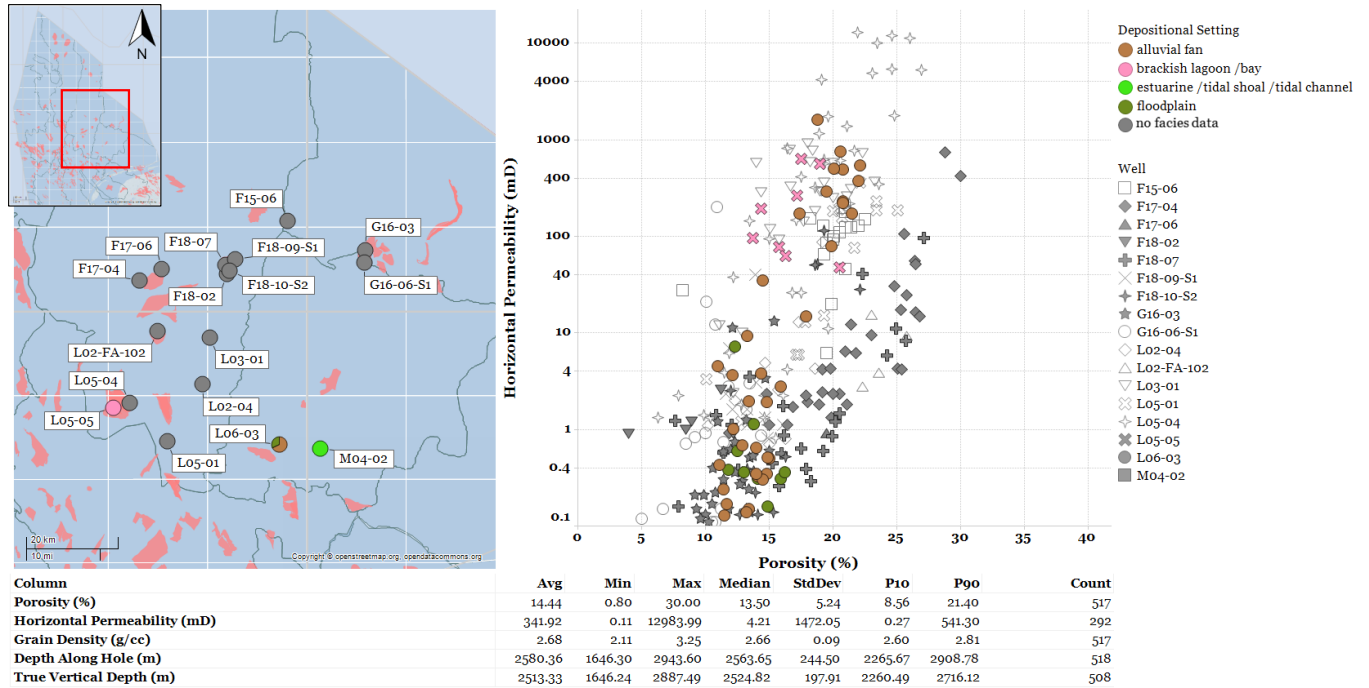


Figure 34. Left: geographical map chart with the locations of all wells that cored the Friese Front Formation. Right: graphic visualization of the plug sample data in a porosity vs permeability plot. Bottom: statistical results of the relevant parameters, where Avg: average, and StdDev: standard deviation. Facies data correlation with plug samples show the dominant depositional environment to be continental, with some depositional settings indicating a more restricted marine environment. Estuarine, tidal shoal/channel deposits are only present in well M04-02 and missing as permeability was measured below the detection limit, which is not included in this plot.

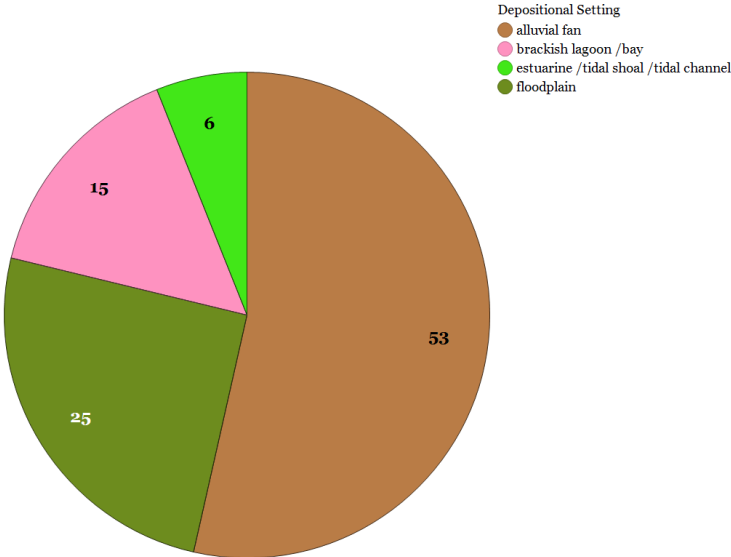


Figure 35. Total amount of plug samples in the Friese Front Formation distributed per facies. Note the dominant environment of deposition is continental.

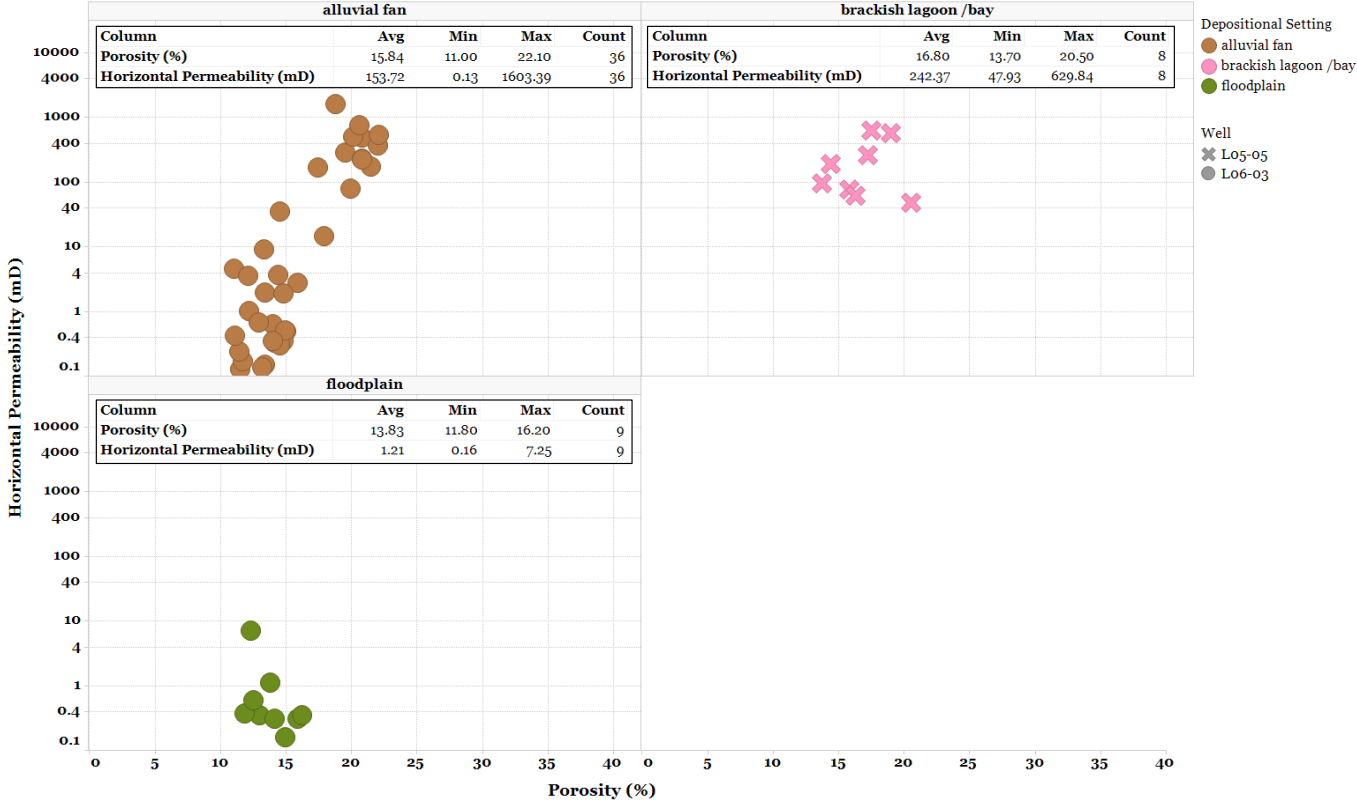


Figure 36. Trellis view of the Friese Front Formation, in which each panel represents a porosity/permeability plot of the total amount of plug samples per facies. Results for the individual facies are shown in the corresponding tables.

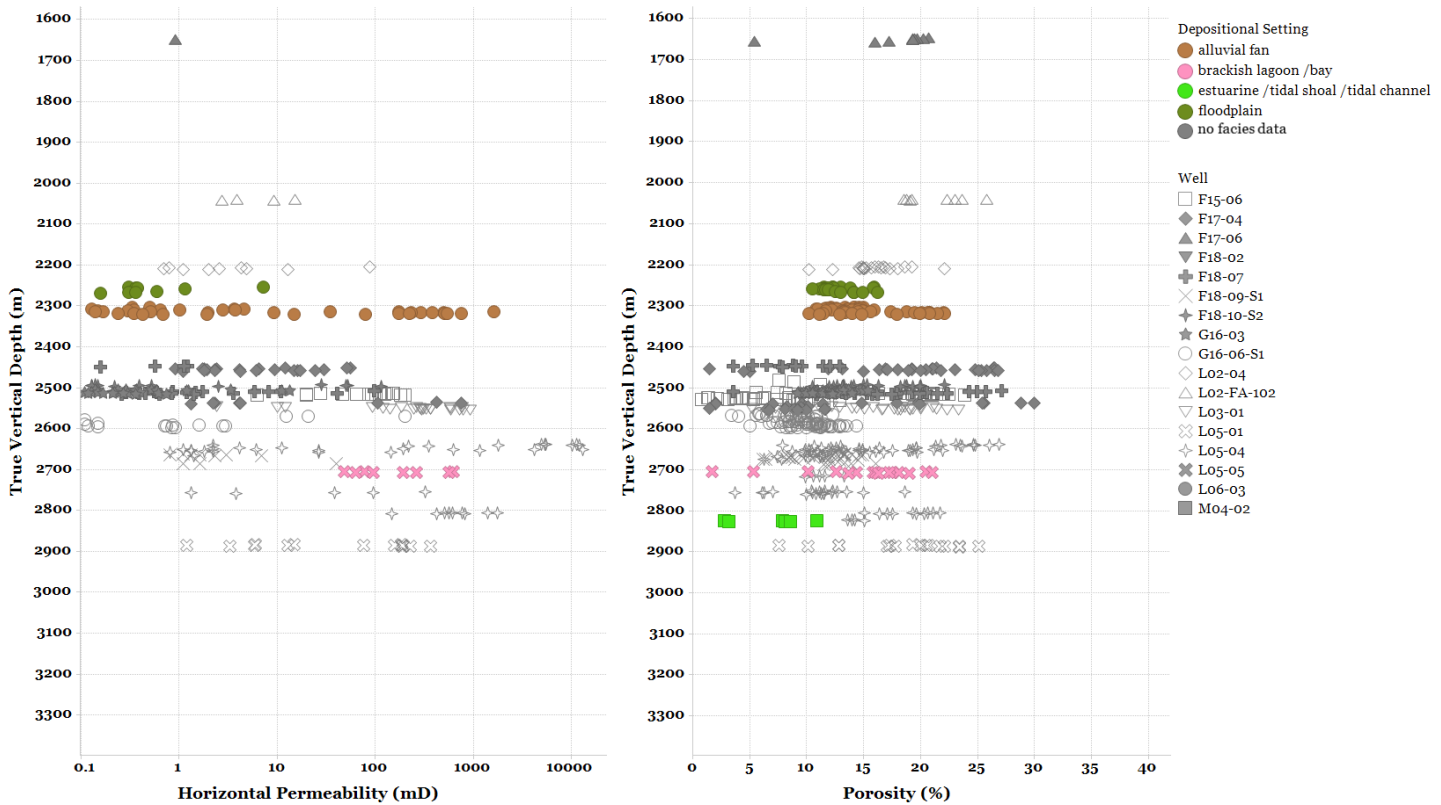


Figure 37. Plug sample data from the Friese Front Formation visualized in a permeability-depth relation (left) and porosity-depth relation (right). Individual facies and wells are specified in color and shape, respectively. Note the relatively high permeability of coarse-grained, cross-bedded fluvial channel sands in wells L05-01, L05-04, and L05-05.

4.5 Skylge Formation (SGSK)

Core data from the Skylge Formation accounted for 426 plug samples from a total core length of 156 m (Table 7). Removal of core plug data below the detection limit resulted in 299 porosity and 296 permeability measurements (Figure 38). Five wells cored the Terschelling Sandstone Member (SGSKT), two wells cored the Noordvaarder Member (SGSKN), and one core was not defined at member level. Hydrocarbon-bearing intervals were cored in L06-02 as part of the L06-FA field, and in well F18-05 within the stranded F18-FA Fregat oil field. The rest of the cores were cut in a dry, water-bearing lithology.

The lithology of the Terschelling Sandstone Member as encountered in the cores consists mostly of medium to (very) fine glauconitic, subrounded to rounded, well-sorted, and occasionally bioturbated sandstone. Thin beds of claystone are present throughout the formation. Especially in wells L06-02 and L06-03, the sandstones are relatively cleaner and coarser, resulting in excellent porosity and permeability. Although the Noordvaarder Member was cored in two wells, only well B13-02 has data on both porosity and permeability. The core from well B13-02 shows a lithology consisting of light grey to grey green, very fine to fine-grained, well sorted, well rounded, glauconitic sandstone. At the bottom of the Noordvaarder Member between 2360 – 2380 m MD, the lithology changes into a conglomerate, with, in addition to euhedral phenocrysts, a bimodal sandstone consisting of fine, rounded grains and very coarse to coarse grains with very poor sorting.

The environment of deposition is predominantly marginal marine, which is characterized by upper shoreface and foreshore deposits present in all wells (Figure 39). To a lesser extent there is also occurrence of sediments deposited in more tidal influenced settings, such as cross-bedded tidal channel complexes in well L06-02, or washover fans deposited in a restricted marine back-barrier environment in well L06-03.

Reservoir quality of the Skylge Formation is generally excellent, as most of the measurements show a porosity within the range of 15 – 30%, with some outliers exceeding 30% and reaching up to 40.0%. Permeability displays an average of 372 mD, with a maximum of 6581 mD. About one fourth of the measurements show a permeability exceeding 100 mD. This is overwhelmingly due to the Terschelling Sandstone Member, which has much better permeability than the Noordvaarder Member.

Estuarine, tidal shoal/channel settings display the best reservoir quality, with a porosity of 2.1 – 38.6% (average 17.4%) and a permeability of up to 6581 mD (average 1016 mD) (Figure 40). Especially well L06-03 shows exceptionally good reservoir quality from sediments deposited in back-barrier washover fans. Upper shoreface, foreshore, and beach settings display a mostly good to excellent reservoir quality, with a porosity of 4.8 – 30.7% (average 19.3%), and a permeability of up to 3303 mD (average 403 mD). Lower shoreface deposits have the lowest reservoir quality, although some samples from well L06-03 show good permeability and excellent porosity.

Although porosity in the Noordvaarder Member is mostly in the 15 – 40% range, permeability has a maximum of only 153 mD (average 28 mD) and reservoir quality is therefore much lower as compared to the Terschelling Sandstone Member. The Noordvaarder member is mostly well-sorted, well-rounded and glauconitic. Only well B13-02 contains measurements on both porosity and permeability. According to the operator, porosity is enhanced in the core due to leaching of oolites. In the core from well F15-02-S1, only permeability measurements were taken. These displayed a range of 0.11 – 6.48 mD (average 0.36 mD), which is low and likely a result of the increased clay content within the cored Noordvaarder Member at that depth.

Interpretation of the porosity vs depth relationship in the Skylge Formation was not possible, as the data display conflicting trends due to an inconsistent distribution along the sampled depth intervals (Figure 41). There is no clear trend that can be derived from the permeability/depth relationship, as permeability appears to be independent of depth. This is especially clear when comparing the plug samples from well L06-02 to the deeper situated plug samples from well M04-02. Permeability is significantly higher in the shallower located plug samples from well L06-02 as compared to well M04-02. However, contrary to what would be expected, porosity from the deeper plug samples of well M04-02 is similar to the core data from well L06-02.

Table 7. Characteristics of wells that cored the Skylge Formation (SGSK). Eight wells cored this interval, resulting in 426 plug samples taken from 156 m of core length. Measured Depth (MD) refers to depth along hole; True Vertical Depth (TVD) refers to depth below Kelly Bushing.

Well	Cored Formation	Cored Member	Number of Plugs	Core Length (m MD)	Depth Interval (m TVD)	Cored Interval Dry or in Field
B13-02	SGSK	SGSKN	35	8.8	2266.7 - 2275.5	Dry
F15-02-S1	SGSK	SGSKN	72	18.3	3248.0 - 3266.3	Dry
F18-05	SGSK	SGSK	45	29.2	2436.5 - 2465.6	F18-FA
L02-04	SGSK	SGSKT	33	16.4	2099.4 - 2115.8	Dry
L06-02	SGSK	SGSKT	112	45.6	2463.3 - 2508.9	L06-FA
L06-03	SGSK	SGSKT	50	15.7	2094.4 - 2110.1	Dry
M01-01	SGSK	SGSKT	27	8.1	2287.2 - 2295.2	Dry
M04-02	SGSK	SGSKT	52	14.0	2636.5 - 2650.4	Dry

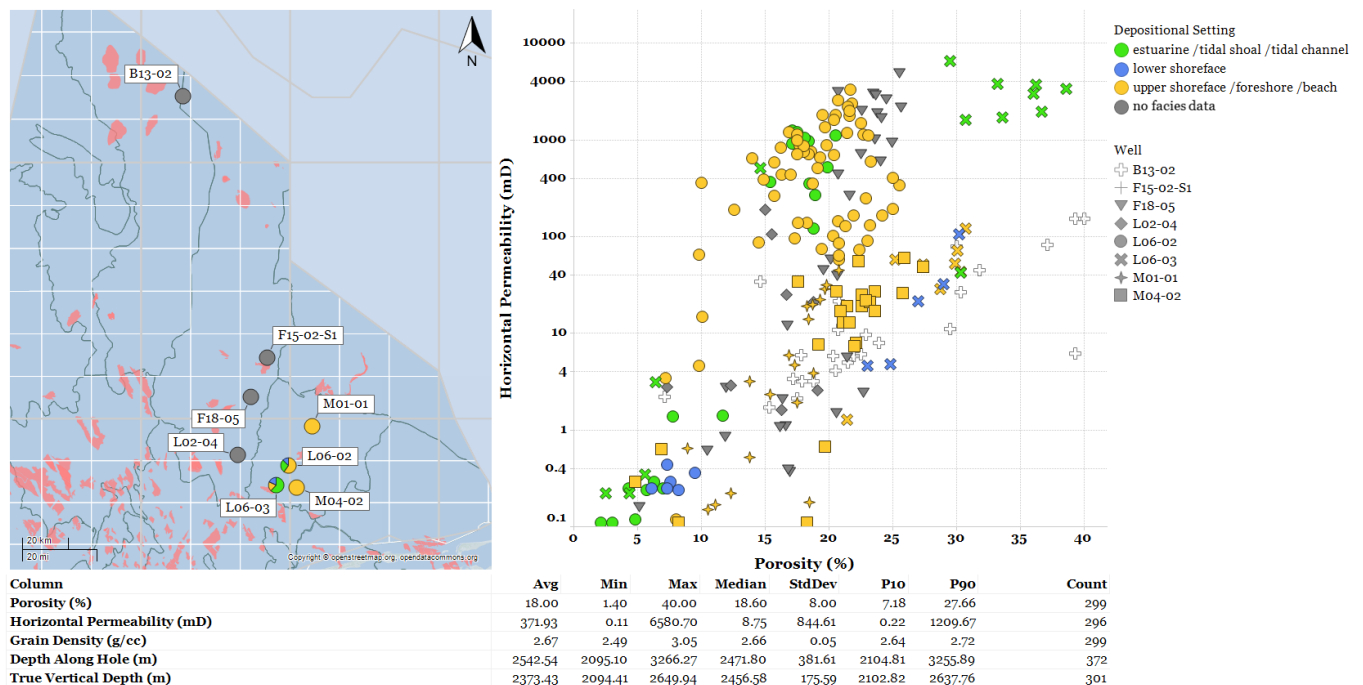


Figure 38. Left: geographical map chart with the locations of all wells that cored the Skylge Formation. Right: graphic visualization of the plug sample data in a porosity vs permeability plot. Bottom: statistical results of the relevant parameters, where Avg: average, and StdDev: standard deviation. Facies data correlation with plug samples show the dominant depositional environment to be marginal marine. L06-02 and L06-03 also have core data that show a restricted marine or even shallow marine environment of deposition. B13-02 is the only well with both porosity and permeability data of the Noordvaarder Member. All other wells cored the Terschelling Sandstone Member, which displays significantly higher porosities and permeabilities compared with the Noordvaarder Member.

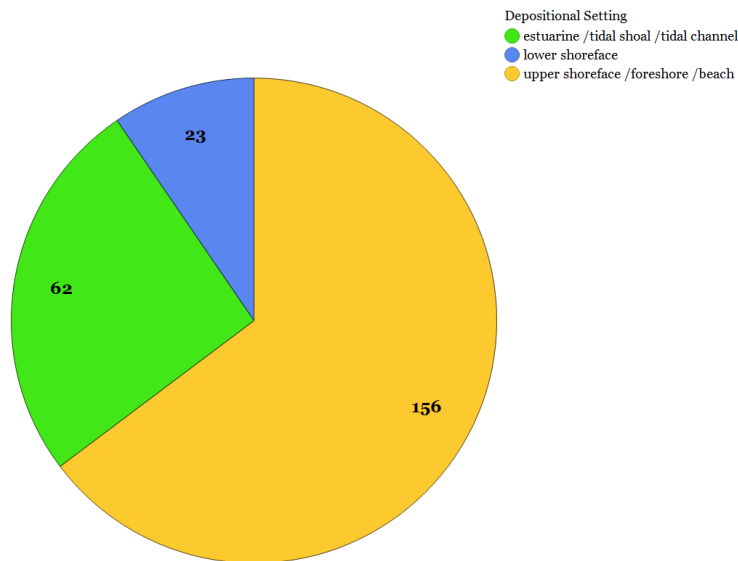


Figure 39. Total amount of plug samples in the Skylge Formation distributed per facies. Note that roughly two-thirds of the core data reflect a mostly marginal marine environment of deposition and one-fourth indicates a restricted marine environment.

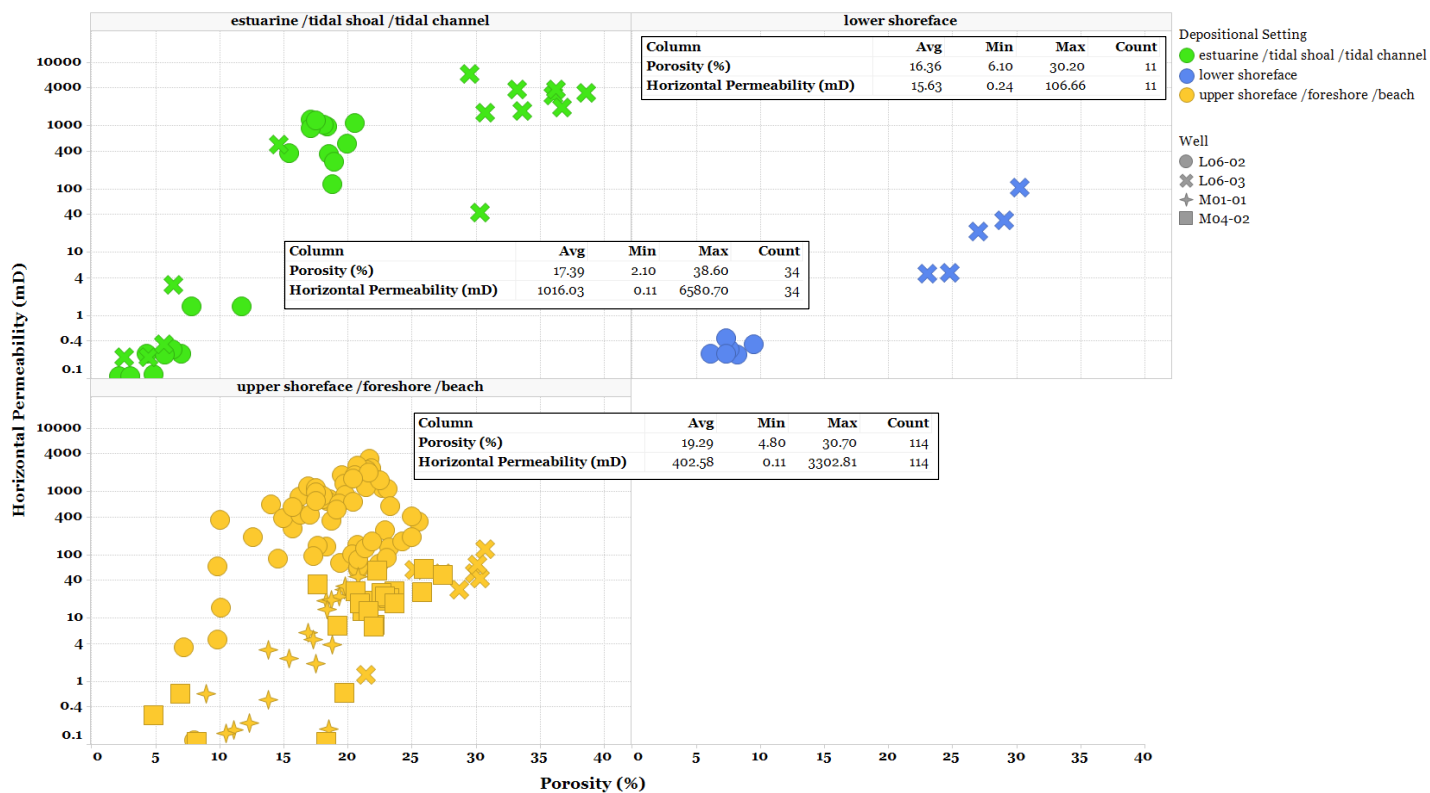


Figure 40. Trellis view of the Skylge Formation, in which each panel represents a porosity/permeability plot of the total amount of plug samples per facies. Results for the individual facies are shown in the corresponding tables.

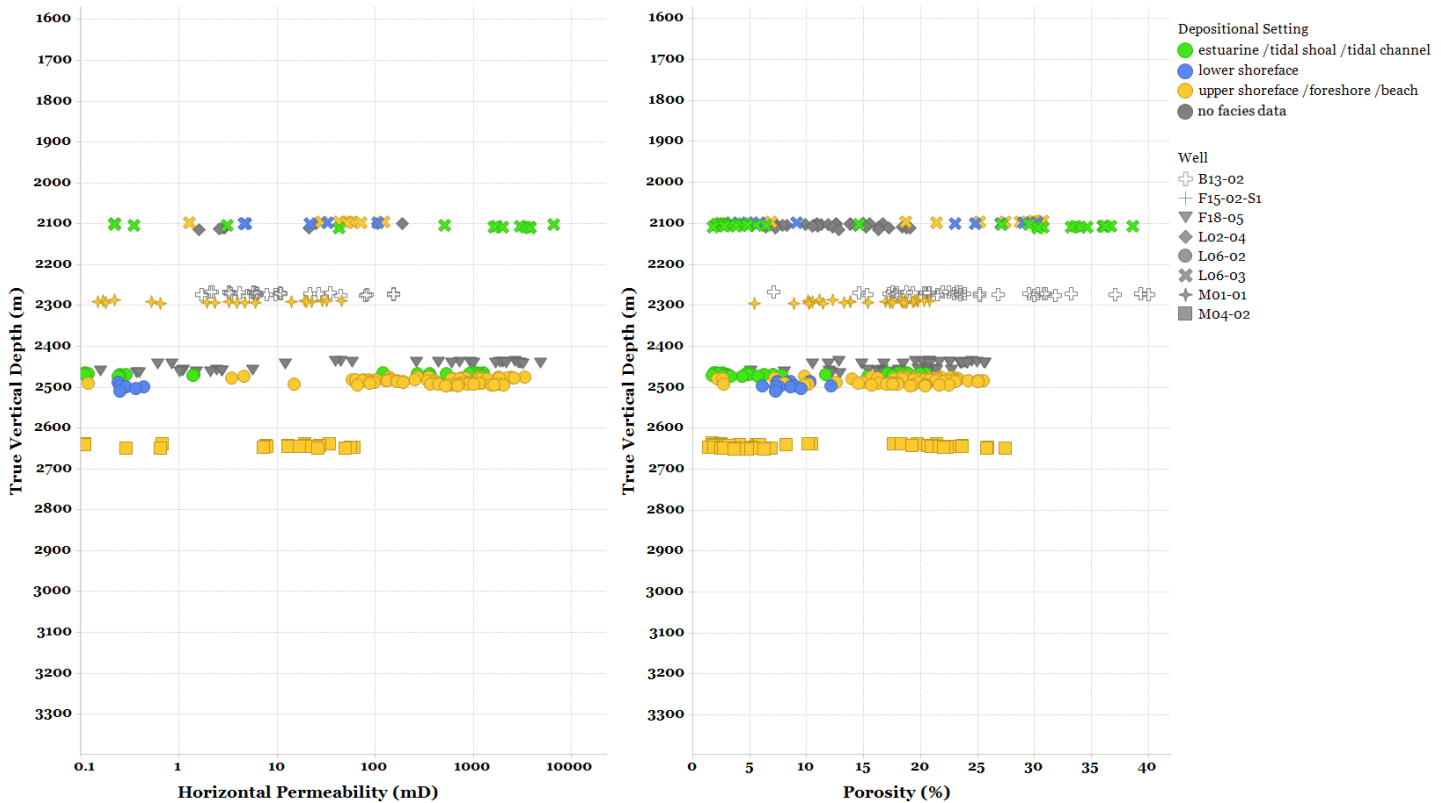


Figure 41. Plug sample data from the Skylge Formation visualized in a permeability-depth plot (left) and porosity-depth plot (right). Individual facies and wells are specified in color and shape, respectively. Note the high porosity in some plug samples from well B13-02 ($>30\%$), whereas permeability is remarkably lower when compared to core data from e.g. wells L06-03, L06-02, and F18-05. These wells contain an overall porosity roughly proportional with permeability.

4.6 Kimmeridge Clay Formation (SGKI)

The Kimmeridge Clay Formation was cored in two wells, with a total of 78 plug samples from 22 m of core length (Table 8). Removal of core plug data below the detection limit resulted in 28 porosity and 21 permeability measurements (Figure 42). The formation consists primarily of clay and shale, with poor reservoir quality as shown by well B14-01. No facies data was available to be linked with the plug samples. The anomalously high reservoir quality of the formation in well F03-FB-107 is likely a result of the presence of sandy streaks at the bottom of the Kimmeridge Clay Formation. When taking the core-depth shift into account, this still shows that about 2.5 m of core was taken from the Kimmeridge Clay Formation, just above the Upper Graben Formation. The core is cut primarily in the Upper Graben Formation, but also partly in the Kimmeridge Clay Formation containing the sandy streaks. These streaks, in contrast with the section of the Upper Graben Formation, were not hydrocarbon-bearing. In well B14-01, the Kimmeridge Clay Formation was specifically cored in a slightly sandier interval, in which the operator recorded oil bleeding. However, although porosity is generally good, permeability is poor. Interpretation of the porosity/depth or permeability/depth relationships revealed no trend (Figure 43).

Table 8. Characteristics of wells that cored the Kimmeridge Clay Formation (SGKI). A total amount of 78 plug samples was taken from 22 m of core length. Measured Depth (MD) refers to depth along hole; True Vertical Depth (TVD) refers to depth below Kelly Bushing. Only two wells cored this interval.

Well	Cored Formation	Cored Member	Number of Plugs	Core Length (m MD)	Depth Interval (m TVD)	Cored Interval Dry or in Field
B14-01	SGKI		61	17.9	2207.5 - 2225.3	Dry
F03-FB-107	SGKI		17	4.3	2542.3 - 2546.4	Dry

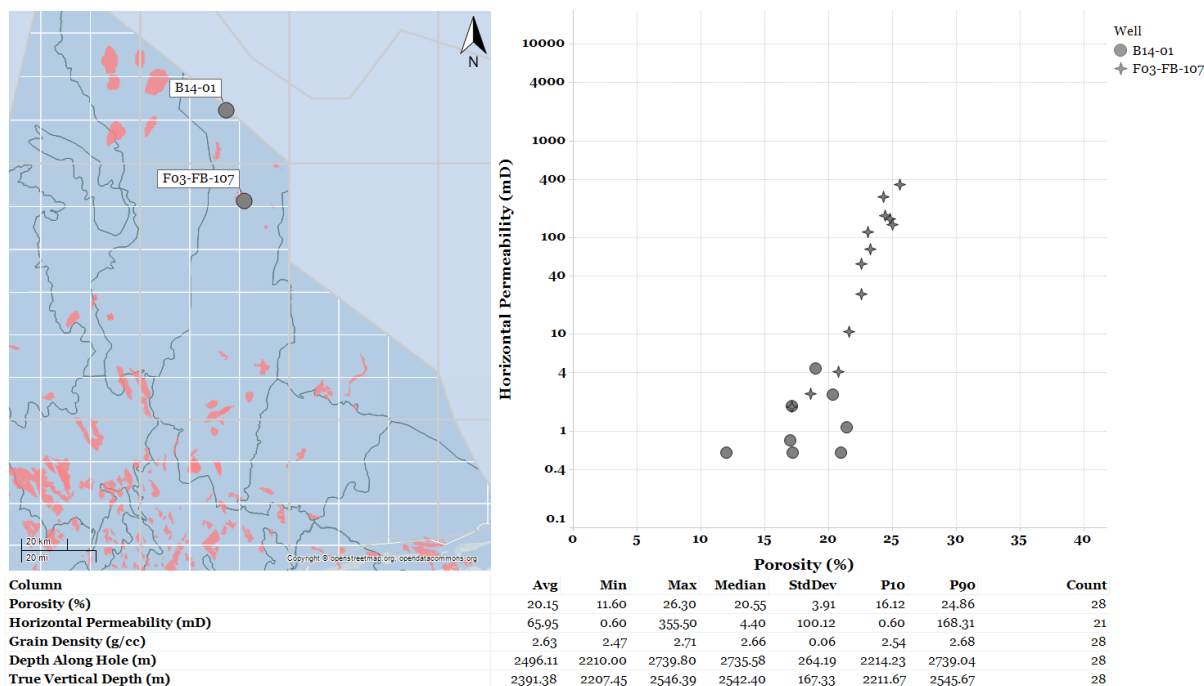


Figure 42. Left: geographical map chart with the locations of all wells that cored the Kimmeridge Clay Formation. Right: graphic visualization of the plug sample data in a porosity vs permeability plot. Bottom: statistical results of the relevant parameters, where Avg: average, and StdDev: standard deviation. Individual wells are specified in shape. No facies data was available for correlation.

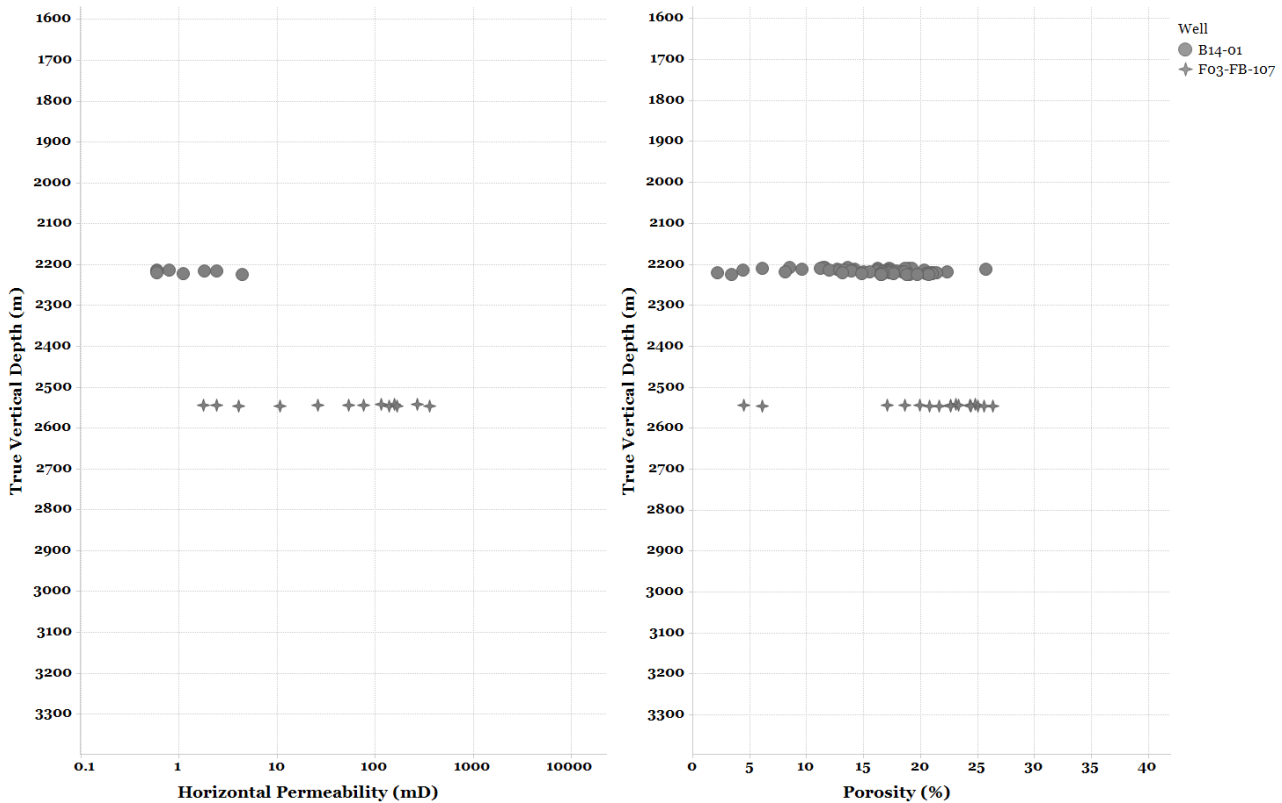


Figure 43. Plug sample data from the Kimmeridge Clay Formation visualized in a permeability-depth plot (left) and porosity-depth plot (right).

4.7 Scruff Greensand Formation (SGGS)

The Scruff Greensand Formation was cored in 17 wells, resulting in 362 m of core length amounting to 1097 plug samples (Table 9). Removal of core plug data below the detection limit resulted in 863 porosity and 531 permeability measurements (Figure 44). The Stortemelk Member was cored in four wells, and the Scruff Spiculite Member was cored in seven wells. Overall, core data from the Scruff Greensand as encountered in the wells consists of a green-colored, often strongly bioturbated sandstone, with varying amounts of glauconite. Grain size varies from well to well. In well L06-02 the grain size is very fine sand, while M07-07 shows medium to coarse sand in the lower 20 m of the core. In addition, well M07-07 also contains thin layers (5-10 cm thick) of very coarse material (gravel and pebbles) within the clean sediments. These layers with angular clasts show reverse grading and are interpreted as gravity flows, as reverse grading is often considered to be a feature of debris flows.

The Scruff Greensand Formation displays a strongly varying reservoir quality. Porosity is poor to excellent and ranges from 3.8 – 37.9%, with an average of 18.4%. Permeability is poor to good, with an average of 6.3 mD and a maximum of 145 mD. The best reservoir quality seems to be more constrained to the north of the Dutch Central Graben in wells F03-01, B18-03, and F03-07. Poor reservoir quality is found in the Terschelling Basin and in most wells in the south of the Dutch Central Graben, with well F18-01 as the only exception. Well M07-07, located in the southeastern most corner of the Terschelling Basin, shows a significantly different distribution of core data, as the cloud of data appears to be shifted to the left with respect of the rest of the wells.

Facies data correlation of 757 plug samples showed that the Scruff Greensand Formation was deposited in a mostly shallow marine environment on a lower shoreface setting (Figure 45). To a lesser extent deposition also took place in a deeper, open marine environment. Distal sediments are encountered in well F15-A-01, L06-02, L06-03 and M07-07. Wells L06-02 and L06-03 contain the most distal sediments, which were deposited in the largest water depths, typically of an open marine environment.

Lower shoreface sands display the best reservoir quality, and can be subdivided into two distinctive trends representing different reservoir qualities, with well M07-07 as the outlier with respect to the rest of the wells (Figure 46). The trend with higher reservoir quality is represented by most of the wells, and displays a porosity of 10.2 – 37.9% (average 24.7%) and a permeability of up to 145 mD (average 14 mD). The trend of lower reservoir quality and only represented by M07-07 shows a porosity of 5.4 – 17.2% (average 12.7%) and a permeability of up to 27 mD (average 3.1 mD).

Open marine sediments have generally poor reservoir quality and show two different trends, with M07-07 again as the outlier. Well M07-07 shows a porosity of 8.3 – 16.9% (average 13.5%) and a permeability of up to 12 mD (average 3.4 mD). The rest of the wells with core data from an open marine setting show a relatively higher reservoir quality, with a porosity of 13.7 – 26.3% (average 19.7%) and a permeability of up to 6.0 mD (average 0.74 mD). The difference for well M07-07 being such a significant outlier is unclear, and multiple potential factors will be provided for explanation later in this study.

Hydrocarbon-bearing intervals within the Scruff Greensand were cored in five wells. In the northern part of the Dutch Central Graben, the wells F03-01 and F03-07 drilled the Scruff Greensand as part of the F03-FA and F03-FC fields, respectively. In well B18-03, the Scruff Greensand turned out to be dry. However, all three wells contain the same lithology, which is characterized by predominantly argillaceous, bioturbated, very fine to fine-grained, well-sorted spiculine sands displaying a light green color due to the presence of glauconite. In wells G16-03 and G16-06-S1, located on the southern border of the Schill Grund Platform, the formation is relatively thin (~10 m), but both wells found hydrocarbons as part of the G16-FA gas field. The G16-03 cored a 2.5 m thick interval with clean sandstone which was gas-bearing. Porosity is poor to good, ranging from 5.9 – 11.6% (average 8.9%), while permeability is poor, with a maximum of 3.4 mD (average 0.42 mD). The cored interval in G16-06-S1 found gas shows in a thin layer of argillaceous sandstones, characterized by abundant presence of glauconite. These sands were deposited in a sandy offshore setting. At the base of the formation, there is a transgressive lag consisting of conglomerate found gas shows in silty sandstones. The argillaceous sandstones and conglomerates within the sandy offshore and transgressive lag display very low permeability with less than 0.11 mD. Locally up to 15% porosity is present, but thin sections show this is mostly microporosity associated with detrital clay matrix and glauconite, and primary porosity is replaced by abundant dolomite cement. Upward fining and increase in clay content reflect deepening of the area during deposition of the Scruff Greensand. Well M07-07 found gas in sands of poor reservoir quality sands (as described above) and defined as the Scruff Spiculite Member.

Table 9. Characteristics of wells that cored the Scruff Greensand Formation (SGGS). 17 wells cored this interval, resulting in 1097 plug samples taken from 362 m of core length. Measured Depth (MD) refers to depth along hole; True Vertical Depth (TVD) refers to depth below Kelly Bushing.

Well	Cored Formation	Cored Member	Number of Plugs	Core Length (m MD)	Depth Interval (m TVD)	Cored Interval Dry or in Field
B18-03	SGGS		48	15.8	2412.1 - 2427.9	Dry
F03-01	SGGS		36	10.5	2359.8 - 2370.3	F03-FA
F03-07	SGGS		73	18.8	2476.5 - 2495.3	F03-FC
F15-02-S1	SGGS	SGGSP	69	8.6	3042.2 - 3050.8	Dry
F15-A-01	SGGS	SGGSS	52	12.7	2558.8 - 2571.4	Dry
		SGGSP	58	6.6	2576.7 - 2583.4	Dry
F16-04	SGGS	SGGSP	15	72.5	3248.8 - 3321.1	Dry
F18-01	SGGS	SGGSP	50	14.7	2200.9 - 2215.6	Dry
F18-10-S1	SGGS	SGGSS	30	8.8	2080.7 - 2087.1	Dry
G16-03	SGGS		11	2.5	2494.4 - 2496.5	G16-FA
G16-06-S1	SGGS		5	1.1	2560.9 - 2561.7	G16-FA
L03-01	SGGS	SGGSP	72	24.0	1996.8 - 2020.8	Dry
L05-01	SGGS		59	18.0	2784.8 - 2802.7	Dry
L05-02	SGGS	SGGSS	59	17.4	2482.4 - 2499.8	Dry
L06-02	SGGS	SGGSP	128	36.0	2226.7 - 2262.7	Dry
L06-03	SGGS		53	17.2	2026.8 - 2043.9	Dry
L09-02	SGGS	SGGSS	90	27.4	2927.9 - 2955.3	Dry
M07-07	SGGS	SGGSP	189	49.2	~2835 - ~2865	M07-B

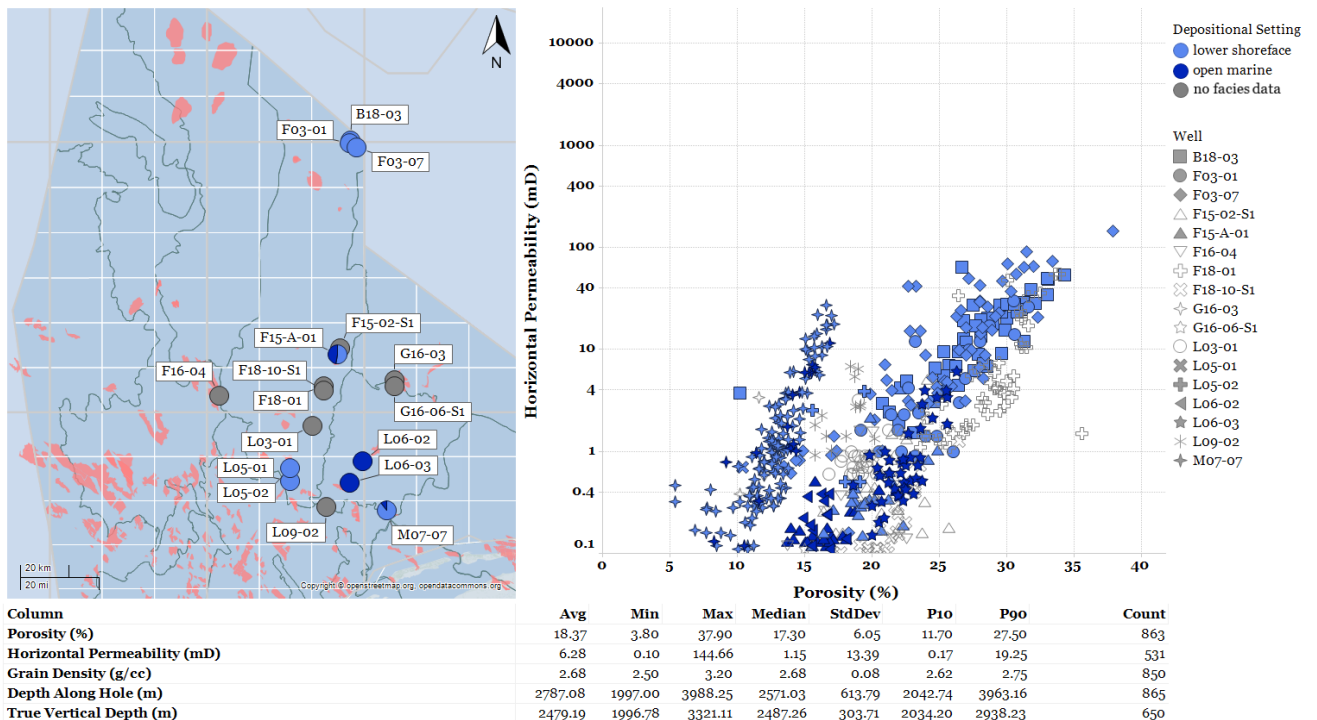


Figure 44. Left: geographical map chart with the locations of all wells that cored the Scruff Greensand Formation. Right: graphic visualization of the plug sample data in a porosity vs permeability plot. Bottom: statistical results of the relevant parameters, where Avg: average, and StdDev: standard deviation. Facies data correlation with plug samples show that the formation was deposited predominantly in a shallow to open marine depositional environment. Note the different trend of the core data from well M07-07.

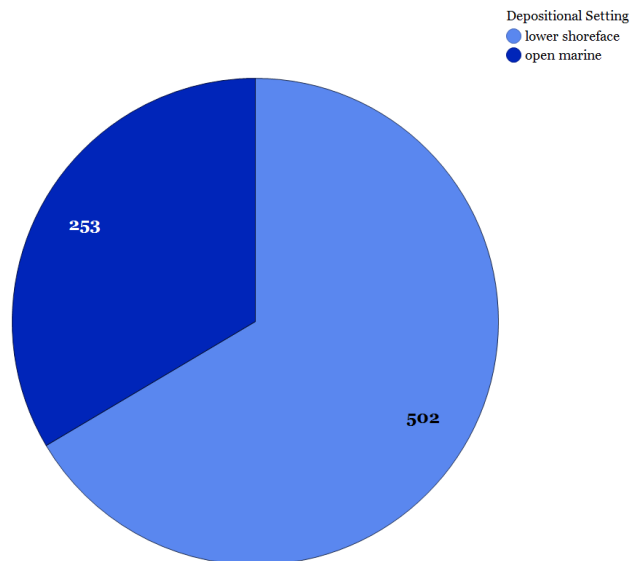


Figure 45. Total amount of plug samples in the Scruff Greensand Formation distributed per facies.

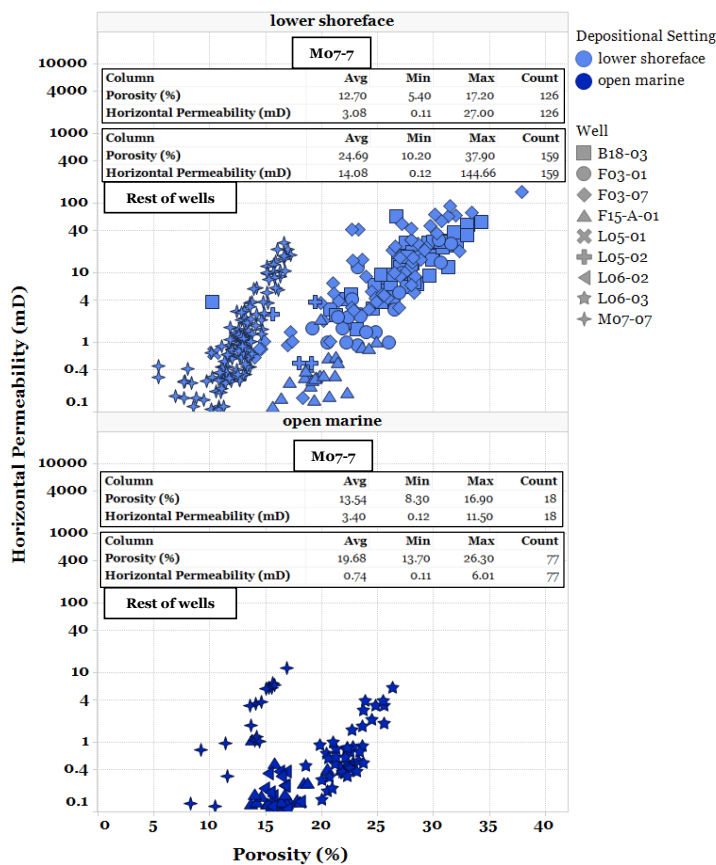


Figure 46. Trellis view of the Scruff Greensand Formation, in which each panel represents a porosity/permeability plot of the total amount of plug samples per facies. Results for the individual facies are shown in the corresponding tables.

Interpretation of the porosity/depth relation is only partly possible due to conflicting data that do not support a conclusive trend for loss of porosity with depth (Figure 47). Especially in the 2000 – 2400 m depth interval, the data do not provide a definite interpretation. When leaving out the core data from well F18-01, one might confidently say that porosity linearly falls with depth, whereas excluding data from well L06-02 suggests a significant increase in porosity. An increase in porosity might be explained by the dissolution of sponge spicules forming the framework grains of the bioclastic sandstone of the Scruff Spiculite Member. A gradual, linear loss of porosity with depth would suggest mechanical compaction as the active porosity-reducing component. For depths between 2400 – 2950 m, this seems to be the case. The permeability/depth trend cannot be constrained with certainty, as the data is conflicting. Moreover, the data suggest that permeability, in contrast with porosity, is practically independent of depth. It must be noted that most measurements were taken in the 2000 – 2600 m depth interval, and that, especially for permeability, below a depth of 2600 m there is not sufficient data to provide a clear interpretation.

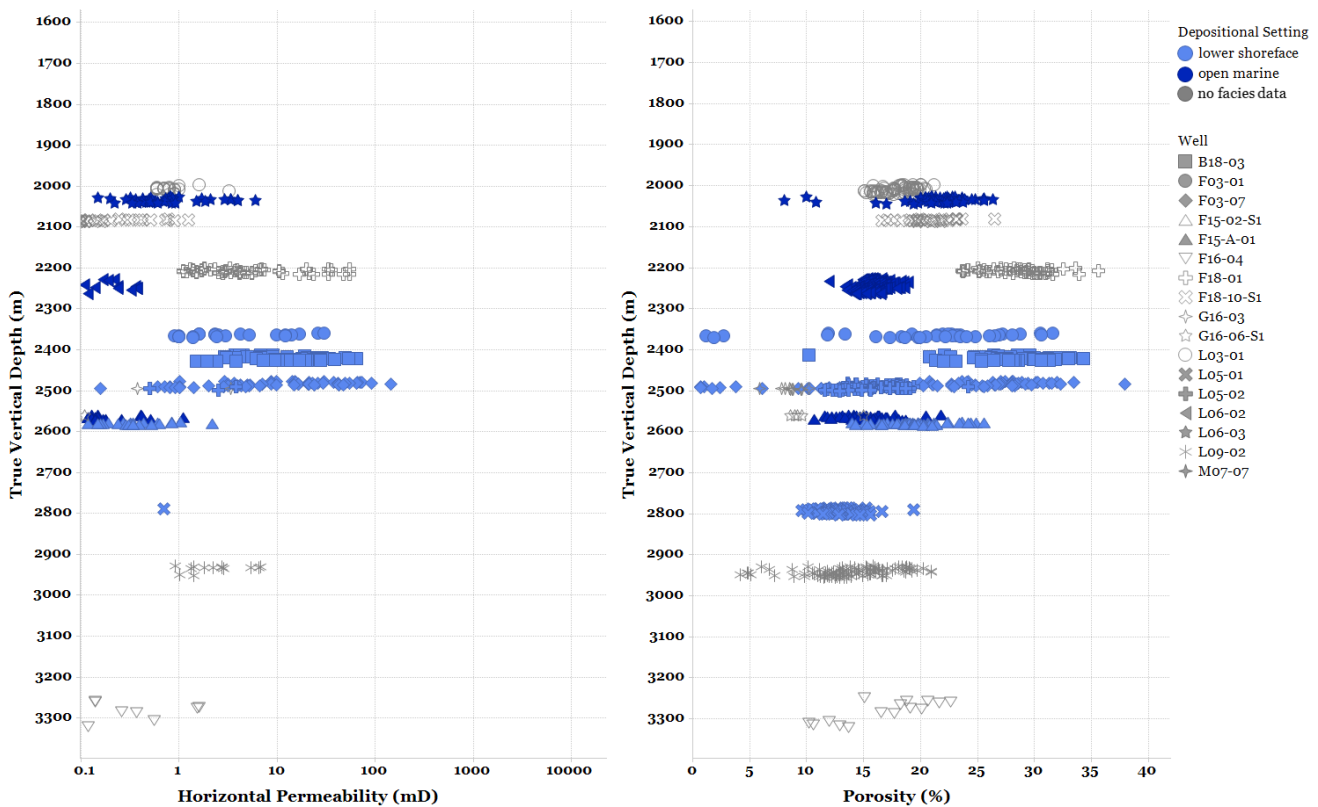


Figure 47. Plug sample data from the Scruff Greensand Formation visualized in a permeability-depth plot (left) and porosity-depth plot (right).

4.8 Lutine Formation (SGLU)

The Lutine Formation was cored only in well M07-03, with 25 plug samples from a 6 m long core. The formation is mostly glauconitic sand with high clay content. Removal of core plug data below the detection limit resulted in 23 porosity and 22 permeability measurements (Figure 48). Well M07-03 shows good porosity, but poor permeability. Reservoir quality is therefore poor. Correlation of facies with plug sample data was not possible due to the lack of facies data. Interpretation of the porosity/depth and permeability/depth relations was not possible due to the lack of sufficient data.

Table 10. Characteristics of wells that cored the Lutine Formation (SGLU). A total amount of 25 plug samples was taken from 6 m of core length. Measured Depth (MD) refers to depth along hole; True Vertical Depth (TVD) refers to depth below Kelly Bushing. Only one well cored this interval.

Well	Cored Formation	Cored Member	Number of Plugs	Core Length (m MD)	Depth Interval (m TVD)	Cored Interval Dry or in Field
M07-03	SGLU	SGLUS	25	6.0	2725.0 - 2731.0	Dry

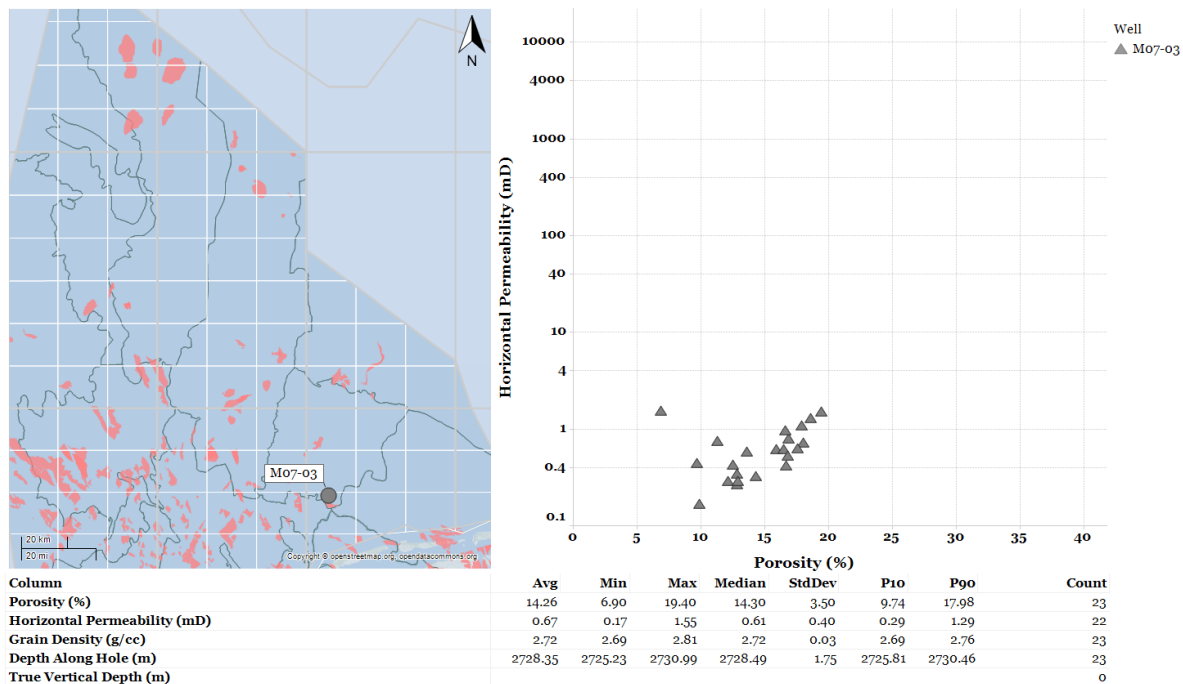


Figure 48. Left: geographical map chart with the locations of all wells that cored the Lutine Formation. Right: graphic visualization of the plug sample data in a porosity vs permeability plot. Bottom: statistical results of the relevant parameters, where Avg: average, and StdDev: standard deviation. No facies data was available for correlation.

5. Results – Controls on Reservoir Properties

5.1 Main findings and uncertainties

Before a sediment undergoes diagenesis, its reservoir properties are primarily controlled by the sediment composition, including its mineralogy and textural characteristics such as grain size, sorting and angularity (Bjørlykke, 2014). The overall composition of a sediment is a function of its provenance and the prevalent depositional environment, where processes such as climate, weathering and erosion play an essential role (Figure 49). After deposition, sediments are altered by diagenesis, which includes the combined effects of burial, bioturbation, compaction, and chemical reactions in the absence of surface processes (Ali et al., 2010).

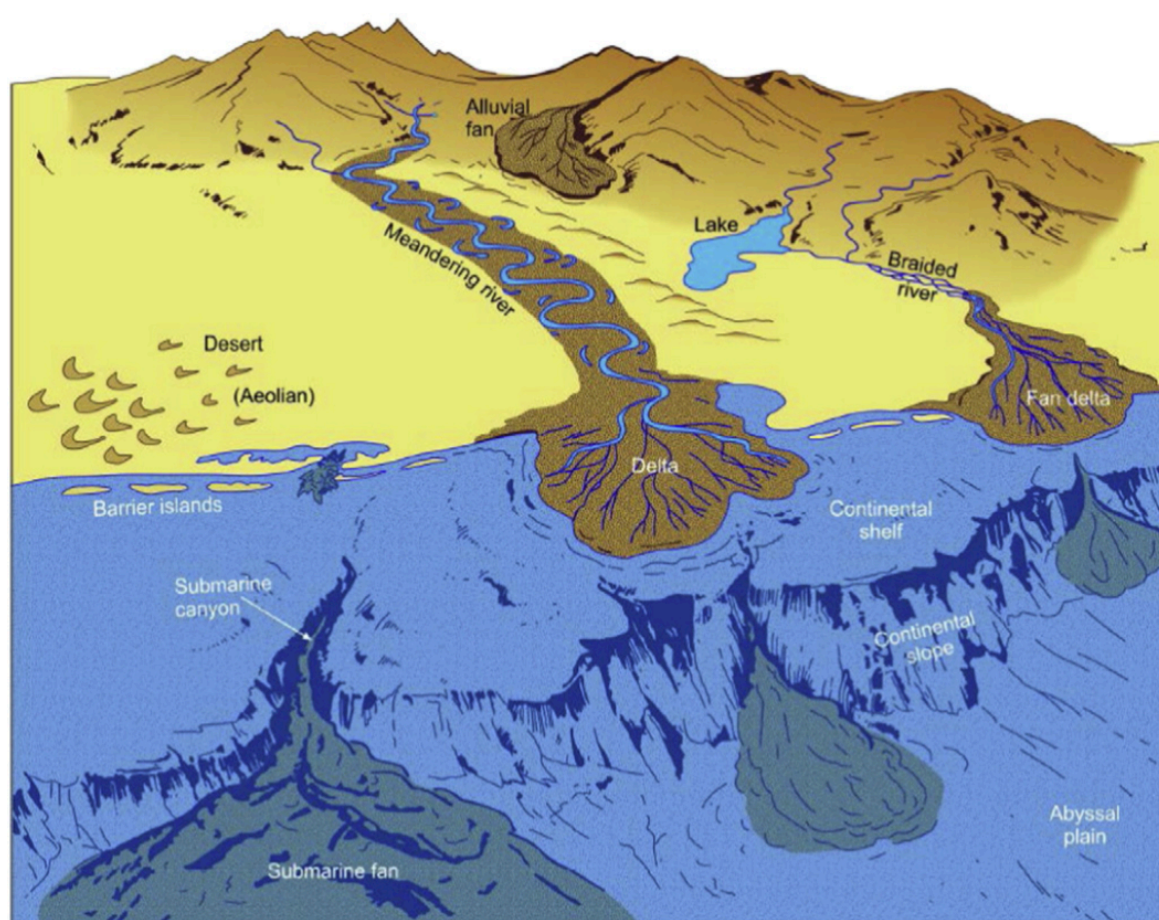


Figure 49. Simplified illustration of common facies on a passive continental margin. Before burial, the depositional environment, provenance, and climate are the most important factors determining reservoir properties by controlling mineralogy and textural characteristics such as grain size, sorting, and angularity. Different depositional settings can have widely different mineralogies. Source: Bjørlykke (2014).

The core plug samples from the Upper Jurassic – Lower Cretaceous formations in this study display a variety of sediment compositions, each of which shows a wide range in reservoir quality. This study looked at the various processes involved in controlling reservoir properties and hence reservoir quality. Although mechanical compaction and clay form the essential part in determining ultimate porosity and permeability, there are various other factors that influence reservoir properties before, during, and after

deposition. Although this study did not incorporate all of these processes, the most important and their effects are discussed below. They vary from processes active at the surface such as depositional environment, provenance, and dissolution due to flushing of meteoric waters, towards burial diagenesis effects such as mechanical compaction, chemical compaction, and dissolution of framework grains. Other factors that are only broadly considered and may affect reservoir properties are allochthonous salt, overpressures, and early hydrocarbon emplacement.

The immediate problems that arise when interpreting the relations between reservoir properties of individual Upper Jurassic – Lower Cretaceous formations and depth is that there is either insufficient uniformly distributed data, or that the data show conflicting trends. This represents the strong heterogeneity of the Upper Jurassic – Lower Cretaceous reservoir sands, which is a direct result of its diverse depositional history. The recognition of the different formations is based on different depositional environments and hence the heterogeneity, and the combined effects of burial diagenesis provide the final footprint on the reservoir quality, which makes distinguishing trends between individual facies even more challenging. However, when viewing the core data from all formations together, as in Figure 21, interpretation of relations between reservoir properties and depth becomes possible. This suggests that the effects of burial diagenesis are similar for vastly differing sediment compositions (Figure 20, Figure 21).

The most important control on initial porosity and permeability is the environment of deposition, which directly affects the presence of clay and hence the degree of cleanness of the sand by filling pores and clogging pore-throats. The ratio of sand to clay and hence the ultimate sediment composition is defined by the prevalent energy conditions. Low-energy conditions generally lead to increased clay content, whereas high-energy conditions tend to lead to increased input of sand. The wide range in reservoir quality and hence porosity and permeability data is a direct result of the many different types of depositional environments that were active in the Late Jurassic to Early Cretaceous times.

After deposition, burial diagenesis is the dominant control on reservoir quality, as mechanical and chemical compaction can significantly reduce porosity and permeability (Figure 50). Primary porosity of sandstones is commonly 25 – 40%, which can be reduced to zero by diagenesis (Bjørlykke, 2014). Furthermore, pore diameter and pore throat size are closely related to particle size and sorting. However, for the samples in this study the lack of a clear relation between permeability and depths up to 3000 m indicate that burial diagenesis exerts only a minor control on permeability. The difference with the linear loss of porosity at depths up to 3000 m suggests a greater control of burial diagenesis on porosity. The onset of permeability loss and increased porosity loss from depths of 3100 m onwards could be due to the start of chemical compaction, resulting in precipitation of clay minerals by process such as cementation and authigenesis, which significantly deteriorate reservoir quality. However, core plug measurements in the 3100 – 3300 m depth are mostly from the Lower Graben Formation in the F03-FB field, and these samples display different depositional environments, which could also explain the difference in permeability and porosity compared with shallower depths.

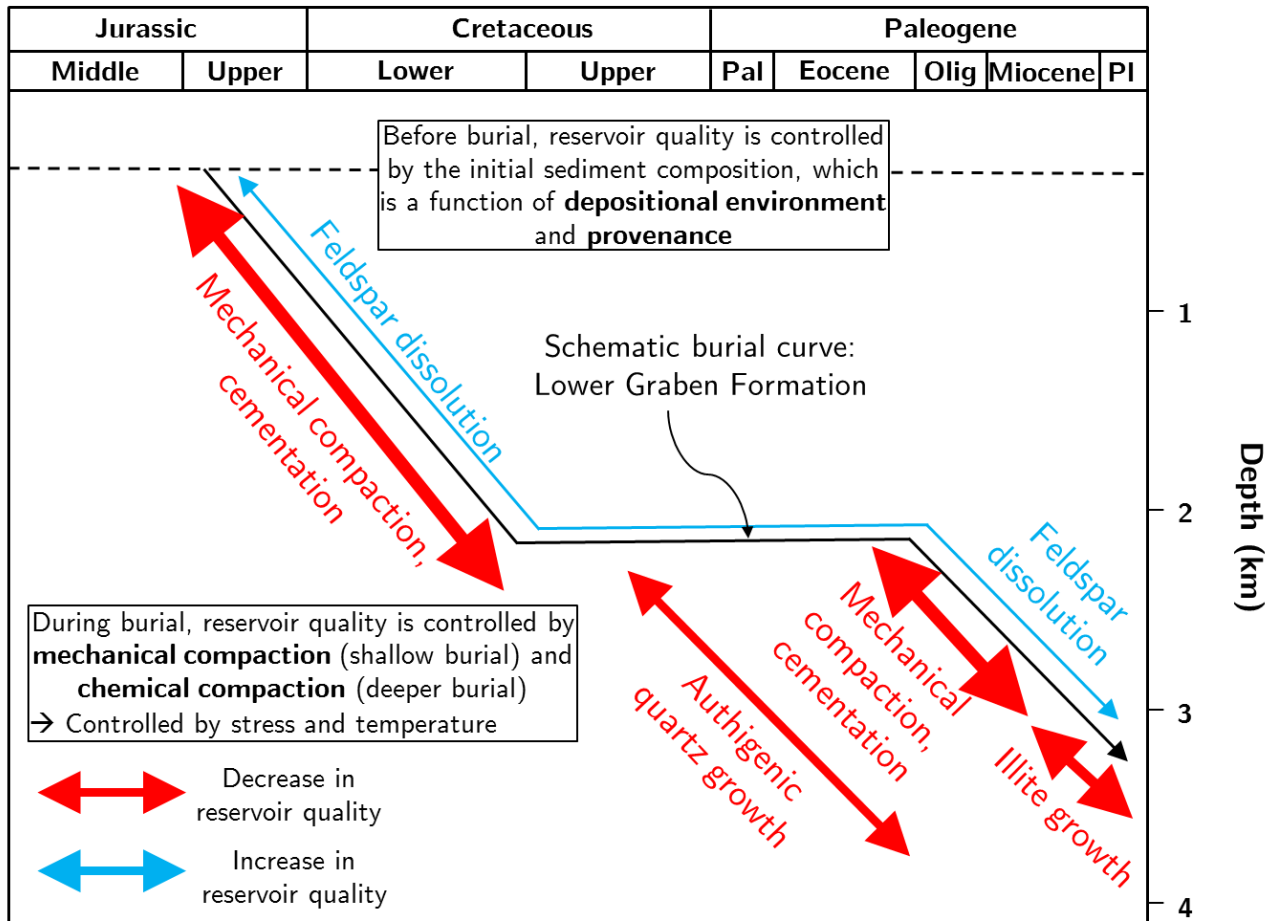


Figure 50. Schematic representation of the main controls on reservoir properties for an example burial curve of the Lower Graben Formation, which underwent the deepest burial in this study. Arrow thicknesses indicate relative impact of each effect. The ultimate reservoir quality displayed by a lithology is the result of the combined effects occurring before and after burial, each of which has a different impact.

5.2 Applicability of the revised lithostratigraphic scheme

The revised lithostratigraphic scheme as proposed by Munsterman et al. (2012) provides a clear differentiation between Upper Jurassic to Lower Cretaceous formations based on depositional environments. This allows for correlation between different sections of the southern North Sea such as the Danish Tail End Graben and the UK Central Graben, which may have been deposited in equivalent environments. In the case of different depositional environments between some sections of the southern North Sea, this could be explained by lateral variation in facies. Especially in the case of the Dutch Central Graben, there are significant differences in depth. As the graben tends to deepen towards the north, this means that different facies can belong to the same system that was deposited in a certain time. However, sea-level fluctuations are not the only factor that determine migration of depositional systems and hence facies. The movement of salt has led to local uplift and erosion, resulting in local deposition of sand, such as the Noordvaarder Member and the Scruff Greensand Formation, which tend to widely vary in presence as well as thickness. Assigning these locally-derived sands to specific sequences resulted in a better understanding of the dispersion of reservoir sands during Late Jurassic – Early Cretaceous times.

Problems arise with correlation with the Entenschnabel, the German sector of the Central Graben. Exploration has taken place in this area, but there is a lack of publicly available information. Although the Entenschnabel is a relatively minor part compared with the rest of the Central Graben, correlating its strata with the Dutch Central Graben and the Danish Tail End Graben would provide a seamless lithostratigraphic fit, which would improve the overall understanding of the southern North Sea basin. Recent interpretations of seismic mapping by Arfai et al. (2015) showed increased sediment thicknesses in rim-synclines, which indicated that most of the salt structures in the German Central Graben had their main growth phase during the Late Jurassic. Therefore, these sediments would correlate well with similar deposits in the Dutch and Danish sections of the Central Graben.

5.3 Lithology and Depositional Environment

As expected, the formations with a lithology consisting of better sorted, cleaner sands, generally display a better reservoir quality than formations with increased clay content, i.e. an inverse relationship exists between clay content and reservoir quality. Clean sands with relatively high porosity ($>15\%$) and permeability (>50 mD) were found in the Lower, Middle, and Upper Graben formations, as well as the Friese Front Formation, the Terschelling Sandstone Member, and the Scruff Greensand Formation. Lithological units with relatively more clay content such as the Kimmeridge Clay, and Lutine formations have comparable porosity (up to 20%), but especially lower permeability (<10 mD), which often reach below the detection limit. Wide ranges in porosity and permeability exist within individual formations and are primarily attributed to the large variations in clay content. Even generally sandy formations rarely – if ever – consistently contain the same degree of cleanness in sands.

The depositional environment plays a very large role in determining the sediment composition prior to burial by controlling sediment distribution, grain size, and sorting (Bjørlykke, 2014). This directly affects sand and clay content of the lithology at the time of deposition. As expected, the classification of the core data according to the prevalent depositional environment reveals that certain facies display a significantly better reservoir quality than others. Intervals with better reservoir quality are generally present in depositional settings with relatively higher energy conditions that produce cleaner, better sorted sands with less clay content (Figure 53).

5.3.1 Lower, Middle, and Upper Graben formations: marginal marine sands

Reservoir sands of the Lower, Middle, and Upper Graben formations have an excellent reservoir quality for each of the three lithostratigraphic intervals. Although there are some differences in reservoir quality, these do not affect the degree of reservoir quality from the oldest to the youngest unit.

The Upper Graben Formation has excellent reservoir quality in well F03-FB-107, with a porosity ranging between $15 - 30\%$ and a permeability of up to 3950 mD. Although no exact information on the depositional environment is available, Munsterman et al. (2012) indicated that these sands were deposited in a marginal marine barrier-island system, which likely explains the excellent reservoir quality. The relatively shallower burial of the Upper Graben Formation compared with the Lower Graben Formation could also explain the relatively higher porosity and permeability due to reduced mechanical and chemical compaction.

The Middle Graben Formation was cored in three wells and has the highest reservoir quality in well F03-FB-105-S3, with a porosity of 20 – 33% and permeability of 2615 mD in a 25 m thick clean sand. This reservoir quality is comparable with the quality of reservoir sands encountered in well F03-FB-107, which is likely due to the relative proximity of these wells in the F03-FB field.

The Lower Graben Formation has excellent reservoir quality in tidal channel sands with a porosity of up to 25% and a permeability of up to 2050 mD. Most of the core data on the Lower Graben Formation comes from the F03-FB field. The fact that the Lower Graben Formation has a somewhat lower porosity and permeability with respect to the Middle and the Upper Graben formations could be due to increased influence of effects related to burial diagenesis such as mechanical and chemical compaction. Giles et al. (1992) showed that at for depths deeper than 3015 m, chemical compaction induces rapid permeability loss due to increased precipitation of clay minerals such as illite and kaolinite. As this depth interval is similar to the depth interval of the Lower Graben Formation, this could be a valid explanation.

5.3.2 Friese Front Formation: alluvial fan deposits and fluvial channel sands

The exceptionally excellent reservoir quality (porosity 15 – 27%; permeability up to ~13000 mD) found in well-sorted sands of the Friese Front Formation in well L05-04 is of special interest. Although well L05-04 cored a dry interval, the reservoir quality is relatively higher than in well L05-05 (porosity 15 – 20%; permeability up to 630 mD), which cored a hydrocarbon-bearing interval. Other wells that cored the Friese Formation have found sands with comparable porosity but with permeability at least one order of magnitude lower. The clean sand intervals within the Friese Front Formation have relatively small thicknesses (5 – 10 m), and the extent of lateral continuation is unknown. Although the exact depositional environment is not known, considering the strongly varying thicknesses and the exceptional cleanness of the sands, this strongly suggests a fluvial origin.

Alluvial fan deposits in the Friese Front Formation also have a remarkably good reservoir quality (porosity 11 – 22%; permeability up to 1600 mD) in some sections due to the increased sand content in the sampled sections. Other sections of excellent reservoir quality include clean, well-sorted fluvial channel sands, that are mostly present in the southernmost part of the Dutch Central Graben, in blocks L02, L03, L05, and L06. Reservoir sands in the relatively northern blocks of F17, F18, and G16 have significantly poorer reservoir quality compared to the southern blocks, which is likely due to increased clay content at the time of deposition, when the Dutch Central Graben deepened towards the north. The outlier, well F15-06, was drilled on the Schill Grund Platform on the southwestern junction of the Dutch Central Graben and the Terschelling Basin. It contains a 5 m interval of Friese Front Formation with good reservoir quality situated between two carbonate intervals below an unconformity, above which there is another 30 m of Friese Front Formation. The existence of an unconformity may have resulted in flushing of meteoric water through the formation, which could have enhanced reservoir quality by weathering effects.

5.3.3 Skylge Formation – Terschelling Sandstone Member: marginal marine sands

The Skylge Formation contains excellent reservoir quality in clean well-sorted sandstones of the Terschelling Sandstone Member, as demonstrated by the consistently high porosity (up to 39%) and permeability (up to 6580 mD). Estuarine & tidal shoal/channel produce the best reservoir quality

(porosity up to 39%; permeability up to 6580 mD). Similar depositional settings also produced good reservoir quality (porosity up to 25%; permeability up to 2050 mD) in the Lower Graben Formation, although the overall quality is less than in the Terschelling Sandstone Member. One explanation for the difference in reservoir quality of the Lower Graben Formation is increased clay content due to differences in formation. Another explanation is increased burial (up to 3300 m) of the Lower Graben Formation resulting in increased mechanical compaction as well as effects attributable to chemical compaction. The significantly shallower burial (2100 – 2600 m) of reservoirs sands of the Terschelling Sandstone Member suggest that at least some quality is retained due to reduced mechanical and chemical compaction.

The upper shoreface barrier island sands of the Terschelling Sandstone Member also display a good reservoir quality (porosity up to 20%; permeability up to 3300 mD), and can form relatively thick deposits of up to 83 m (Munsterman et al., 2012). They can be compared to sands of the Heno Formation in the Danish Central Graben, which are the product of deposition in a similar setting. Johannessen et al. (2010b) investigated unusually (~88 m) thick Upper Jurassic transgressive barrier island and shoreface sandstones of the Heno Formation that characterize the Freja oil field in the Danish Central Graben. The unusual thickness of the barrier island complex could be explained by an analogue barrier island system in the Danish part of the NW European Wadden Sea. This barrier island developed during a relative sea-level rise of ~15 m during the last 8000 years and is up to 20 m thick. An explanation is that sedimentation kept pace with rapid sea-level rise, resulting in aggradation and even seaward progradation of the barrier island due to abundant supply of sand (Johannessen et al., 2010b). The striking similarities between the Heno Formation and the Terschelling Sandstone Member of the Skylge Formation in timing, thickness, architecture, and depositional environment, strongly suggests that a large surplus of sand could also have caused aggradation and/or progradation of Sequence 2 sands not only in the Terschelling Basin, but also in other unexplored parts of the Dutch Central Graben.

5.3.4 Skylge Formation – Noordvaarder Member: shallow marine sands and mass-flow sandstones of the Brae Formation in the UK

The Noordvaarder Member was only cored in two wells (B13-02 and F15-02-S1), and only well B13-02 had sands with good reservoir quality (porosity 15 – 40%; permeability up to 150 mD). Well F15-02-S1 showed a consistent poor permeability of <0.50 mD, with no data on porosity. The poorly sorted sands may explain the lower permeability, even though porosity is high.

The depositional environment of the Noordvaarder Member is considered shallow marine by Munsterman et al. (2012), and although it had only one core with both porosity and permeability data, the potential is promising in other sections of the Dutch Central Graben. Numerous wells that drilled this interval showed thick, clean sands and in the case of well B13-02 the lower part of the member is a conglomerate and the thickness exceeds 170 m. Local deposition of these sands could have occurred in response to movement of salt resulting in the further tilting of fault blocks (Figure 51). Dipping of the strata and the presence of thick Noordvaarder sands indicate that salt movement was active during deposition of Sequence 2. Furthermore, areas with thicker Noordvaarder sandstones were identified along the northern graben fault, with thinner sands further away from the structure.

An analogue in the UK Central Graben can be the reservoir sands in the Fife field, which were deposited partly in a shoreface setting and partly by similar gravity-flow processes, which have led to deposition of massive, partly channelized, sub-marine fan sands that constitute large reservoirs with good reservoir quality (Johnson et al., 2005). Furthermore, in the Kimmeridge Clay, mass-flow processes formed local bodies of sandstone known as e.g. Ribble Sandstone. In the Heather Formation, similar sand bodies are referred to as e.g. the Freshney Sandstone Member. Recent research of the provenance of Upper Jurassic to Lower Cretaceous gravity-flow sandstones in the deep-marine Farsund Formation indicates that deposition in the Danish Tail End Graben was controlled by multiple locally sourced mass-flow systems and not by one basin axial flow (Nielsen et al., 2015). Proven hydrocarbon-bearing Upper Jurassic sandstone reservoirs at depths deeper than 5 km have been found in the northern part of the Danish Central Graben with the recently discovered Hejre field, and this HPHT sandstone play provides a future exploration target (Johannessen et al., 2010a). Intercalation of gravity-flow sandstones in offshore claystones were mainly deposited during the Late Kimmeridgian to Early Volgian, and the Late Middle Volgian to Ryazanian in the central part of the Tail End Graben (Johannessen et al., 2010a).

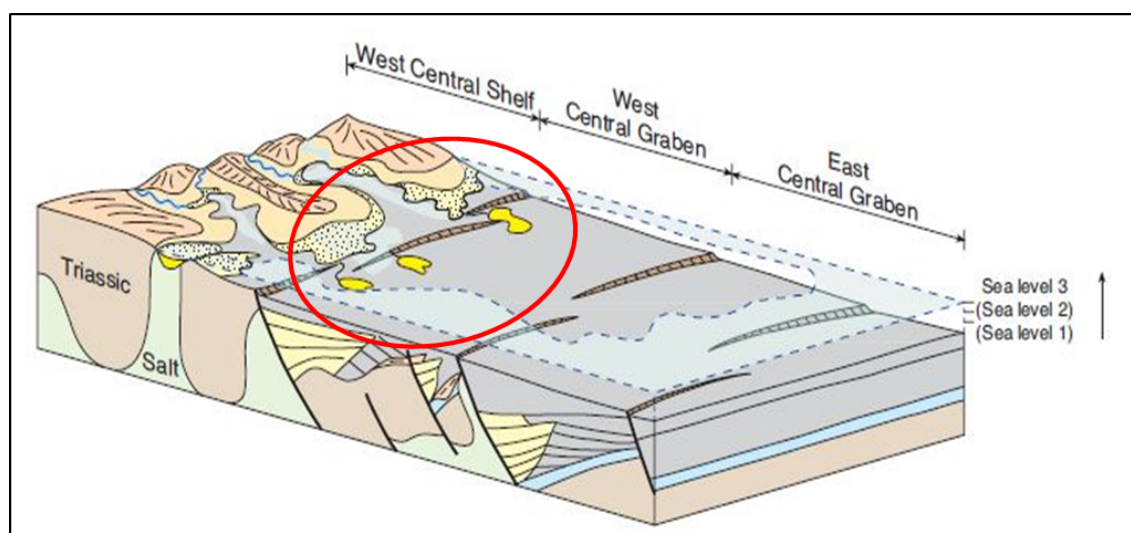


Figure 51. Postulated depositional environment of the Noordvaarder Member, which suggests local deposition of sand bodies due to salt movement and/or fault activity. Source: Fraser et al. (2003).

Due to the similarities between the Dutch and Danish sectors of the Central Graben, gravity-flow sand bodies are also expected in the Kimmeridge Clay Formation and perhaps also in the Lutine Formation within the northern Dutch offshore. Currently, there are no known studies that have addressed this subject. According to Erratt et al. (2010), the relative lack of deep marine mass-flow reservoirs in the central and southern North Sea can be caused by provenance and reservoir fairway development resulting from the basin architecture. However, the absence of mass-flow deposits within deep-marine mudstones of the Kimmeridge Clay Formation in the current lithostratigraphic framework for the northern Dutch offshore does not mean that they have not been deposited at all, as the amount of data currently available is limited. The South Viking Graben and Moray Firth have highly successful deep-marine systems due to their abundant coarse sediment provenance from the Fladen Ground Spur and the Scottish Mainland. Heavy mineral analysis of Fulmar sands indicate that sediments were derived from finer-grained and mixed lithologies in the Triassic and Middle Jurassic sequences, indicating a less effective reservoir provenance than those feeding the South Viking Graben and Moray Firth systems

(Erratt et al., 2010). Furthermore, the basin architecture plays a significant role in developing sediment fairways. In the case of the South Viking Graben, a single half-graben formed one depocentre along a relatively narrow basin, with major footwall uplift across the main bounding fault resulted in significant erosion of the Paleozoic basement rock, whereas the Moray Firth benefited from an abundant supply of clastics from the Scottish mainland (Erratt et al., 2010). Compared with these analogues, the Dutch Central Graben consists of a series of smaller sub-basins, with extension dissipated across a network of bounding faults, leading to reduced footwall uplift and hence no regional exposure of Paleozoic rocks that may result in erosion of coarse clastics. In addition, the role of salt movement could play an inhibiting role in delivering sand to deeper marine environments by forming sediments traps in e.g. relatively shallow-marine salt mini-basins, thereby reducing the potential for sediment bypass (Erratt et al., 2010).

5.3.5 Scruff Greensand Formation: lower shoreface sands and enhanced porosity due to dissolution of sponge spicules

The lower shoreface deposits of the Scruff Greensand Formation constitute a relatively deep depositional environment with a widely varying reservoir quality. The formation has a relatively reduced reservoir quality compared with the other sandy formations, which is likely a result of increased clay content due to deposition in a more distal environment with relatively lower energy conditions.

The interval with the best reservoir quality is the Scruff Spiculite Member, which is a bioclastic sandstone consisting of a framework of sponge spicules. The porosity of the reservoir depends on the amount of dissolution of the sponge spicules (Abbink et al., 2006). The fact that the best reservoir quality is observed in the northern part of the Dutch Central Graben, is likely due to increased dissolution of sponge spicules. As this section of the Dutch Central Graben is relatively deeper buried than the rest of the graben, it could indicate increased degrees of dissolution due to elevated temperatures and pressures leading to enhanced spiculine dissolution. In the case of the F03-FA gas field, dissolution of sponge spicules is thought to exert a significant control on reservoir quality (Abbink et al., 2006).

Wonham et al. (2014) found that spiculitic Fulmar sandstones of the Elgin and Franklin fields displayed enhanced secondary porosity through dissolution of feldspar and sponge spicules. The dissolution of sponge spicules does not enhance permeability due to its secondary nature and limited pore connectivity. This results in a one-dimensional shift of the core data compared with spiculitic sandstones that have not undergone spicule dissolution. This shift can also be observed in core data from the Scruff Greensand Formation from well M07-07 (Figure 52). In addition, lining of pore spaces with microcrystalline quartz resulted in inhibition of later quartz overgrowth (Wonham et al., 2014). This coating of the grains with microcrystalline quartz is not observed in the Scruff Greensand Formation in the northern Dutch offshore.

Another analogue of the Scruff Spiculite Member from the UK is the Fife field, the reservoir of which consists of Kimmeridgian to Volgian sandstones of sheet-like, heavily bioturbated, fine-grained, silty shelf sands with abundant sponge spicules (Shepherd et al., 2003). Porosities range between 19 – 31%, with a typical permeability of less than 100 mD, which is comparable with the reservoir quality of the Scruff Greensand Formation. The origin of some coarse-grained intervals and a general northward

thickening towards an E-W trending fault, suggests that part of the reservoir may represent gravity flows or submarine toes of fan deltas sourced from the footwall area of the fault (Shepherd et al., 2003). This fits with the interpretation that accommodation space for the Fife Sandstone was controlled by growth faulting (Møller & Rasmussen, 2003).

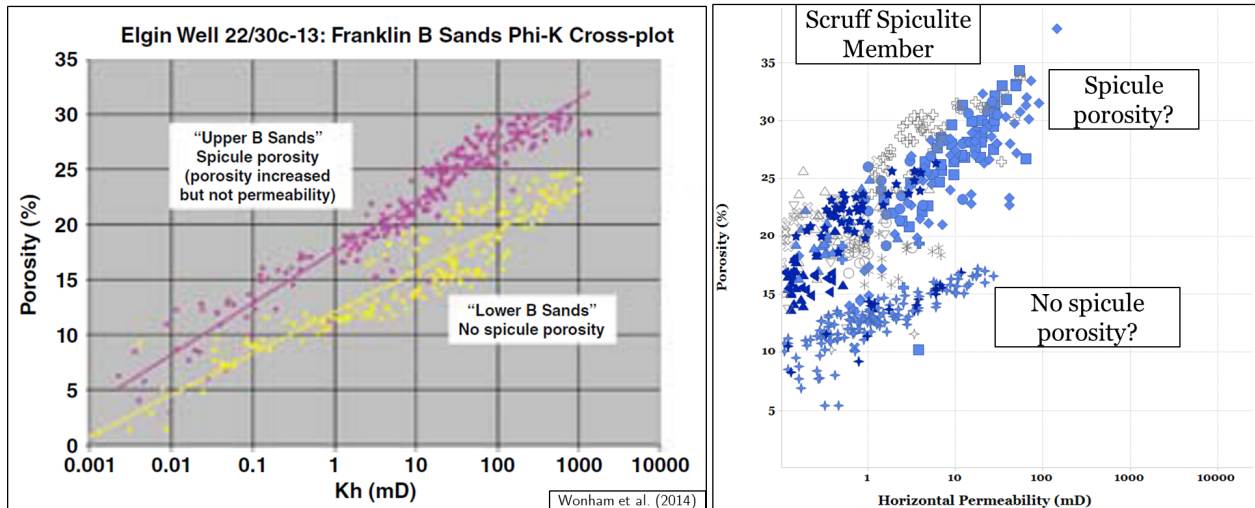


Figure 52. Left: spiculitic shoreface sands belonging to the Fulmar Formation from the UK sector with (yellow) and without spicule porosity (purple). As spicule porosity only leads to an increase in porosity, the core data shifts only in one dimension. Right: spiculitic lower shoreface sands from the Scruff Greensand Formation from the northern Dutch offshore. Notice the same one-dimensional shift of the core data towards higher porosities, while permeability remains roughly the same. Well M07-07 consists of spiculitic sands that have not undergone spicule dissolution.

5.3.6 Kimmeridge Clay Formation and Lutine Formation: open marine clay-rich sediments

The Kimmeridge Clay and Lutine formations, which are predominantly composed of clay, were deposited in a distal, open marine environment and display a significantly poorer reservoir quality with medium to high porosity (15 – 20%) but low permeability (<1 mD). In the case of well F03-FB-107, the formation was very likely not a target at all, but the formation was cored due to its proximity to the underlying reservoir sand. In the case of wells B14-01 and M07-03, the cored intervals had some sand content, but the predominant lithology consisted of clay. It is therefore not surprising that these formations were cored in few wells. Still, although permeability is poor in all three wells, overall porosity is relatively high with a range of 15 – 20%. This distinct difference between permeability and porosity is a characteristic property of clay, which has a very small grain size, which does not necessarily affect porosity, but will result in negligible permeability due to few connected pores.

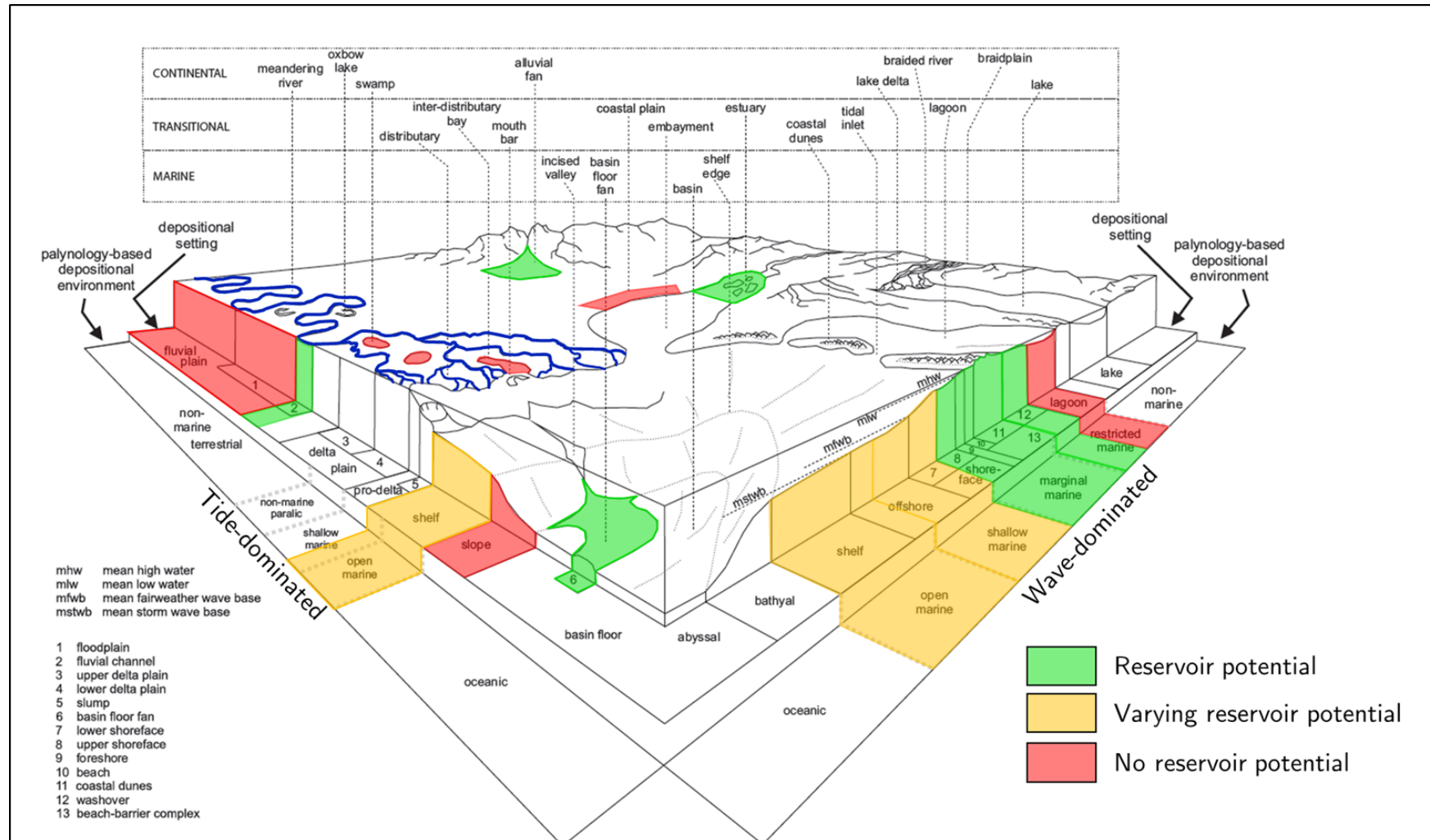


Figure 53. Schematic overview of typical depositional settings within their corresponding depositional environments. Encountered depositional settings in this study are highlighted. Green indicates settings that lead to deposition of clean sands with relatively good reservoir quality, whereas red indicates settings that cause deposition of sediments with increased clay content and hence relatively poor reservoir quality. Orange areas indicate depositional settings that lead to deposition of sediments varying in composition and therefore variable reservoir quality (modified after Munsterman et al., 2012).

5.4 Mineralogy

Mineralogy plays an important part in determining the degree of mechanical and chemical compaction that a sediment will undergo due to the varying of reaction rates. Although the mineralogy of a sediment is predominantly controlled by provenance and weathering processes, the depositional environment largely controls its distribution in a basin (Bjørlykke, 2014). Clay minerals are differentially distributed in deltaic and coastal environments, as kaolinite is enriched in the proximal facies while illite and smectite are more abundant in the distal and offshore facies (Weaver, 1989). Early diagenetic processes may modify the mineralogy of a sediment, e.g. in a humid climate, this kind of diagenesis is due to freshwater (meteoric) flow, while in a dry climate this is due to precipitation of evaporite minerals (Bjørlykke, 2014). There are significant spatial and temporal differences in distribution of diagenetic alterations in siliciclastic rocks caused by mass transfer in sedimentary basins (Morad et al., 2000). The mineralogy of a sediment depends on its position in a depositional system. Determining the exact mineralogies of the Upper Jurassic to Lower Cretaceous formations and their relation with the depositional environments was beyond the scope of this study.

5.5 Diagenesis

Diagenesis is a process that takes over as soon as sediments are deposited and subjected to burial. At or below the depositional interface, the sediments may be reworked and altered by all sorts of organisms, a process commonly known as bioturbation (Ali et al., 2010). The continued burial of the sediments to greater depths leads to a changing chemical environment with increased pressures and temperatures. This promotes the consolidation and cementation of loose sediment into lithified rock.

According to Ali et al. (2010), the course of diagenesis is controlled by sedimentary and environmental factors. The sedimentary factors include particle size, fluid content, organic content, and mineralogical composition. Environmental factors are temperature, pressure, and chemical conditions. Diagenesis can affect sediment particles by various processes:

- compaction: when pressure pushes grains into closer contact with each other;
- cementation: when material precipitates on the surface of grains to act as a coating;
- recrystallization: when particles change in size or form, while retaining composition;
- replacement: when particles change composition, while retaining size or shape;
- differential solution: when some particles undergo (partial or complete) dissolution, while other particles are unaffected;
- authigenesis: when changes in size, shape, and composition are controlled by chemical alterations.

After deposition, diagenesis becomes the main control on reservoir properties. A classification scheme relates diagenetic regimes to the evolution of sedimentary basins and can be divided into three stages, some of which may be bypassed or reactivated repeatedly: eogenesis, mesogenesis, telogenesis (Ali et al., 2010) (Figure 54).

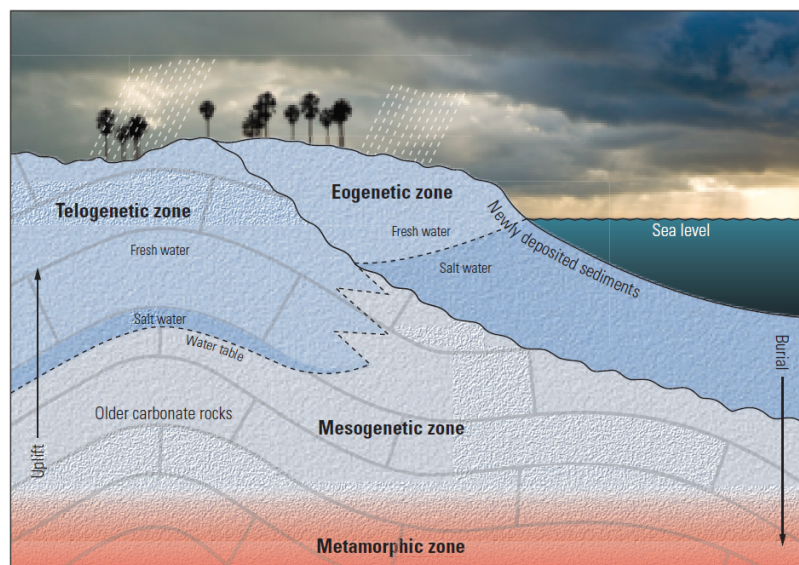


Figure 54. Classification of diagenetic regimes. The eogenetic zone is the earliest phase of diagenesis and includes near-surface processes such as meteoric water dissolution. Further burial introduces the sediments into the mesogenetic zone, where the sediments are no longer influenced by processes related to the surface. Ultimately, continued burial will bring the rocks into the metamorphic zone. However, sufficient uplift will reintroduce the rock to meteoric water flow in the telogenetic zone (Ali et al., 2010).

Eogenesis refers to the earliest stage of diagenesis and is dominated by near-surface processes, such as flushing of meteoric water. The most significant change in the eogenetic zone is the reduction of porosity from cementation by carbonate or evaporite minerals (Ali et al., 2010). During mesogenesis, also referred to as burial diagenesis, sediments are buried to depths, at which they are no longer influenced by processes active at the surface. Major porosity reducing processes in the mesogenetic zone are mechanical compaction and cementation, whereas dissolution is only of minor influence. Telogenesis reintroduces the rocks to the surface via uplift and erosion. Here, meteoric water flow leads to renewed dissolution and enhancing of porosity.

The presence of multiple unconformities within Upper Jurassic – Lower Cretaceous formations indicate that the underlying sediments could have been re-exposed to meteoric water flow in the telogenetic zone. Well L05-04 cored sands that showed the highest permeability encountered in this study, and which were situated about 35 – 50 m below an unconformity separating it from the overlying Vlieland Claystone Formation. Meteoric water flow can significantly alter reservoir properties by dissolution. The precise extent of the influence of flushing by meteoric water was not considered in this study, and requires further research that addresses anomalously high reservoir quality sandstones.

5.5.1 Mechanical Compaction

Mechanical compaction is the most important factor in controlling porosity loss during burial diagenesis and is a function of effective stress and the textural and mineralogical composition of the sediment (Figure 55) (Bjørlykke, 2014). Pore space and the overall thickness is reduced by mechanical compaction. Mechanical compaction is active until sufficient burial leads to chemical compaction, which then becomes the dominant process reducing porosity and permeability.

For the core data in this study, porosity loss shows roughly two different trends with increasing burial: one for depths up to 3000 m, and one trend for depths between 3100 – 3300 m. No data is available for depths between 2950 – 3100 m, hence it is not possible to establish the boundary between the two trends. Permeability loss is only detectable for depths between 3100 – 3000 m and at a rate proportional to porosity loss in the same depth interval. The lack of a clear relationship between permeability and depth for depths up to 3100 m suggests a (so far) lack of evidence for a significant influence of mechanical compaction on permeability. A similar behavior of permeability with depth was found in a study of the Brent Group by Giles et al. (1992), which found no relation for depths up to 3105 m, but rapid loss of permeability with depth after 3105 m. The two different trends of porosity vs depth found in this study were also observed by Giles et al. (1992).

The lack of a clear relationship between grain density and depth suggests that mechanical compaction is only of minor influence and only on porosity. A more plausible cause for significant loss of porosity could be cementation, or differences in depositional environments leading to differences in sorting.

Finally, some facies seem to be limited to certain depth intervals. Furthermore, facies such as upper shoreface/foreshore/beach and brackish lagoon/bay do not appear to vary much in reservoir properties even if they are buried at relatively greater depths. This brings a significant uncertainty in interpreting the influence of mechanical compaction on reservoir properties with increasing depth.

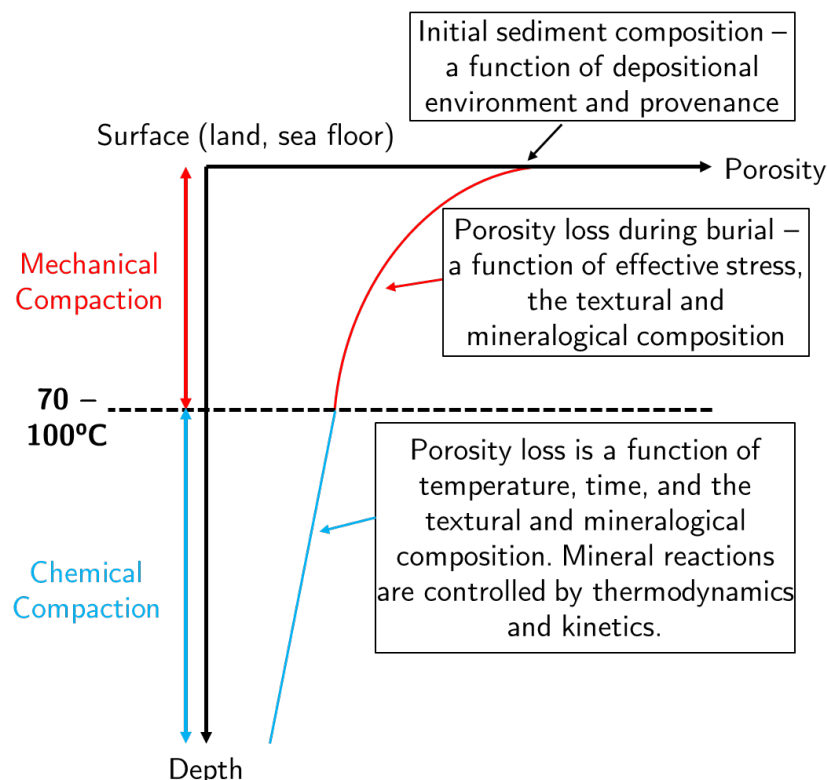


Figure 55. Schematic plot showing the two processes of compaction and their control on porosity in sedimentary systems. Temperature controls the transition from mechanical compaction to chemical compaction. Mechanical compaction is controlled by effective stress from the overlying rock and the primary sedimentary composition, which is a direct result of depositional environment and provenance. Chemical compaction is controlled by the reaction rates, which are dependent of mineralogy, temperature, and time (after Bjørlykke, 2014).

6. Discussion

6.1 Chemical Compaction

At sufficient burial, chemical compaction controls diagenesis and mineral reactions are controlled by thermodynamics and kinetics towards a more stable mineral assemblage with a lower Gibbs Free Energy (Bjørlykke, 2014). Dissolution and precipitation of minerals reduce porosity and increase density. This characterizes the mesogenetic zone, where surface processes no longer influence diagenesis.

Chemical compaction comes in various forms, but the most important one in sandstone diagenesis is cementation. When minerals precipitate from pore fluids onto framework grains, they act as cement. Quartz cementation and compaction are the most important processes that significantly reduce porosity in quartz and feldspar-rich sandstones during burial toward 4000 m (Ramm et al., 1997). The reaction rates generally increase with temperature, therefore at certain depths cementation is stimulated and can lead to enhanced loss of porosity and permeability (Bjørlykke, 1998). Common minerals that form cement are: calcite, quartz, anhydrite, dolomite, feldspar, siderite, and clay minerals (Ali et al., 2010). Kaolinite and illite are the most abundant authigenic clays, and early precipitation of kaolinite is generally related to flushing by meteoric waters (Lanson et al., 2002). Fibrous illite can precipitate from dissolution of K-feldspar and fill pores, thereby significantly reducing permeability at deep burial (Ramm, 2000) (Figure 56). For the Brent Group, illitization leading to the presence of increased quantities of illite is associated with significant permeability decrease at depths greater than 3100 m (Giles et al., 1992). Porosity decrease in the Brent Group was related to mechanical compaction together with burial cementation of quartz and iron-rich carbonates (Giles et al., 1992).

The same behavior of permeability with depth is also observed in this study. Thoroughly illitized feldspar was found in the Lower Graben Formation in the F03-FB field. However, it is essential to note that practically all core data from the 3100 – 3300 m depth interval comes from the Lower Graben Formation in the F03-FB field. In addition, the Lower Graben Formation has mostly been cored in the 3100 – 3300 m depth interval, and there is no comparison possible with the same formation at shallower depths. As precise mineral contents are not used in this study, the exact extent of the illitization process can therefore not be determined. Therefore, the extent of illitization and its influence on reservoir quality in relatively deeper buried reservoir sands is suggested for future studies.

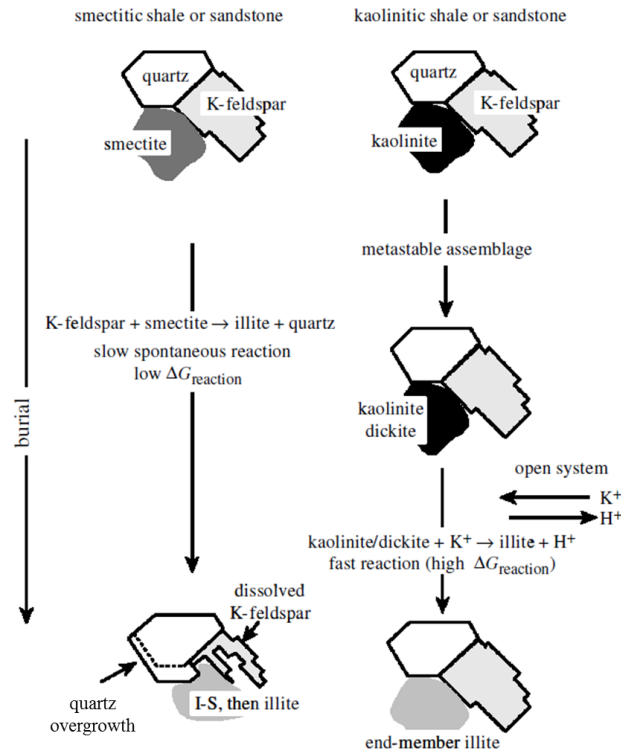


Figure 56. Schematic overview of the illitization process in sandstones as a function of the initial clay mineralogy (Lanson et al., 2002).

Glaucinite is also widely present in Upper Jurassic – Lower Cretaceous sandstones in the northern Dutch offshore and can significantly reduce reservoir quality by forming a pseudomatrix that occludes the original primary porosity (Diaz et al., 2002).

6.2 Dissolution of framework grains

In some reservoir sandstones such as the Brent Group, feldspar dissolution has led to secondary porosity (Giles et al., 1992). However, the total addition to intergranular porosity is considered volumetrically minor (<2%) (Taylor et al., 2010). The primary control on dissolution of feldspars and precipitation of kaolinite in sandstones and carbonates is meteoric water flow (Figure 57) (Bjørlykke, 2014). In the northern Dutch offshore, some sands that are situated below unconformities e.g. well F15-06 suggest that meteoric water could have flushed out minerals such as feldspars, thereby enhancing the overall reservoir quality.

In this study, dissolution of sponge spicules was encountered in the Scruff Spiculite Member and led to enhanced porosity (Abbink et al., 2006). Currently, there are no known studies that have addressed the extent of dissolution of sponge spicules and the induced enhancing of porosity. As additional porosity results in more pore volume for the storage of hydrocarbons, studying the extent of dissolution and its relation with e.g. diagenesis is relevant.

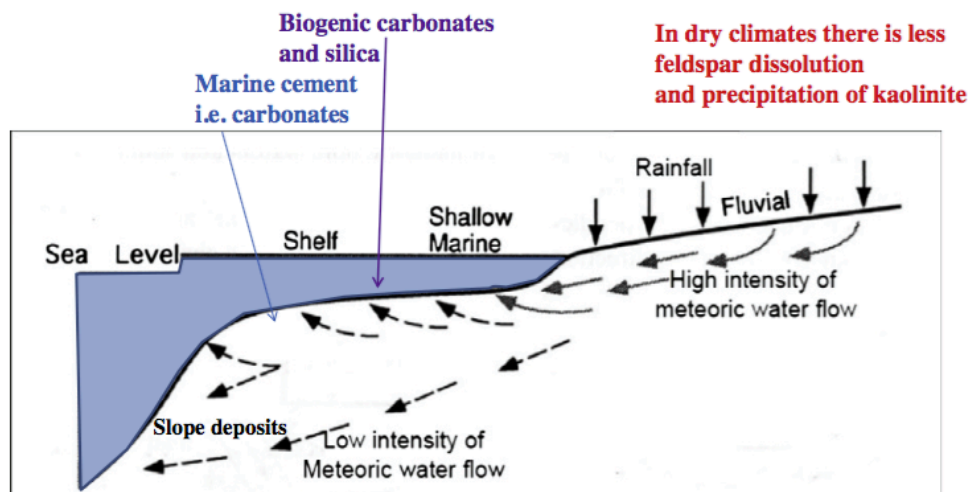


Figure 57. Schematic depiction of meteoric water flow, which is the main control on feldspar dissolution and precipitation of kaolinite in sandstones and carbonates. Meteoric water flow gradually loses its influence when reaching more distally located sediments, and its primary control is climate. Source: Bjørlykke (2014).

6.3 Grain Coating

Numerous studies have addressed microquartz coating on framework grains in sandstones and found that microquartz coating can hinder quartz precipitation and late diagenetic chemical compaction. In the Norwegian Central Graben, two oil discoveries in deeply buried (>4000 m) Upper Jurassic sandstones preserved high porosity (>20%) due to the pervasive microquartz coating on framework grains (Ramm et al., 1997). Burial history-dependent factors such as high pore pressure, low thermal maturity, or early oil emplacement were ruled out. Ramm et al. (1997) explains the occurrence of microcrystalline coatings within specific layers by relating it to the input of amorphous silica such as volcanic glass and sponge spicules during deposition. In this study, no core data are available on deeply buried Upper Jurassic sandstones such as in the Norwegian Central Graben, as the maximum depth of the core data is ~3300 m TVD. In addition, for the northern Dutch offshore, there are currently no known public studies that address the preservation of porosity by microquartz coating on framework grains such as in deeply buried (>4000 m) Upper Jurassic reservoir sands in the Norwegian Central Graben. Its presence could be studied in the deeper parts of the Dutch Central Graben. Therefore, currently no sufficient proof is available to suggest that microquartz coating of framework grains has a significant influence on Upper Jurassic – Lower Cretaceous formations in the northern Dutch offshore. Studying the possible effect of grain coating on the preservation of reservoir quality will be relevant for deeper buried Upper Jurassic reservoirs in the Dutch Central Graben.

6.4 Allochthonous Salt

Changes in heat-flow associated with allochthonous salt bodies can result in suppressed thermal exposure, thereby slowing the rate of quartz cementation in some subsalt sands (Taylor et al., 2010). Because of the high thermal conductivity of salt compared to shale and sand, heat is transmitted more easily away from the underlying strata. The thermal conductivity of salt is dependent on temperature and decreases with increasing temperature, so this effect is strongest at shallow burial depths, where the contrast in heat is greatest. Therefore, temperatures above large salt bodies are typically elevated

compared to laterally depth-equivalent strata farther away from salt (Taylor et al., 2010). This has significant influence on the precipitation of quartz cement, which is primarily controlled by temperature and the available quartz surface area. Quartz precipitation rates increase exponentially with temperature, and therefore suppression of temperature over time could have a significant impact on the loss of porosity. Especially sandstones that lack grain-coating clay are susceptible to quartz cementation at high temperatures.

Upper Jurassic – Lower Cretaceous reservoirs in the northern Dutch offshore are almost always situated above or next to large salt bodies, the most important of which is the Permian Zechstein, which tends to vary widely in thickness due to salt tectonics. This has triggered piercing salt diapirs, which may extend to almost the depth of the sea-floor. This implies that sand reservoirs at shallow depths could have experienced relatively high temperatures compared to laterally equivalent strata. This study did not address the effect of heat flow perturbations of salt bodies on reservoir sandstones. As salt is abundant in the northern Dutch offshore, this could provide additional ground for studying.

6.5 Overpressure

Fluid overpressure occurs when the fluid pressure becomes greater than the hydrostatic gradient for the fluid at the top of the water column (Dickinson, 1953). Fluid overpressures tend to bear some of the mass of the overlying rock column, thereby reducing the overall effective stress (Bloch et al., 2002). As effective stress exerts a major control on sandstone compaction, fluid overpressures may in some cases help preserve porosity. However, while overpressures can slow the rate of compaction, they do not result in porosity increase, as compaction of sand is an irreversible process (Taylor et al., 2010). The control of fluid overpressure on preservation of porosity is largely dependent on the timing of the development of overpressures, and on the mechanical properties of the reservoir sandstones (Bloch et al., 2002). According to Osborne & Swarbrick (1997), fluid overpressures form (1) when the rate of pore volume reduction is faster than the rate of fluid release, (2) when the rate of pore fluid expansion is faster than the rate of fluid release, and (3) as a response to large-scale fluid movements. The first two mechanisms are transient flow conditions and control the development of overpressures in the North Sea (Bloch et al., 2002).

Pressure data show consistent overpressures in Upper Jurassic to Lower Cretaceous reservoirs (Scruff and Schieland groups) within the northern Dutch offshore in the Central Graben and the Terschelling Basin (Verweij et al., 2012). However, no studies have been performed that address the preservation of porosity through the existence of overpressures. Studying and comparing porosity data of Upper Jurassic to Lower Cretaceous formations from different overpressures in the Dutch Central Graben and Terschelling Basin could provide an indication of how this process has affected reservoir quality.

6.6 Early Hydrocarbon Emplacement

The influence of early hydrocarbon emplacement on the preservation of porosity due to inhibition of quartz cementation is disputed. Recent studies such as Taylor et al. (2010) evaluated detailed available field data, and concluded that there is not enough proof for the hypothesis that hydrocarbon pore fluids suppress porosity loss due to quartz cementation. The effect of (early) hydrocarbon emplacement on

reservoir properties of Upper Jurassic – Lower Cretaceous formations was not investigated in this study. Studying this effect will further constrain how reservoir quality is affected or preserved during diagenesis.

6.7 Provenance

Distribution of clastics is strongly controlled by facies, as energy conditions in proximal and distal facies can lead to wide spatial variations in mineralogy (Ramm, 2000). Provenance determines the supply of sediments and minerals, and therefore different areas of provenance will lead to different sediment compositions in sedimentary basins. As addressed before, the success of mass-flow sands in the northern North Sea could be attributed to sediment provenance. The Southern Viking Graben experienced massive footwall uplift, thereby exposing Paleozoic basement rocks, resulting in coarse clastic sediment supply (Erratt et al., 2010). The Upper Jurassic deep-water sandstones had their sediment supply from the Scottish mainland, which also consisted of coarse clastics. This shows the significant impact that provenance can make in determining reservoir quality. The impact of provenance on reservoir properties and the origin of clean, well-sorted reservoir sands is an important field for further research.

6.8 Inversion

It is known that inversion during the Late Cretaceous caused widespread uplift and erosion in the Dutch rift basins, with differences in structural expression of inversion related to the Zechstein salt, which acted as an important detachment zone (De Jager, 2003). In the northern Dutch offshore, relatively strong inversion took place throughout Dutch Central Graben. This inversion has also caused uplift of Upper Jurassic – Lower Cretaceous formations, reintroducing them to relatively lower depths and therefore a different diagenetic regime with different prevailing diagenetic processes. The maximum burial depth is therefore likely not the burial depth as shown by the current data. Studying the effects of inversion on reservoir properties helps in revealing previous (maximum) burial depths and explain differences in reservoir quality related to the magnitude of inversion.

7. Conclusions

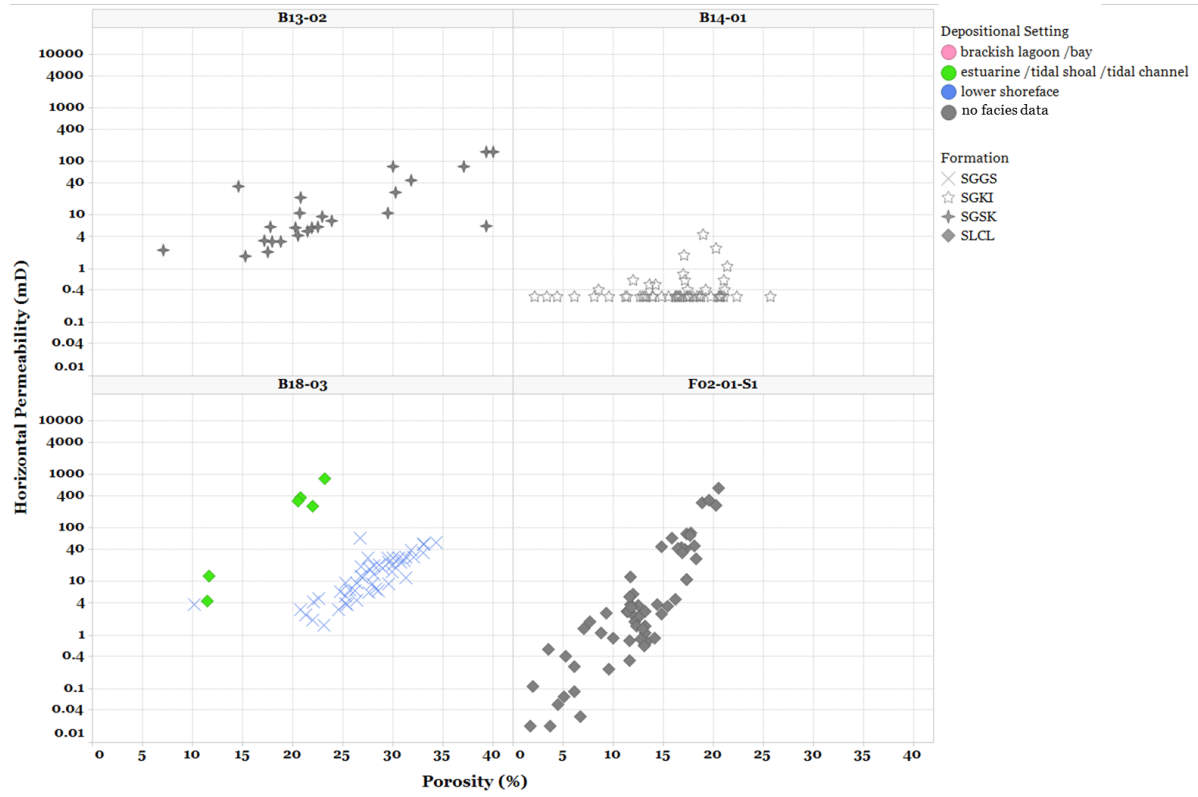
- Reservoir properties of Upper Jurassic – Lower Cretaceous formations in the northern Dutch offshore are characterized by wide variations that reflect the combined influence of individual factors affecting reservoir quality in descending order of magnitude: depositional environment, mechanical compaction, and chemical compaction.
- The dominant control on reservoir quality is the original environment of deposition, which directly affects the clay content of the lithology. The clay content tends to increase from proximal towards distal facies due to changes in energy conditions. Differences in energy conditions between various depositional environments tend to produce a wide range of sand/clay ratios with different mineralogies leading to major differences in reservoir quality.
- High clay content significantly reduces porosity and permeability. The three mega-sequences deposited during Late Jurassic to Early Jurassic times display an overall transgressive change in prevalent environments of deposition from Sequence 1 to 3, i.e. from proximal to distal facies.
- Reservoirs with high clay content buried at relatively shallow depth have compacted less, but show a significantly lower porosity and permeability. Conversely, reservoirs with clean, well-sorted sands can be buried at higher depth yet still retain a relatively high reservoir quality. This is especially visible in the Lower Graben Formation, which has relatively high porosity and permeability at depths of 3100 – 3300 m. Here, porosity is more affected by mechanical compaction and burial cementation.
- Restricted and marginal marine facies are primarily represented in formations of Sequence 1, which have the largest spread in reservoir quality. The best reservoir quality is found in the Friese Front Formation, with excellent porosity and permeability in clean, well-sorted channel sands and alluvial fan deposits. The Lower, Middle, and Upper Graben formations have good to excellent reservoir quality in marginal marine sands. Poor reservoir quality is preserved in brackish lagoon/bay settings of the Lower Graben Formation, which underwent additional reduction in porosity and permeability due to effects of burial diagenesis.
- Formations in Sequence 2 are relatively more distal, although it depends on the position in the northern Dutch offshore. In the Dutch Central Graben, the Kimmeridge Clay Formation was deposited in an open marine environment and primarily consists of clay, resulting in a poor reservoir quality. However, good reservoir quality is found in clean, well-sorted sands of beach barrier complexes of the Terschelling Sandstone Member and the shallow marine Noordvaarder Member.
- Sequence 3 has good reservoir quality in lower shoreface deposits of the Scruff Greensand Formation. Local dissolution of sponge spicules created some additional porosity in the Scruff Spiculite Member, but did not enhance permeability. The Lutine Formation is more distal and primarily composed of clay with a poor reservoir quality.
- After deposition, diagenetic processes during burial become the dominant effect on reservoir quality. Mechanical compaction has a significant effect on reservoir properties, but only tends to affect porosity until a certain depth and temperature, after which chemical compaction takes

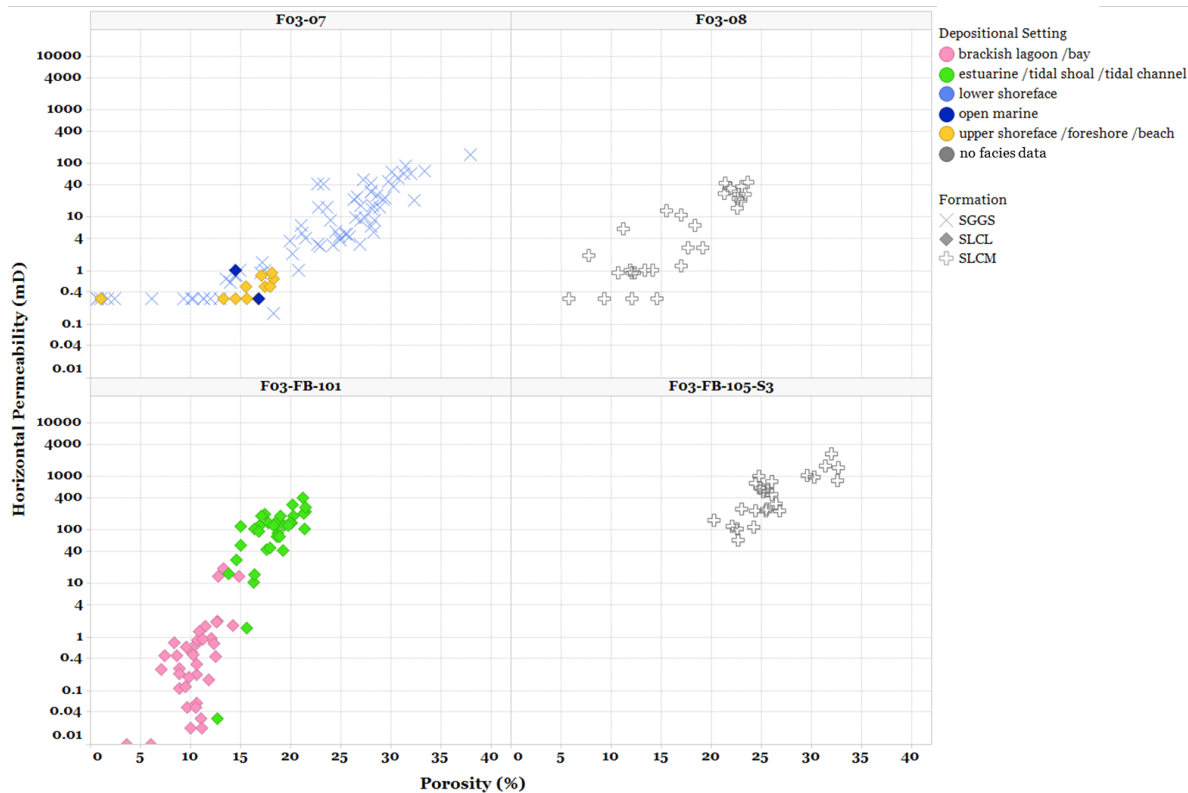
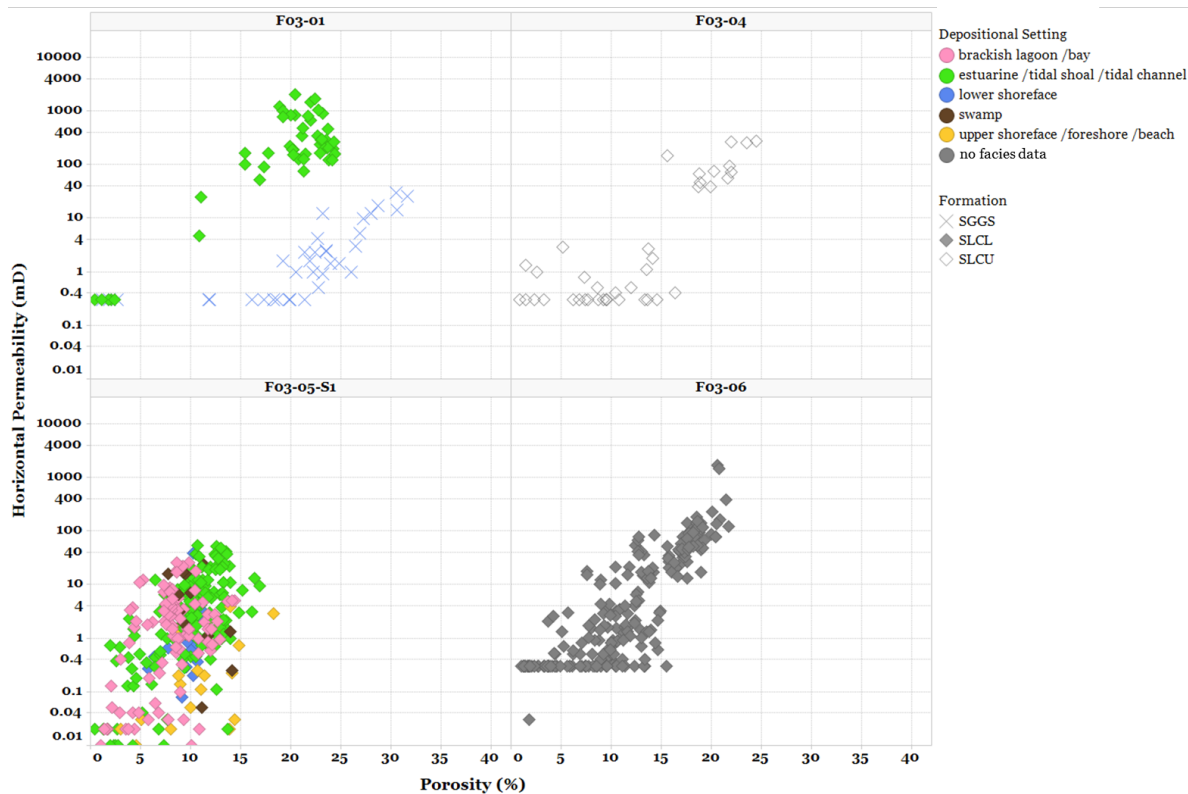
over. Core data show that porosity decreases linearly with depth due to mechanical compaction and burial cementation. Permeability shows no clear trend with depth.

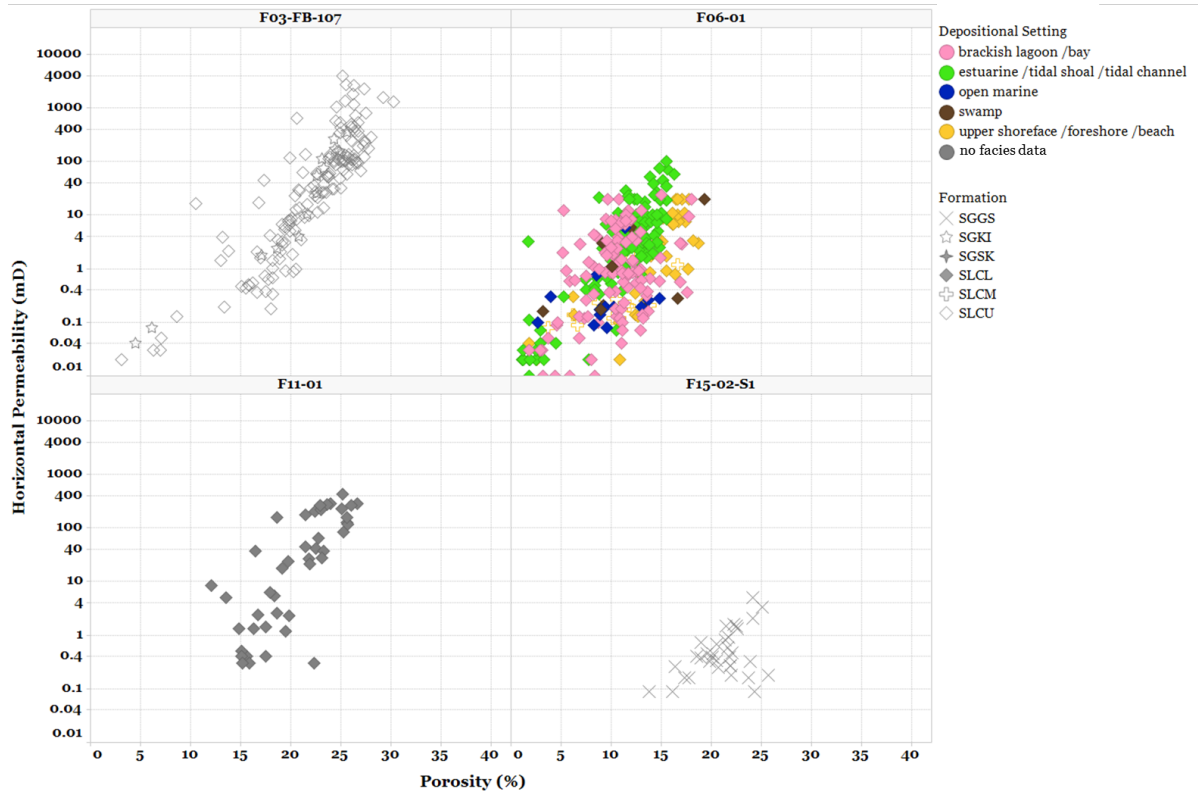
- Core data from the F03-FB field show rapid losses of porosity and permeability at depths greater than 3100 m, which suggests chemical diagenesis as the dominant control on reservoir quality. Permeability losses at depths greater than 3100 m are in 1 to 2 orders of magnitude, which is attributed to chemical diagenesis due to the precipitation of clays such as illite at increased pressures and temperatures. The same porosity vs depth behavior was observed in the Brent Group in the UK.
- For individual formations, determining the porosity/depth and the permeability/depth relations was not always possible as the data displayed conflicting trends due to inconsistent distributions along the sampled depth intervals.
- Chemical compaction is interpreted to be the driving factor controlling loss of porosity and permeability with depth from 3100 m onwards. Precipitation of burial cement through illitization of feldspars results in severe loss of permeability, while significantly decreasing porosity.
- Most formations tend to be concentrated at specific depth intervals, and hence certain facies are not widely distributed along depth ranges. This makes determining the exact porosity/depth and permeability/depth relations challenging.

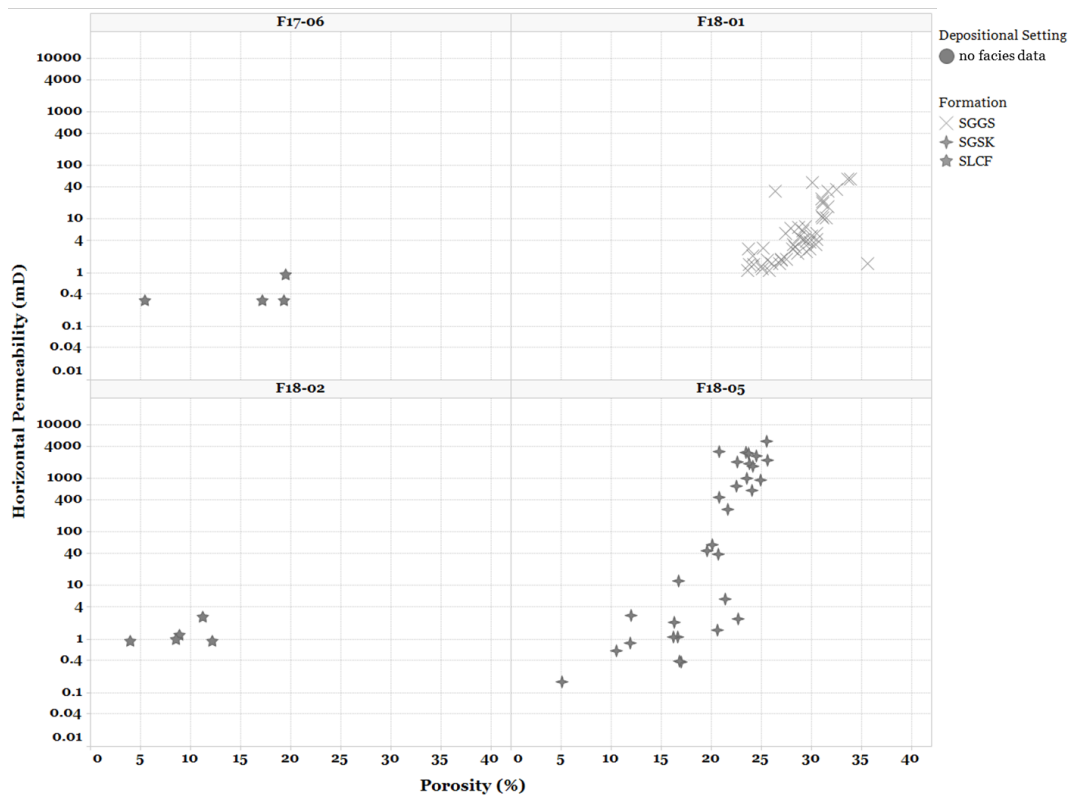
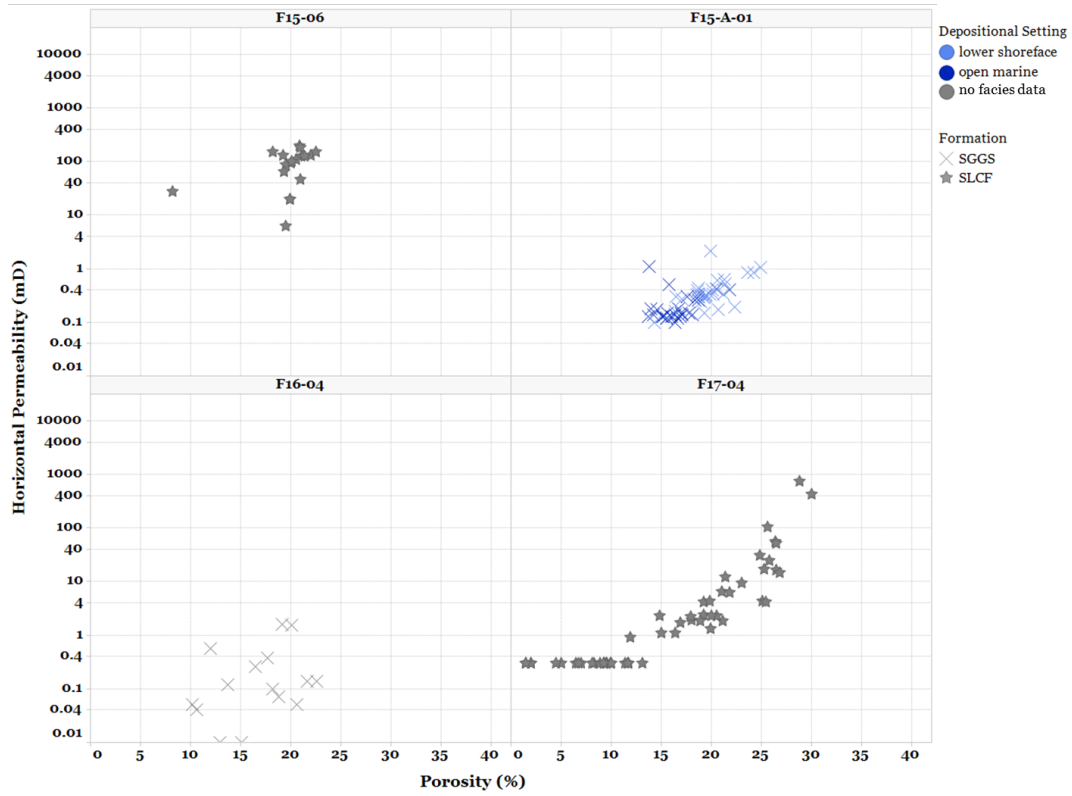
8. Appendices

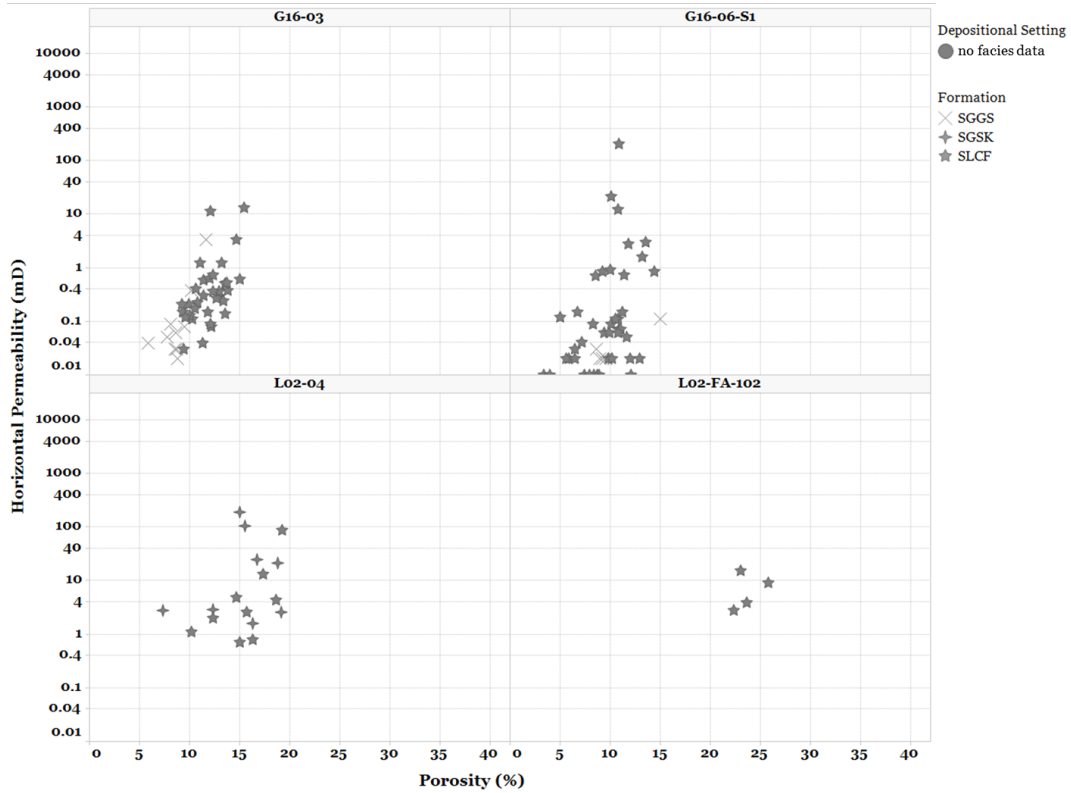
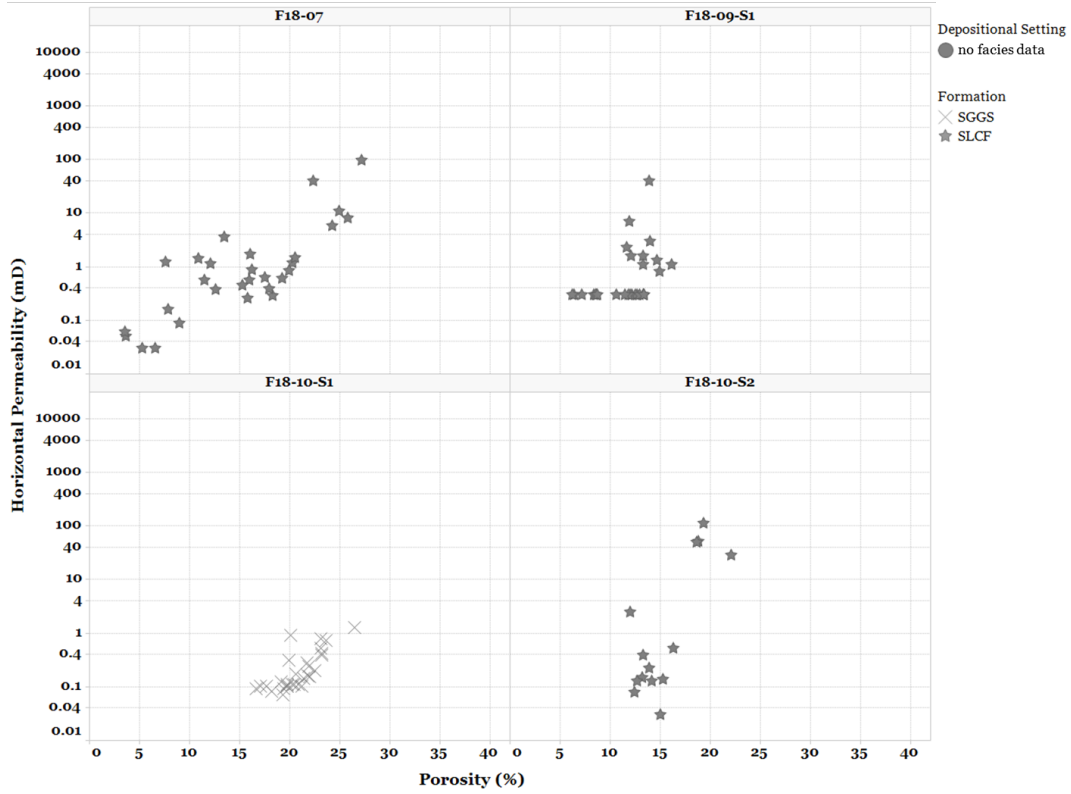
8.1 Appendix A – Raw data per well

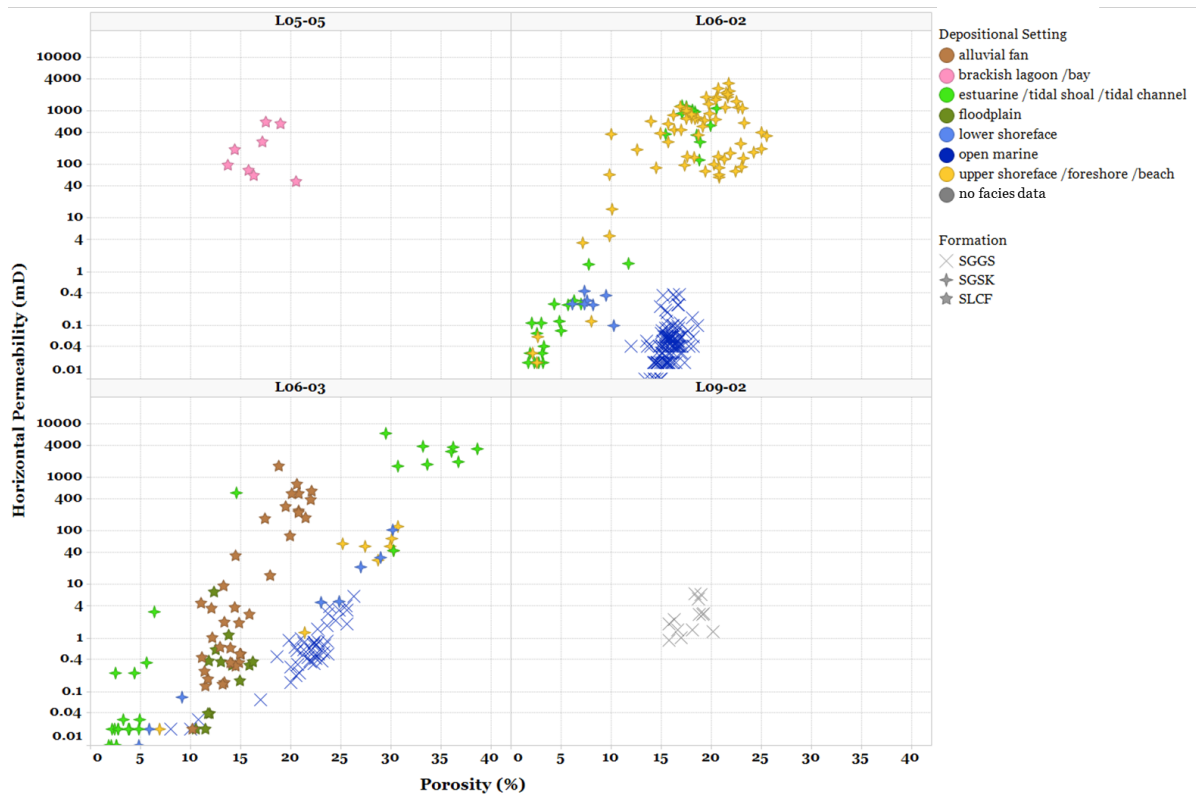
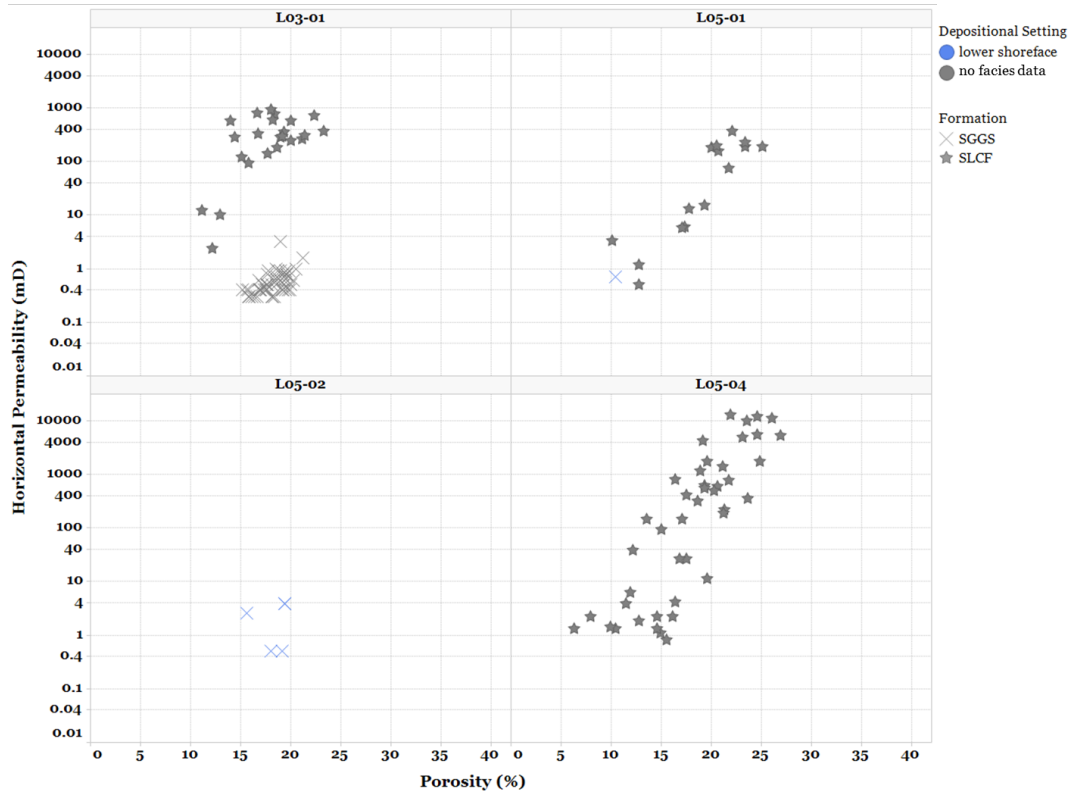


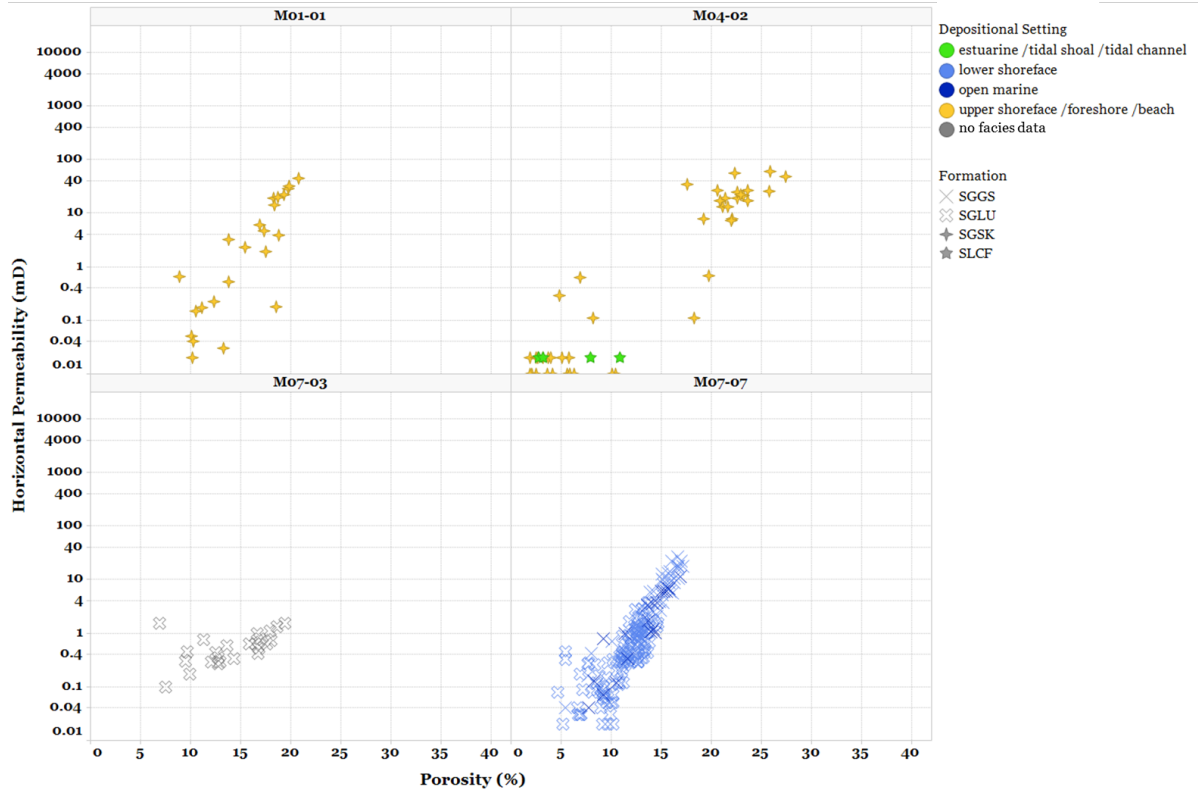




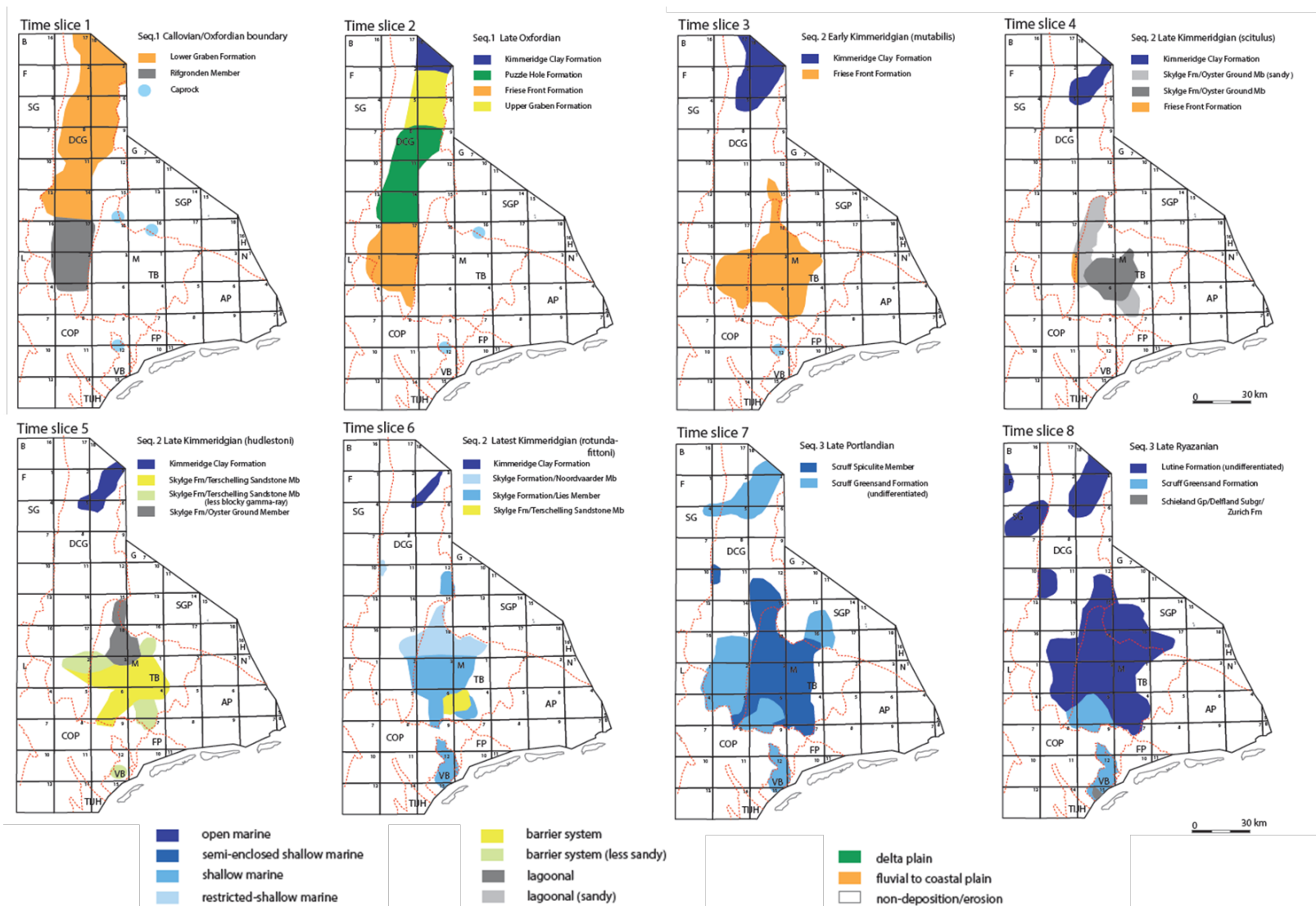








8.2 Appendix B – Late Jurassic to Early Cretaceous time slices of the facies distribution in the northern Dutch offshore through time. (Munsterman et al., 2012)



9. References

- Abbink, O.A., Mijnlief, H.F., Munsterman, D.K., & Verreussel, R.M.C.H. (2006). New stratigraphic insights in the 'Late Jurassic' of the Southern Central North Sea Graben and Terschelling Basin (Dutch Offshore) and related exploration potential. *Netherlands Journal of Geosciences—Geologie en Mijnbouw*, 85(3), 221-238.
- Ali, S.A., Clark, W.J., Moore, W.R., & Dribus, J.R. (2010). Diagenesis and reservoir quality. *Oilfield Review*, 22(2), 14-27.
- Andsbjerg, J. & Dybkjær, K. (2003). Sequence stratigraphy of the Jurassic of the Danish Central Graben. *The Jurassic of Denmark and Greenland. Geological Survey of Denmark and Greenland Bulletin*, 1, 265-300.
- Arfai, J., Jähne, F., Lutz, R., Franke, D., Gaedicke, C., & Kley, J. (2014). Late Palaeozoic to Early Cenozoic geological evolution of the northwestern German North Sea (Entenschnabel): New results and insights. *Netherlands Journal of Geosciences*, 93(4), 147.
- Bjørlykke, K. (2014). Relationships between depositional environments, burial history and rock properties. Some principal aspects of diagenetic process in sedimentary basins. *Sedimentary Geology*, 301, 1-14.
- Bjørlykke, K. (1998). Clay mineral diagenesis in sedimentary basins—a key to the prediction of rock properties. Examples from the North Sea Basin. *Clay minerals*, 33(1), 15-34.
- Bloch, S., Lander, R.H., & Bonnell, L. (2002). Anomalously high porosity and permeability in deeply buried sandstone reservoirs: Origin and predictability. *AAPG bulletin*, 86(2), 301-328.
- Boldy, S.A.R. & Fraser, S.I. (1999). Introduction and review. *In: Geological Society, London, Petroleum Geology Conference series (Vol. 5, 825-826). Geological Society of London.*
- Coward, M.P., Dewey, J., Hempton, M., & Holroyd, J. (2003). Tectonic evolution. *In: Evans, D.J., Graham, C., Armour, A. & Bathurst, P. (eds): The Millennium Atlas: Petroleum Geology of the Central and Northern North Sea. The Geological Society (London): 17-33.*
- De Jager, J. (2007). Geological development. *In: Wong, T.E., Batjes, D.A.J., & De Jager, J. (eds): Geology of the Netherlands. Royal Netherlands Academy of Arts and Sciences (KNAW) (Amsterdam): 5-26.*
- De Jager, J. (2003). Inverted basins in the Netherlands, similarities and differences. *Geologie en mijnbouw (en).*
- Diaz, E., Prasad, M., Mavko, G., & Dvorkin, J. (2003). Effect of glauconite on the elastic properties, porosity, and permeability of reservoir rocks. *The Leading Edge*, 22(1), 42-45.
- Dickinson, G. (1953). Geological aspects of abnormal reservoir pressures in Gulf Coast Louisiana. *AAPG Bulletin*, 37(2), 410-432.
- Donato, J.A., Martindale, W., & Tully, M.C. (1983). Buried granites within the mid North Sea High. *Journal of the Geological Society*, 140(5), 825-837.
- Duin, E.J.T., Doornenbal, J.C., Rijkers, R.H.B., Verbeek, J.W., & Wong, T.E. (2006). Subsurface structure of the Netherlands—results of recent onshore and offshore mapping. *Netherlands Journal of Geosciences*, 85(4), 245.
- Erratt, D., Thomas, G.M., Hartley, N.R., Musum, R., Nicholson, P.H., & Spisto, Y. (2010, January). North Sea hydrocarbon systems: some aspects of our evolving insights into a classic hydrocarbon province. *In Geological Society, London, Petroleum Geology Conference series (Vol. 7, pp. 37-56). Geological Society of London.*
- Fraser, S.I., Robinson, A.M., Johnson, H.D., Underhill, J.R., Kadolsky, D.G.A., Connell, R., Johannessen, P.N., & Ravnås, R. (2003). Upper Jurassic. *In: Evans, D., Graham, C., Armour, A., & Bathurst, P. (eds): The Millennium Atlas: Petroleum Geology of the Central and Northern North Sea. The Geological Society (London): 157-189.*

- Geluk, M.C. (2007). Permian. *In*: Wong, T.E., Batjes, D.A.J., & De Jager, J. (eds): Geology of the Netherlands. Royal Netherlands Academy of Arts and Sciences (KNAW) (Amsterdam): 63-83.
- Giles, M.R., Stevenson, S., Martin, S.V., Cannon, S.J.C., Hamilton, P.J., Marshall, J.D., & Samways, G.M. (1992). The reservoir properties and diagenesis of the Brent Group: a regional perspective. Geological Society, London, Special Publications, 61(1), 289-327.
- Glennie, K.W. (1986). The structural framework and the pre-Permian history of the North Sea area. *In*: Glennie, K.W. (ed.): Introduction to the Petroleum Geology of the North Sea. Blackwell Scientific Publications (Oxford): 25-62.
- Goldsmith, P.J., Hudson, G., & Van Veen, P. (2003). Triassic. *In*: Evans, D. J., Graham, C., Armour, A., & Bathurst, P. (eds): The Millennium Atlas: Petroleum Geology of the Central and Northern North Sea. The Geological Society (London): 105-27.
- Guterch, A., Wybraniec, S., Grad, M., Chadwick, R.A., Krawczyk, C.M., Ziegler, P.A., Thybo, H., & De Vos, W. (2010). Crustal structure and structural framework. *In*: Doornenbal, J.C. & Stevenson, A.G. (eds): Petroleum Geological Atlas of the Southern Permian Basin Area. EAGE Publications B.V. (Houten): 11-23.
- Herngreen, G.W., Kouwe, W.F., & Wong, T.E. (2003). The Jurassic of the Netherlands. Geological Survey of Denmark and Greenland Bulletin, 1, 217-229.
- Herngreen, G.F.W. & Wong, T.E. (1989). Revision of the 'Late Jurassic' stratigraphy of the Dutch Central North Sea Graben. In Coastal Lowlands. Springer Netherlands, 73-105.
- Heybroek, P. (1974). Explanation to tectonic maps of The Netherlands. Geologie en Mijnbouw, 53(2), 43-50.
- Heybroek, P. (1975). On the structure of the Dutch part of the Central North Sea Graben. *In*: Woodland, A.W. (ed.): Petroleum and the Continental Shelf of North-West Europe. Applied Science Publishers Ltd (London): 339-352.
- Johannessen, P.N., Dybkjær, K., Andersen, C., Kristensen, L., Hovikoski, J., & Vosgerau, H. (2010a, January). Upper Jurassic reservoir sandstones in the Danish Central Graben: new insights on distribution and depositional environments. In Geological Society, London, Petroleum Geology Conference series (Vol. 7, pp. 127-143). Geological Society of London.
- Johannessen, P.N., Nielsen, L.H., Nielsen, L., Møller, I., Pejrup, M., & Andersen, T.J. (2010b, January). Architecture of an Upper Jurassic barrier island sandstone reservoir, Danish Central Graben: implications of a Holocene-Recent analogue from the Wadden Sea. In Geological Society, London, Petroleum Geology Conference series (Vol. 7, pp. 145-155). Geological Society of London.
- Johnson, H., Leslie, A.B., Wilson, C. K., Andrews, I., & Cooper, R.M. (2005). Middle Jurassic, Upper Jurassic and Lower Cretaceous of the UK Central and Northern North Sea. British Geological Survey.
- Johnson, H.D. & Fisher, M.J. (2009). North Sea plays: geological controls on hydrocarbon distribution. Petroleum Geology of the North Sea: Basic Concepts and Recent Advances, Fourth Edition, 463-547.
- Kley, J. & Voigt, T. (2008). Late Cretaceous intraplate thrusting in central Europe: Effect of Africa-Europe-Iberia convergence, not Alpine collision. Geology 36: 839-842.
- Kombrink, H., Doornenbal, J.C., Duin, E.J.T., Den Dulk, M., Ten Veen, J.H., & Witmans, N. (2012). New insights into the geological structure of the Netherlands; results of a detailed mapping project. Netherlands Journal of Geosciences, 91(04), 419-446.
- Lanson, B., Beaufort, D., Berger, G., Bauer, A., Cassagnabere, A., & Meunier, A. (2002). Authigenic kaolin and illitic minerals during burial diagenesis of sandstones: a review. Clay minerals, 37(1), 1-22.
- Lott, G.K., Wong, T.E., Duser, M., Andsbjerg, J., Mönnig, E., Feldman-Olszewska, A., & Verreussel, R.M.C.H. (2010). Jurassic. *In*: Doornenbal, J.C. & Stevenson, A.G. (eds): Petroleum Geological Atlas of the Southern Permian Basin Area. EAGE Publications b.v. (Houten): 175-193.

- Michelsen, O., Nielsen, L.H., Johannessen, P.N., Andsbjerg, J., & Surlyk, F. (2003). The Jurassic of Denmark and Greenland: Jurassic lithostratigraphy and stratigraphic development onshore and offshore Denmark.
- Michelsen, O. & Wong, T.E. (1991). Discussion of Jurassic lithostratigraphy in the Danish, Dutch, and Norwegian central Graben areas. DGU, Danmarks Geologiske undersøgelse. Serie B, (16), 20-28.
- Morad, S., Ketzer, J.R.M., & De Ros, L.F. (2000). Spatial and temporal distribution of diagenetic alterations in siliciclastic rocks: implications for mass transfer in sedimentary basins. *Sedimentology*, 47(s1), 95-120.
- Møller, J. J., & Rasmussen, E. S. (2003). Middle Jurassic–Early Cretaceous rifting of the Danish Central Graben. *The Jurassic of Denmark and Greenland. Geological Survey of Denmark and Greenland Bulletin*, 1, 247-264.
- Munsterman, D.K., Verreussel, R.M.C.H., Mijnlief, H.F., Witmans, N., Kerstholt-Boegehold, S., & Abbink, O.A. (2012). Revision and update of the Callovian-Ryazanian stratigraphic nomenclature in the northern Dutch offshore, i.e. Central Graben Subgroup and Scruff Group. *Netherlands Journal of Geosciences*, 91(04), 555-590.
- NAM (1994). Sedimentology, Petrology, and Reservoir Properties of the Late Jurassic Lower Graben Sand Formation (CGLS) Deposits in Core 1 from Well F03-FB-101. NLOG: <http://nlog.nl/nlog/requestData/nlogp/allBor/metaData.jsp?tableName=BorLocation&id=106529888>
- NAM & RGD (1980). Stratigraphic nomenclature of the Netherlands. *Verhandelingen van het Koninklijk Nederlands Geologisch Mijnbouwkundig Genootschap* 32, 77 pp.
- Nielsen, M.T., Weibel, R., & Friis, H. (2015). Provenance of gravity-flow sandstones from the Upper Jurassic–Lower Cretaceous Farsund Formation, Danish Central Graben, North Sea. *Marine and Petroleum Geology*, 59, 371-389.
- Osborne, M J., & Swarbrick, R.E. (1997), Mechanisms for generating overpressure in sedimentary basins: a reevaluation: *AAPG Bulletin*, v. 81, p. 1023–1041.
- Pharaoh, T.C., Dugar, M., Geluk, M.C., Kockel, F., Krawczyk, C.M., Krzywiec, P., Scheck-Wenderoth, M., Thybo, H., Vejbaek, O.V., & Van Wees, J.D. (2010). Tectonic evolution. In: Doornenbal, J.C. & Stevenson, A.G. (eds): *Petroleum Geological Atlas of the Southern Permian Basin Area*. EAGE Publications b.v. (Houten): 24-57.
- Ramm, M. (2000). Reservoir quality and its relationship to facies and provenance in Middle to Upper Jurassic sequences, northeastern North Sea. *Clay Minerals*, 35(1), 77-77.
- Ramm, M., Forsberg, A.W., & Jahren, J.S. (1997). Porosity--Depth Trends in Deeply Buried Upper Jurassic Reservoirs in the Norwegian Central Graben: An Example of Porosity Preservation Beneath the Normal Economic Basement by Grain-Coating Microquartz.
- Roberts, D.G., Thompson, M., Mitchener, B., Hossack, J., Carmichael, S., & Bjørnseth, H.M. (1999, January). Palaeozoic to Tertiary rift and basin dynamics: mid-Norway to the Bay of Biscay—a new context for hydrocarbon prospectivity in the deep water frontier. In *Geological Society, London, Petroleum Geology Conference series (Vol. 5, pp. 7-40)*. Geological Society of London.
- Roberts, A.M., Yielding, G., Kuszniir, N.J., Walker, I.M., & Dorn-Lopez, D. (1995). Quantitative analysis of Triassic extension in the northern Viking Graben. *Journal of the Geological Society*, 152 (1), 15-26.
- Scheck-Wenderoth, M., Krzywiec, P., Zühlke, R., Maystrenko, Y., & Froitzheim, N. (2008). Permian to Cretaceous tectonics. In: McCann, T. (ed.): *The Geology of Central Europe*. The Geological Society (London): 990-1030.
- Schroot, B.M. (1991). Structural development of the Dutch Central Graben. In: Michelsen, O. & Frandsen, F. (eds): *The Jurassic in the Southern Central Trough*. Danmarks Geologiske Undersøgelse series B 16: 32-35.

- Shepherd, M., MacGregor, A., Bush, K., & Wakefield, J. (2003). The Fife and Fergus Fields, Block 31/26a, UK North Sea. Geological Society, London, Memoirs, 20(1), 537-547.
- Surlyk, F. & Ineson, J.R. (2003). The Jurassic of Denmark and Greenland: key elements in the reconstruction of the North Atlantic Jurassic rift system. *In: Ineson, J.R. & Surlyk, F. (eds): The Jurassic of Denmark and Greenland. Geological Survey of Denmark and Greenland Bulletin 1: 9-20.*
- Taylor, T.R., Giles, M.R., Hathon, L.A., Diggs, T.N., Braunsdorf, N.R., Birbiglia, G.V., ... & Espejo, I.S. (2010). Sandstone diagenesis and reservoir quality prediction: Models, myths, and reality. AAPG bulletin, 94(8), 1093-1132.
- Ter Borgh, M.M., Jaarsma, B., & Rosendaal, E.A. (2015, June). Go North-A Fresh Look at the Paleozoic Structural Framework and Hydrocarbon Charge in the Dutch Northern Offshore. In 77th EAGE Conference and Exhibition 2015.
- TNO-NITG (2004). Geological Atlas of the Subsurface of the Netherlands – onshore. TNO-NITG (Utrecht): 103 pp.
- Torsvik, T.H., Carlos, D., Mosar, J., Cocks, L.R.M., & Malme, T.N.M. (2002). Global reconstructions and North Atlantic paleogeography 440 Ma to recent. *In: Eide, E.A. (ed.): Batlas – Mid Norway plate reconstruction atlas with global and Atlantic perspectives. Geological Survey of Norway (Trondheim): 18-39.*
- Underhill, J.R. & Partington, M.A. (1993). Jurassic thermal doming and deflation in the North Sea: implications of the sequence stratigraphic evidence. *In: Parker, J.R. (ed): Petroleum Geology of Northwest Europe: Proceedings of the 4th Conference. The Geological Society (London): 337-345.*
- Van Adrichem Boogaert, H.A. & Kouwe, W.F.P. (1993-1997). Stratigraphic nomenclature of the Netherlands, revision and update by RGD and NOGEP. Mededelingen Rijks Geologische Dienst, 50.
- Van den Haute, P. & Vercoetere, C. (1990). Apatite fission track evidence for a Mesozoic uplift of the Brabant Massif – preliminary results. *Annales Societe Geologique de Belgique 112: 443-452.*
- Van Wijhe, D.H. (1987). The structural evolution of the Broad Fourteens Basin. *In: Brooks, J. & Glennie, K. (eds): Petroleum Geology of North-West Europe. Graham & Trotman (London): 315-323.*
- Verreussel, R.M.C.H., Munsterman, D.K., Ten Veen, J.H., Van de Weerd, A., Dybkjaer, K., & Johannessen, P.N. (2014, June). Late Jurassic rifting in the southern central Graben - A complex story simplified. In 76th EAGE Conference and Exhibition 2014.
- Verweij, J.M., Simmelink, H.J., Underschultz, J., & Witmans, N. (2012). Pressure and fluid dynamic characterization of the Dutch subsurface. *Netherlands Journal of Geosciences, 91(04), 465-490.*
- Weaver, C.E. (1989). Clays, Muds, and Shales: Development in Sedimentology, 44.
- Wong, T.E. (2007). Jurassic. *In: Wong, T.E., Batjes, D.A.J., & De Jager, J. (eds): Geology of the Netherlands. Royal Netherlands Academy of Arts and Sciences (Amsterdam): 107-126.*
- Wonham, J.P., Rodwell, I., Lein-Mathisen, T., & Thomas, M. (2014). Tectonic control on sedimentation, erosion and redeposition of Upper Jurassic sandstones, Central Graben, North Sea. From Depositional Systems to Sedimentary Successions on the Norwegian Continental Margin, 473-512.
- Zanella, E & Coward, M.P. (2003). Structural framework. *In: Evans, D., Graham, C., Armour, A., & Bathurst, P. (eds): The Millennium Atlas: Petroleum Geology of the Central and Northern North Sea. The Geological Society (London): 45-59.*
- Ziegler, P.A. (1982). Geological Atlas of Western and Central Europe. Shell Internationale Petroleum Maatschappij b.v.; Elsevier Scientific Publishing Company: 130 pp.
- Ziegler, P.A. (1988). Evolution of the Arctic, North Atlantic and western Tethys. American Association of Petroleum Geologists: 198 pp.

- Ziegler, P.A. (1990a). Geological Atlas of Western and Central Europe (2nd edition). Shell Internationale Petroleum Maatschappij b.v.; Geological Society Publishing House (Bath): 239 pp.
- Ziegler, P.A. (1990b). Tectonic and paleogeographic development of the North Sea rift system. *In*: Blundell, D.J. & Gibbs, A.D. (eds): Tectonic Evolution of the North Sea rifts. Oxford Science Publications (Oxford): 1-36.